



Email to: reports@lrl.leg.mn

August 20, 2018

Chris Steller
Legislative Reference Library
645 State Office Building
100 Rev. Dr. MLK Jr. Blvd.
St Paul, MN 55155

RE: PT contract #108837 MN Department of Agriculture (MDA) and University of Minnesota, Office of Sponsored Projects Final Report

Project: Research to optimize woodchip bioreactors to reduce nitrogen and phosphorus in subsurface drainage water

Dear Chris:

Here are two complete copies of the final report submitted to the Minnesota Department of Agriculture Pesticide and Management Division. The electronic copy was emailed to you on August 20, 2018.

This report was prepared by the contractor and according to the project manager is not mandated by law.

Please contact me at (651) 201-6196 if you have questions.

Sincerely,

Kam Carlson

Kam Carlson
Contracts & Grants Coordinator
Pesticide & Fertilizer Management Division
Minnesota Department of Agriculture
625 Robert Street N.
St. Paul, MN 55155-2538

Enclosures: Two copies of final report for project listed above

Optimizing Woodchip Bioreactors to Treat Nitrogen and Phosphorus in Subsurface Drainage Water

Final Report for MDA Project #108837

Prepared by

Gary Feyereisen, Carl Rosen, Satoshi Ishii, Ping Wang, Ehsan Ghane, and Mike Sadowsky

July 2018

(intentionally blank page)

Acknowledgments

Dedicated technicians Ed Dorsey and Scott Schumacher; Ping Wang, Emily Anderson, Jeonghwan Jang, Todd Schumacher, and a host of staff and students.

(intentionally blank page)

Executive Summary

Nutrient losses from agriculture contribute to harmful algal blooms in streams, rivers and lakes of Minnesota (Heiskary et al., 2014) and to the Hypoxic Zone in the Gulf of Mexico, prompting concern over the deleterious effects on tourism, fisheries, and ecosystem function. In response, the Gulf Hypoxia Action Plan called for a minimum of 45% reduction in total nutrient loads in the Mississippi River (Mississippi River/Gulf of Mexico Watershed Nutrient Task Force, 2008), and the Minnesota Pollution Control Agency has also set reduction goals of 45% for nitrogen (N) and phosphorus (P) loads to the Mississippi River (MPCA, 2014). The focus of this study was to contribute to water quality nutrient reduction goals by demonstrating, evaluating, and improving upon the effectiveness of the agricultural best management practice (BMP) of woodchip bioreactors for treating agricultural subsurface (tile) drainage.

Two specific objectives of the study were 1) to identify microbial community composition in woodchip bioreactors and in their environs and to isolate and select low-temperature-adapted denitrifiers for field study, and 2) to compare N and P removal in a replicated field study by inoculating with the selected denitrifiers (bioaugmentation) or by supplementing with readily available carbon (biostimulation). The hypotheses were that 1) addition of microorganisms will enhance nitrate removal due to increasing the microbial populations that contribute to N and P removal, and 2) addition of acetate will enhance nitrate removal due to stimulation of microbial denitrification.

Low temperature-adapted denitrifying bacteria were isolated from the woodchip samples collected from the bioreactor near Willmar, Minnesota, on October 2nd, 2014. In addition, denitrifying bacteria were isolated from either biofilm or woodchips in other woodchip bioreactors located in Blue Earth, Olmsted County, and Lamberton, Minnesota. Denitrifiers were identified, isolated, and tested for denitrification rate. Best candidates were chosen and prepared for use in the field experiment. The field experiment was conducted on a Discovery Farm near Willmar, Minnesota. Subsurface drainage water was pumped to a supply tank and fed to replicated 38-ft long by 5.6-ft wide woodchip bioreactor beds. Treatments included woodchip control, bioaugmentation, and biostimulation. Experimental treatments were applied with subsequent water quality monitoring during fall 2016, Spring and Fall 2017, and spring 2018.

Results from spring 2017 suggested that bioaugmentation increased nitrate removal for one month, but the effect was then lost. Biostimulation dramatically reduced nitrate outlet concentration for six weeks, but stimulated biofouling of the bed, which restricted flow. Nutrient removal corresponded to an increase in *nosZ* gene (encoding nitrous-oxide reductase, N_2O to N_2) abundance for the biostimulation treatment. Based on the spring results, adjustments were made to the inoculation procedure and C source addition for fall 2017. Some nitrate removal increase was observed for both bioaugmentation and biostimulation, but the effects were short-lived. Results from spring 2018 are in the process of being analyzed and were not ready for inclusion in this report. There was a slight increase in ammonium with bioaugmentation presumably due to increased microbial activity related to dissimilatory nitrate reduction to ammonium (DNRA).

While total P reductions were consistently seen for all treatments, the mechanism for P removal was not identified. Part of the benefit may be attributable to steady flow rate in these experiments in contrast to event flow rate fluctuations that flush P in typical installations.

Bioaugmentation shows some promise at enhancing nitrate removal; however, additional research needs to focus on viability of the microbial community over time and to minimize DNRA. Biostimulation, which has shown promise in the laboratory, has potential to significantly increase nitrate removal rates. Additional work is needed to identify an optimum and economical C source and to overcome bioclogging.

Table of Contents

Acknowledgments.....	3
Executive Summary	5
1.0 Introduction	8
2.0 Objectives	11
3.0 Methods and Materials	12
3.1. Location and Experimental Setup.....	12
3.2. Microbial Materials and Methods.....	14
3.3. Nutrient Removal Materials and Methods.....	17
4.0 Results and Discussion	21
4.1. Microbial Results and Discussion.....	21
4.2. Nutrient Removal Results and Discussion.....	28
5.0 Education and Outreach Summary	38
6.0 References	41
7.0 Peer-reviewed publications based on this project	43
8.0 Appendices (Pending peer-reviewed scientific papers)	
A: Bioreactor Tracer Hydraulics.....	47
B: Woodchip Bioreactor Microbial Communities.....	74
C: Selection of Psychophilic Denitrifiers.....	98

1.0 Introduction

1.1. Rationale and significance

Farmers in humid and semi-humid regions install perforated drains to remove excess water from farmland. This practice is generally referred to as subsurface (tile) drainage, which enhances agricultural productivity in the Midwest by providing better conditions for root growth and improving soil trafficability for timely planting and harvesting (Ward et al., 2016). However, one tradeoff is that with the removal of excess water through subsurface drainage, portions of soluble nitrogen (N) and phosphorus (P) are leached from the soil profile and make their way into surrounding waterways. Consequently, excess nutrients in downstream water bodies can cause adverse effects of harmful algal blooms and hypoxia (oxygen depletion) (Huffman et al., 2013).

Harmful algal blooms in streams, rivers and lakes of Minnesota during warmer months are prompting concern on the deleterious effects on tourism, fisheries, and ecosystem function (Heiskary et al., 2014). Therefore, the United States Environmental Protection Agency (USEPA) has called for a minimum of 45% reduction in total nutrient loads in the Mississippi River (USEPA, 2013), and the Minnesota Pollution Control Agency has also set reduction goals of 45% for N and P loads to the Mississippi River (MPCA, 2014). Our proposed research will contribute to the MPCA goal of 45% nutrient reduction by optimizing the best management practice (BMP) of woodchip bioreactors. The Minnesota Department of Agriculture has also set priorities for impaired waters that includes demonstrating and evaluating N and P removal effectiveness of common agricultural best management practices. Therefore, our work is important since it demonstrates and evaluates the effectiveness of N and P reduction from drainage water using microbiologically-optimized woodchip bioreactors, and thus, alleviating the adverse effects associated with hypoxia and harmful algal blooms.

1.2. A proposed solution to the water quality problem

There are a number of agricultural conservation practices that reduce nutrient transport in drainage water. Some of these practices include controlled drainage, wetlands, woodchip bioreactors, crop rotations, and the use of cover crops (Dinnes et al., 2002). Among them, woodchip bioreactors (also known as denitrification beds) have shown promise due to their low maintenance and relatively small surface footprint while reducing nitrate concentration before it enters surface water (Fig. 1) (Schipper et al., 2010; Bednarek et al., 2014). Bioreactors, installed in several locations in the Midwest, have shown nitrate load reductions per year of about 12% to 57% depending on the bioreactor dimension, drainage system, and weather pattern (Christianson et al., 2012). While such reduction of nitrate load is comparable to or slightly lower than the reduction of 35% to 55% by wetlands (Brauer et al., 2015), most previous studies have been done using non-replicated and uncontrolled systems with little or no attempts to optimize the microbiology of the systems.

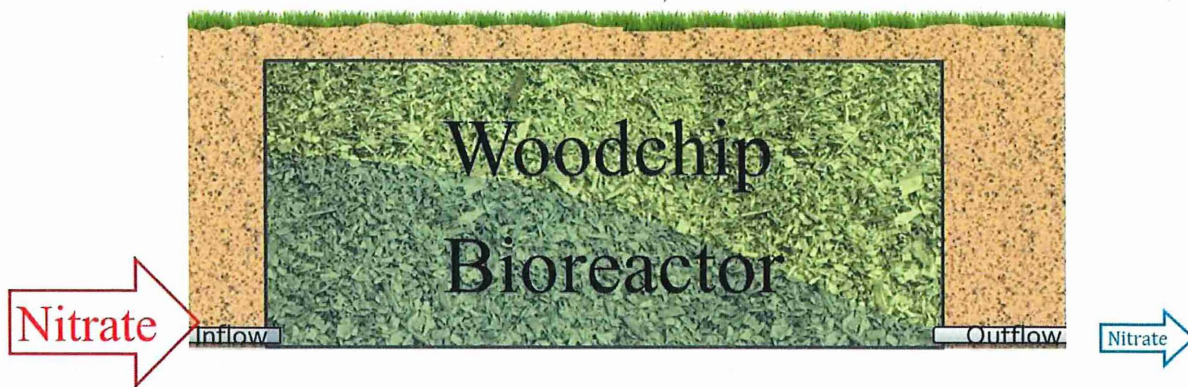


Fig. 1. Conceptual diagram of a woodchip bioreactor reducing nitrate concentration from drainage water.

A woodchip bioreactor is a trench filled with woodchips through which subsurface drainage water is routed (Fig. 1). In these systems, denitrification is the main nitrate removal mechanism through which nitrate is microbiologically converted to N_2 gas (Warneke et al., 2011).

Denitrification occurs under anaerobic conditions wherein the woodchips constitute the main source of carbon (C) for the denitrifying microbial community, while nitrate in the drainage outflow serves as the electron acceptor in the absence of oxygen. When these denitrifying bacteria have an ample supply of C for growth, favorable temperatures, and anaerobic conditions, the bioreactor removes nitrate from drainage water.

While a majority of the annual drainage outflow occurs during spring season, the water temperature from late March to May is too cold to obtain optimum nitrate removal using a woodchip bioreactor. Christianson et al. (2013) reported only a 9% load reduction in May 2011 at an average temperature of 48.2°F (9.0°C) for a bioreactor in Iowa. Similarly, based on the data in Ghane et al. (2015), nitrate load removal from drainage water was 12% at an average temperature of 47.5°F (8.6°C) during April 2014 in Ohio. However, drainage water temperatures in Minnesota are generally lower than that of Ohio, and thereby, nitrate load reduction can be lower. In this regard, Ranaivoson et al., (2012) reported annual nitrate load removal of only 24% (2009) and 10% (2010) in Minnesota. Therefore, there is a need for strategies to improve bioreactor performance at cold temperatures if we are to reach the MPCA goal of 45% nutrient reduction in Minnesota. To achieve this goal, we proposed to conduct a unique replicated experiment to evaluate strategies that would enhance bioreactor performance.

1.3. Strategies to improve bioreactor performance

One strategy for enhancing nitrate removal under cold temperatures is supplementing additional C to the woodchip bioreactor, which would be more readily available than the C in the woodchips. Findings that support this strategy include those of Feyereisen et al. (2016), who found that denitrification at cold temperatures (35°F/1.5°C) was limited by available C, rather than by population of denitrifying microbes. Greenan et al. (2006) reported on the success of this

strategy by improving denitrification in woodchips by adding soybean oil in laboratory columns under room temperature. We have recently shown that adding acetate to woodchips improve nitrate removal in laboratory columns at water temperatures of 41°F (5°C) (Roser et al., 2018). Therefore, there is a need to evaluate this strategy at the field scale and under cold water temperatures typically present during spring flow periods.

Another strategy for enhancing nitrate removal is the addition of cold-adapted and metabolically-active denitrifying bacteria that are more efficient at lower temperatures. This strategy is referred to as bioaugmentation. We already have a handful of rapidly-denitrifying bacteria that were isolated from the bioreactor in 2015. These microorganisms were introduced into the bioreactor beds for improvement of the bioreactor's performance. To date, while design and performance factors have been monitored at bioreactor sites, there has been little work to characterize the microbial community. Consequently, our results will potentially be a game changer in allowing more rapid nitrate removal under lower temperatures.

1.4. Phosphorus removal using bioreactors

In addition to nitrate removal, it has been observed that load reduction of other pollutants such as soluble P and atrazine can also occur with wood-based media (Choudhury et al., 2015; Krause Camilo et al., 2016), although results with P have been mixed (David et al., 2015; Keegan Kult, pers. comm.). Any reduction in P is likely attributed to polyphosphate accumulating microorganisms (PAOs). This group of microorganisms is further classified as denitrifying PAO (DPAOs) if they use nitrate. Therefore, we will also investigate P removal in our replicated experiment.

2.0 Objectives

Our overall goal is to demonstrate, evaluate, and improve upon the effectiveness of the agricultural BMP of woodchip bioreactors for treating tile water. To achieve this goal, we initiated a field-scale experiment to evaluate the effect of labile C (i.e., acetate) and cold-adapted denitrifying bacteria addition to bioreactors. The two specific objectives of this project were:

Objective 1: Identify the microbial community composition within the bioreactor. It is expected that the results of this section will aid in identifying and isolating the most efficient nitrate and P removing microbial populations.

Objective 2: Compare N and P removal by bioaugmentation (i.e., addition of cold-adapted denitrifying bacteria) and biostimulation (i.e., supplementing additional C source of acetate) throughout the growing season.

Our hypotheses include, 1) addition of acetate will enhance nitrate removal due to stimulation of microbial denitrification through addition of labile C that is otherwise not readily available under suboptimal growth temperatures, and 2) the addition of microorganisms will enhance nitrate removal due to increasing the microbial populations that contribute to nitrogen and P removal.

3.0 Materials and Methods

3.1 Location and Experimental Setup

In October 2014, we redesigned a plastic-lined woodchip bioreactor (349 ft long and 5.6 ft wide), which was originally installed on a private farm near Willmar, Minnesota, in November 2010 through the Discovery Farm program, into eight bioreactor beds (Figs. 2, 3). This redesign was made possible through funding from the University of Minnesota MnDRIVE program. As constructed, the setup allowed simultaneous analysis of two independent variables (i.e., bacteria and C source) that have the potential to enhance bioreactor performance. This unique system allowed us to control flow rate and to add bacteria and C to optimize bioreactor performance in a manner that was not previously possible. During the installation, we collected woodchip samples from each bed to characterize their physical, chemical, and microbiological properties.

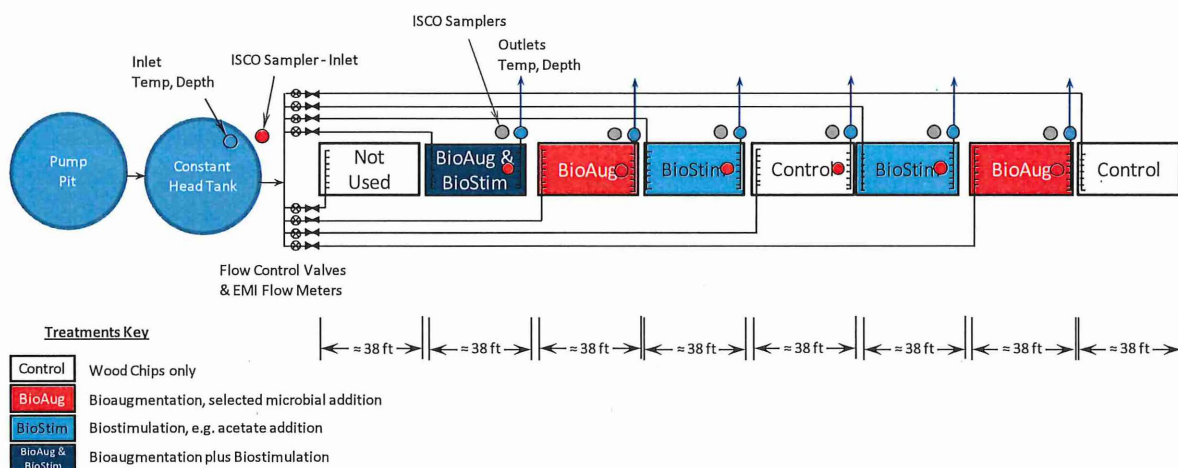


Fig. 2. Schematic of the redesigned replicated bioreactor beds.

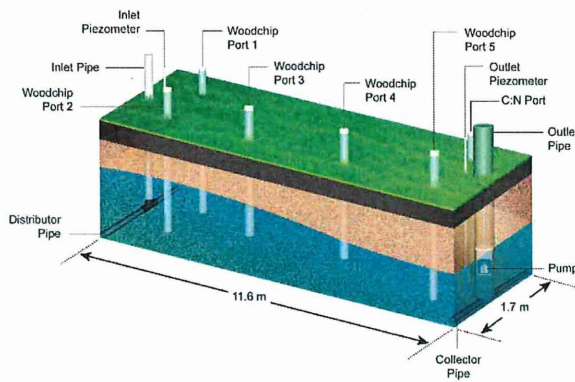
This redesign resulted in eight plastic-lined beds, each 38 ft long and 5.6 ft wide, with ≈ 2 ft of soil cover (Fig. 4a). Each of the eight beds was separated from adjacent beds using a compacted soil berm, and plastic sheets were inserted before and after the soil berms to prevent water movement between beds. Drainage water from adjacent cropped fields flows into a vertical pit from which the water is pumped into a 3,000-gallon constant-head supply tank. The water head in the supply tank causes gravity flow of water to each bed via a manifold and 1.5-in. (3.8-cm) diameter PVC piping. The flow rate for each bed is independently adjustable, and paddlewheel flow sensors are used to measure flow rate into and out of each bed (Fig. 3). Each bed was equipped with a set of PVC pipes ("ports") that were installed vertically to the bottom of the bed and used to monitor water quality parameters along the bed length. The ports were placed ≈ 30 cm downstream of the inlet, at 1/3 and 2/3 the length of the bed, and at ≈ 30 cm upstream of the outlet (Fig. 4a). Each port contained a basket with ≈ 30 "woodchip balls" that were used for microbial analysis (Fig. 4b).



Fig. 3. Photos of the supply tank and the tile-water distribution system to each bioreactor bed.

We determined the physical (i.e., particle size) and chemical (i.e., N and C content) properties of the woodchips in each bioreactor bed (Ghane et al., 2018). These results showed that the woodchips in bed numbers 3 to 8 have similar properties, so these six beds were used to conduct the replicated experiment to explore the nutrient removal performance of the experimental treatments (bioaugmentation and biostimulation). One of the remaining two beds (number 2) was used as a demonstration treatment, receiving both bioaugmentation and biostimulation treatments. One of the beds (number 1) was not used because flow through it was impacted by an old tile line located under it.

(a)



(b)



Fig. 4. (a) Diagram of an individual bioreactor bed. (b) Port baskets containing woodchip balls.

The following replicated ($n=2$) treatments were established: control - woodchip beds left as is; bioaugmentation - addition of selected cold-tolerant denitrifying bacteria; biostimulation - addition of acetate, a readily available C source. Bioreactor bed numbers 3 through 8 were randomized for the fall 2016 experimental campaign. Since there were no microbial nor nutrient removal treatment differences, beginning in the spring 2017 the beds were blocked based on landscape position and randomized within each block. The blocks consisted of numbers 3 through 5, and numbers 6 through 8. The higher numbered beds (6 through 8) were at a lower

elevation in the landscape and more likely to be influenced by high ground water table after large precipitation events.

Construction and troubleshooting of the beds, piping, and instrumentation was a large effort and was completed by summer's end 2016. Four experimental "campaigns" were conducted: Fall 2016, Spring 2017, Fall 2017, and Spring 2018. Each campaign consisted of inoculation of the bioaugmentation beds with selected denitrifiers and introduction of acetate into the biostimulation beds. Intense water and woodchip sampling were performed on bed numbers 2 through 8 by an interdisciplinary team just prior to the inoculation and one, two, and/or three weeks after inoculation. During these intense sampling events, water and woodchip collection occurred at the outlets, ports, and inlets of each bed. Further details concerning the materials and methods for the microbial (Section 3.2) and nutrient removal (Section 3.3) objectives follow.

3.2 *Microbial Materials and Methods*

3.2.1. *Isolation of low temperature-adapted denitrifying bacteria*

Low temperature-adapted denitrifying bacteria were isolated from the woodchip samples collected from the bioreactor near Willmar (bioreactor WB) on October 2nd, 2014. In addition, denitrifying bacteria were isolated from either biofilms or woodchips in other woodchip bioreactors located in Blue Earth (bioreactor BE), Olmsted County (bioreactor DC) and Lamberton (bioreactor LB), Minnesota. The ages of the woodchip bioreactors varied from 2 months (bioreactor BE) to 6 years (bioreactor WB). Woodchips were collected from submerged areas of the bioreactors and were immediately placed in a cooler. Clogging as a result of biofilm formation occurred in Rochester, Lamberton, and Willmar bioreactors. Denitrifying bacteria were also isolated from these biofilms.

The woodchip and biofilm samples (1 g) were suspended in phosphate buffered saline (PBS, pH 7.4) and then plated on R2A agar containing 5 mM nitrate and 10 mM acetate (R2A-NA). Plates were incubated anaerobically at 15°C using an AnaeroPak system (Mitsubishi Gas Chemical) and continually restreaked until individual colonies appeared. Initial strain isolation work done at 10 and 4°C was unsuccessful, most likely due to slow bacterial growth; therefore, subsequent work was carried out at 15°C, which is relatively low compared to an optimum growth temperature range of typical denitrifying bacteria (30 to 35°C).

The ability of the strains to denitrify was examined by using the acetylene inhibition assay (Tiedje, 1994). In brief, fresh cell cultures (300 µl) were inoculated into R2A-NA broth (10 ml) in 27 ml test tubes. After replacing the air phase with Ar:C₂H₂ (90:10) gas, the test tubes were incubated at 30°C. After 2-week incubation, gas samples were taken via a gastight syringe and analyzed for N₂O production by GC as described above. In addition, liquid samples were collected and analyzed for nitrate, nitrite and ammonium concentrations using the SEAL AA3 HR AutoAnalyzer. Strains that reduced ≥40% nitrate, converted <10% of nitrate to ammonium, and produced significant amount of N₂O (>100 ppm) were considered as denitrifiers. The GC

system used in this study was too sensitive, and the upper quantification limit was often exceeded. Therefore, we could not calculate the percentage of nitrate reduced to N_2O .

3.2.2. Identification and characterization of the denitrifying strains.

All nitrate-reducing microorganisms were identified based on 16S rRNA gene sequencing. First, DNA was extracted by heating cells at 95°C for 15 min and then diluted 10-fold for PCR. The reaction mixture (50 μl) contained 1x Ex Taq buffer (Takara Bio, Otsu, Japan), 0.2 μM of each primer (27F and 1492R; ref), 0.2 mM of each dNTP, 1 U of Ex Taq DNA polymerase (Takara Bio), and 2 μl of DNA template. PCR was performed using a Veriti Thermal Cyclers (Life Technologies) and the following conditions: initial annealing at 95°C for 5 min, followed by 30 cycles of 95°C for 30 s, 55°C for 30 s and 72°C for 1.5 min, and one cycle of 72°C for 7 min. Amplification was confirmed using agarose gel electrophoresis and PCR products were purified using AccuPrep PCR Purification Kit (Bioneer) and then quantitated using PicoGreen dsDNA quantitation assay (Thermo Scientific). The purified PCR products were bidirectionally sequenced using the Sanger method by at the University of Minnesota Genomics Center. The resulting forward (27F) and reverse (1492R) reads were aligned using the phred, phrap, consed software (Ewing et al. 1998) and strain identity was determined using Naïve Bayesian classifier (Wang et al. 2007).

3.2.3. Denitrification rate measurement

Potential cold-adapted denitrifiers chosen for further testing were selected based on the following criteria: greater than 49% nitrate-N was reduced, less than 10% N was converted to ammonium, and no nitrite-N was produced.

Denitrification rates were measured using ^{15}N -labeled nitrate and a gas chromatograph-mass spectrometer (GC-MS). Having confirmed that these strains are capable of reducing nitrate, the ^{15}N -labeled nitrogenous gases would allow us to track nitrate through the denitrification process, showing whether or not complete denitrification is occurring. In brief, denitrifying bacteria grown in R2A-NA broth under anaerobic conditions were washed in piperazine-N, N'-bis (PIPES) buffer (pH 7.4). Denitrifying bacteria were incubated at 15°C in triplicate 50 ml PIPES buffer (pH 7.4) containing 10 mM acetate and 5 mM ^{15}N -labeled nitrate in 160 ml airtight bottles. The gas phase was exchanged for He. 10 μl gas samples were taken at hours 0, 24, 48, 72 and 1 week and 2 weeks and immediately analyzed using a GCMS-QP2010 SE (Shimadzu) equipped with Rt-Q-BOND column (30 m \times 0.32 mm \times 10 μm ; Restek) to measure the absorbance values of $^{30}\text{N}_2$ and $^{46}\text{N}_2\text{O}$. A standard curve was created by injecting different volumes of $^{30}\text{N}_2$ gas and comparing absorbance values to known concentrations. Data were analyzed according to this standard curve and results were calculated as pmol-N $^{46}\text{N}_2\text{O}$ and $^{30}\text{N}_2$ produced per cell, based on OD_{600} values. The denitrification rate was calculated as pmol-N/cell/hour for $^{30}\text{N}_2$ gas based on the slope of the trendline where $^{30}\text{N}_2$ gas was produced linearly.

3.2.4. Aerobic denitrification confirmation

While denitrification is thought to be an anaerobic process, some microorganisms have recently been identified that are capable of aerobic denitrification (Takaya et al. 2003) and explanations for compatible aerobic respiration and denitrification have been hypothesized (Chen and Strous 2013). Aerobic denitrification would serve an important role in wastewater treatment, particularly in woodchip bioreactors where fluctuating water depth corresponds to a fluctuation in oxygen levels. To test for aerobic denitrification, potential denitrifying bacteria were incubated under the same conditions as the denitrification rate test except the gas phase was not exchanged. Gas samples were taken at the same time intervals.

3.2.5 Materials and methods for qPCR

3.2.5.1 Sample collection

Two-liter water samples were collected from the woodchip bioreactors. All water samples were transported on ice to the lab, and stored at 4°C for less than 24 hours prior to filtration

3.2.5.2 Sample processing and DNA extraction

Water samples were pre-filtered through 5µm nitrocellulose filters (Millipore-Sigma, St. Louis, MO) to remove debris. Water was subsequently filtered through 0.45µm, and then 0.22µm, nitrocellulose filters (Millipore-Sigma, St. Louis, MO) to capture all bacteria. Filters were transferred into 50ml conical tubes containing 3ml of 0.01% sodium pyrophosphate buffer, pH 7.0 containing 0.2% Tween 20 (polyethylene glycol sorbitan monolaurate) and vortexed for 3 min at room temperature. Each conical tube held up to four filters, and the 0.45µm and 0.22µm filters were placed in the same tube. The supernatant containing re-suspended cells from the filters was transferred to a 1.7 mL Eppendorf tube and centrifuged for 3 min at 13,300×g, discard the supernatant and keep the cell pellets in the tube. It was performed twice for the above vortex and centrifuge procedures, combine the cell pellets in the same tube. Samples were stored at -80°C until DNA was extracted. DNA from water sample pellets was extracted using the DNeasy PowerSoil DNA extraction kit (Qiagen, CA, USA), as per kit directions. DNA concentrations were measured on a Qubit 2.0 fluorometer (Life Technologies).

3.2.5.3 Quantification of denitrifying genes

Quantitative Polymerase chain reaction (qPCR) was used to determine the accuracy and efficiency of the DNA primers for each gene. The genes investigated in this project encompass some key steps of the denitrification pathway, and included genes for nitrite reductase (nirS and nirK) and nitrous oxide reductase (nosZ). The total bacteria abundance in each sample was also determined by targeting the v4 region of 16S rRNA gene. For all genes, gBlock Gene Fragments (Integrated DNA Technologies, Inc., USA) were created from the primers for each selected gene.

Quantitative PCR (qPCR) was used to determine the concentration (abundance) of each gene in water samples. The qPCR analysis used the iTaq™ Universal SYBR® Green Supermix (Bio-Rad, CA) and was performed on a Roche Light Cycler 480 Real-Time PCR (Roche Life Sciences, Indianapolis, IN). The specific primers used were U515F and U806R for 16S rRNA (BAC515F), nirK876F and nirK1040R for nirK (Bru et al., 2011; Petersen et al., 2012), m-cd3AF and m-R3cd for nirS, nosZ2F and nosZ2R for nosZ3 (Bru et al., 2011; Petersen et al., 2012). The qPCR efficiencies for all genes ranged from 85% to 105%, with R2 values over 0.99 for all calibration curves. Negative, no-template controls were included with each qPCR run. Gene abundances were normalized per 100 mL water sample for analysis.

3.3 Nutrient Removal Materials and Methods

3.3.1 Flow Measurement

Flow to each bed was controlled with a 3/4-in. diameter gate valve near the manifold near the supply tank. At the outlet end of each bed, effluent flowed through a collection manifold across the width of the bed toward a center sump consisting of a 7-gallon bucket. Water inside the sump was pumped with a submersible pump through a paddle wheel sensor connected to a datalogger. A paddle wheel sensor was also connected to the inlet of each bed, close to the control valves. The inlet paddle wheel readings were correlated with the outlet readings and used to fill any gaps in the outlet flow data. A nominal flow rate of 10 L/min (8 to 9-h hydraulic residence time, HRT) was established.

3.3.2 Water Sample Collection

Three water sampling regimes were used throughout the project: weekly manual sampling, continuous automated sampling, and intensive manual sampling related to microbial inoculation and sampling. Automated water samplers (ISCO 6712, Teledyne ISCO, Lincoln, NE) were installed in storage huts at the supply tank and the outlet of each bed. Power was supplied by 12-volt deep cycle batteries recharged by solar panels.

3.3.2.1 Weekly Manual Sampling Regime

Manual sampling occurred mid-week throughout the period from Spring 2016 through Summer 2018 as long as subsurface drainage water was flowing. The system was shut down during winter and early spring to avoid freeze up. For the Fall 2016 and Spring 2017 campaigns, 250-mL water samples were collected in polyethylene bottles from the outlet sumps of each bed. For the Fall 2017 and Spring 2018 campaigns, 250-mL water samples were collected in polyethylene bottles using the automated samplers, which drew water from outside the outlet sump bucket. Inlet samples were collected from a sampling port on the inlet manifold. Within one hour of collection, six 17-mL samples were filtered (0.45 mm); two of these, along with two unfiltered

17-mL samples were acidified (Clesceri et al., 1998). Samples were placed on ice, transported to the laboratory in St. Paul, Minnesota, and frozen until analysis.

3.3.2.2 Automated Sampling Regime

The automated sampler at the supply tank was programmed to pump 160-mL subsamples at 4-hour intervals into a 1-L bottle containing 1.25 mL concentrated H₂SO₄ daily. The water was pumped from inside the supply tank, ≈12 in. from its bottom, near the outlet to the manifold. For the Fall 2016 campaign, the same sampling regime (one 1-L bottle per day) was used for outlet sampling of all the beds. In order to reduce the sample handling and analysis load, outlet sampling for Spring and Fall 2017 was reduced to one acidified 1-L bottle each 3 days: 80-mL subsamples at 6-hour intervals. In order to increase the number of data points for the final campaign, Spring 2018, a 2-day acidified 1-L bottle regime was used: 80-mL at 4-hour intervals. Weekly, the 1-L bottles were placed in coolers and transported to St. Paul, Minnesota, and stored in a cooler (4°C). Filtered (0.45 mm) and unfiltered samples were prepared for analysis and archival (frozen) purposes.

3.3.2.3 Inoculation-related Intensive Sampling Regime

Table 1 indicates the dates when intense water sampling occurred. The sampling immediately preceded inoculation of the bioaugmentation treatment beds and was repeated one, two, and/or three weeks after inoculation. Beginning with the control beds, water was pumped from the outlet sump, 4 ports from the outlet to the inlet, and the inlet with a peristaltic pump connected to a polycarbonate tube inserted into the ports to a depth of ≈1 to 2 in. from the bottom of the bed. Water for nutrient analysis was collected in 250 mL polyethylene bottles and processed on site. Filtered (0.45 mm) and unfiltered samples (17 mL) were poured into scintillation vials, acidified per sample plan, placed in iced coolers, transported to St. Paul, and stored (frozen) until analyzed. Water for microbial analysis was collected from the outlet, the four ports (2016) or two mid-ports (2017 and 2018), and from the inlets by pumping into 1-L (2016) or 2-L (2017 and 2018) autoclaved polyethylene bottles.

Table 1. Intensive water sampling dates associated with bed inoculation – prior to and after.

Sampling Dates	Inoculant
October 20, 2016	<i>Bacillus pseudomycooides</i> I32.
October 27, 2016	No inoculation.
May 8, 2017	<i>Cellulomonas</i> sp. strain WB94
May 15, 2017	No inoculation.
June 23, 2017	No inoculation.
October 17, 2017	<i>Microvirgula</i> sp. strain BE2.4, <i>Lelliottia</i> sp. strain BB2.1

October 31, 2017	<i>Microvirgula</i> sp. strain BE2.4, <i>Lelliottia</i> sp. strain BB2.1
November 14, 2017	No inoculation.
November 28, 2017	No inoculation.
May 2, 2018	<i>Microvirgula</i> sp. strain BE2.4, (<i>Cellulomonas</i> sp. strain WB94 did not grow)
May 16, 2018	<i>Microvirgula</i> sp. strain BE2.4, (<i>Cellulomonas</i> sp. strain WB94 did not grow)
May 30, 2018	<i>Microvirgula</i> sp. strain BE2.4, <i>Cellulomonas</i> sp. strain WB94
June 20, 2018	No inoculation.

3.3.3 Delivery of Carbon Source (Biostimulation Treatment)

Acetate solution was stored in a 55-gallon drum in the storage huts at the head ends of the two biostimulation treatment beds and bed number 2. The solution was delivered into the inlet flow stream with a peristaltic pump controlled by a datalogger. Concentrations, duty cycles, and flow rates are shown in Table 2. Changes were made throughout the project to optimize nitrate removal yet overcome bioclogging.

Table 2. Acetate concentrations and C:N ratios from Fall 2016 through Spring 2018.

	October 2016	May 2017	July 2017	October 2017	November 2017	May 2018
Acetate-C Conc (mg C/L)	2,770	28,500	27,900	6,050	9,940	20,400
Acetate Pumping Rate (mL/min)	200	200	200	13	13	13
Duty Cycle # cycles, timing length of ea cycle	5 min on, 10 min off for 1 hr each 8 hrs	21 sec each 5 min 7%	†21 sec each 5 min 7%	†100%	†100%	†100%

Design NO ₃ -N Concentration (mg N/L)	19	22	14	15	16	15.5
Design Bed Flow Rate (gal/min)	2.5	2.5	2.5	2.7	2.7	7.5
Design C:N (mole C:mole N)	0.15	2.52	1.00	0.60	0.57	1.46

†Pump controlled by water level in inlet pipe. Pumping of acetate ceased until backup from bioclogging diminished.

3.3.4 Water Analysis

Samples were analyzed by flow-injection colorimetry (Lachat QuikChem 8500, Hach Co.) for nitrate-N (NO₃-N + NO₂-N) (method number 10-107-04-1-A), ammonium-N (method number 10-107-06-2-A), dissolved reactive P (DRP) (method number 10-115-01-1-A), and sulfate-S (method number 10-116-10-1-A). Samples for total-N and total-P were digested (alkaline persulfate, Patton and Kryskalla, 2003) prior to the nitrate-N and DRP flow-injection analysis methods identified above. Dissolved C was determined by combustion (Elementar vario TOC Cube Select, Elementar, GmbH) and infrared spectrometry; dissolved inorganic C (DIC) was determined by purging with phosphoric acid and dissolved organic C (DOC) was calculated as the difference between DC and DIC.

4.0 Results and Discussion

4.1 Microbial Results and Discussion

4.1.1. Isolation of potential denitrifying bacteria

A total of 207 microorganisms were isolated under cold temperatures from woodchip or biofilm samples from four woodchip bioreactors in Minnesota. Of these, 79 strains were identified as cold-adapted nitrate-reducers. Table 3 shows the identity and denitrification potential of all isolates across all sites. While nitrate reduction and ammonium production varied widely, overall little to no nitrite was produced. From the bioreactor BE woodchip samples, a total of 25 bacteria were isolated, all of which were confirmed nitrate reducers and many potential denitrifiers. The isolated nitrate-reducers from this site belonged mostly to the genera *Microvirgula* and *Enterobacter*. Six isolated bacteria were considered to be potential denitrifiers (>49% nitrate reduced, <10% ammonium produced) and belonged to a more diverse group of genera, including *Microvirgula*, *Delftia*, *Raoultella*, *Clostridium* and *Buttiauxella*.

From bioreactor WB, 104 and 16 bacterial strains were isolated under denitrifying conditions from the woodchips and biofilm, respectively. Of these, 21 isolates from woodchips and five isolates from biofilm were confirmed nitrate-reducers and both samples contained unique microorganisms. A total of three potential denitrifiers were identified from the WB woodchips, two of which belonged to the genus *Clostridium* and one to *Cellulomonas*. Of the five nitrate-reducers isolated from the biofilm, many demonstrated relatively high nitrate reduction (32-62%), but correspondingly high ammonium concentrations, indicating that these strains are likely performing dissimilatory nitrate reduction to ammonium (DNRA). Production of ammonium is undesirable in a bioreactor and therefore strains with the lowest possible DNRA were selected for inoculation.

A total of nine nitrate-reducing bacteria were isolated from the LB bioreactor biofilm, none of which were identified as potential denitrifiers. Similarly, no potential denitrifiers were isolated from the DC woodchip bioreactor, which belonged almost exclusively to the genus *Bacillus*. The isolated nitrate-reducers from the DC biofilm produced little ammonium, but the presence of nitrite was detected in all but one sample.

Table 3. Nitrate-reducing bacteria isolated from woodchip bioreactors in Minnesota and their N transformations. Strains shown in bold were used for bioaugmentation experiments.

Isolate ID	Source	%N to ammonium	% Nitrate reduced	%N to nitrite	N ₂ O (ppm)	Identification
BE1.1	Blue Earth woodchips	32.73	100.00	0.00	2020.21	<i>Enterobacter</i>
BE 1.2	Blue Earth woodchips	7.95	69.84	0.00	1532.52	<i>Delftia</i>
BE 1.3	Blue Earth woodchips	27.30	99.85	0.00	3348.41	<i>Enterobacter</i>
BE 1.4	Blue Earth woodchips	34.33	100.00	0.00	2786.80	<i>Microvirgula</i>
BE 1.5	Blue Earth woodchips	21.57	81.02	0.00	2695.12	<i>Microvirgula</i>
BE1.6	Blue Earth woodchips	48.00	87.50	0.00	1861.03	<i>Kosakonia</i>
BE 1.7	Blue Earth woodchips	29.51	74.58	0.00	17.97	<i>Enterobacter</i>
BE 2.1	Blue Earth woodchips	6.82	70.09	0.00	1815.50	<i>Raoultella</i>
BE 2.2	Blue Earth woodchips	14.89	73.63	0.00	2072.18	<i>Clostridium</i>
BE 2.3	Blue Earth woodchips	33.49	99.80	0.00	3693.00	<i>Microvirgula</i>
BE 2.4	Blue Earth woodchips	-0.23	62.05	0.00	2072.18	<i>Microvirgula</i>
BE2.5	Blue Earth woodchips	7.78	66.83	0.00	316.15	<i>Klebsiella</i>
BE 2.6	Blue Earth woodchips	-0.30	62.12	0.00	88.76	<i>Buttiauxella</i>
BE2.7	Blue Earth woodchips	21.84	78.40	0.00	1898.18	<i>Enterobacter</i>
BE 3.1	Blue Earth woodchips	18.12	74.79	0.00	2111.09	<i>Serratia</i>
BE3.2	Blue Earth woodchips	36.77	99.89	0.00	939.63	<i>Enterobacter</i>
BE 3.3	Blue Earth woodchips	16.46	73.87	0.00	1567.94	<i>Microvirgula</i>
BE 3.4	Blue Earth woodchips	35.22	100.00	0.00	2919.65	<i>Raoultella</i>
BE 3.5	Blue Earth woodchips	33.60	49.99	0.00	917.43	<i>Lelliottia</i>
BE 3.6	Blue Earth woodchips	26.66	60.11	0.00	2073.42	<i>Enterobacter</i>
BE 3.7	Blue Earth woodchips	73.59	100.00	0.00	3504.32	<i>Microvirgula</i>
BE 3.8	Blue Earth woodchips	66.17	99.92	0.00	3706.89	<i>Microvirgula</i>
BE 3.9	Blue Earth woodchips	39.12	56.90	0.00	1668.99	<i>Enterobacter</i>
BE 3.10	Blue Earth woodchips	74.68	100.00	0.00	3333.53	<i>Microvirgula</i>
BE 3.11	Blue Earth woodchips	4.83	62.38	0.00	64.93	<i>Clostridium</i>
17	Willmar woodchips	40.88	98.31	0.00	1401.13	<i>Microvirgula</i>
18	Willmar woodchips	44.86	98.30	0.00	1479.26	<i>Microvirgula</i>
19	Willmar woodchips	4.06	-6.92	0.00	63.11	<i>Clostridium</i>
21	Willmar woodchips	5.78	-12.89	0.00	224.02	<i>Clostridium</i>
22	Willmar woodchips	42.11	98.41	0.00	1496.52	<i>Microvirgula</i>
23	Willmar woodchips	6.96	-16.99	0.00	9.45	<i>Clostridium</i>
24.2	Willmar woodchips	7.26	-15.18	0.00	7.11	<i>Clostridium</i>
26	Willmar woodchips	-7.50	33.45	0.00	2.45	<i>Clostridium</i>
29	Willmar woodchips	-6.47	31.96	0.00	1.26	<i>Clostridium</i>
39	Willmar woodchips	7.12	39.44	0.00	68.83	<i>Clostridium</i>
40	Willmar woodchips	2.04	3.77	0.00	5.12	<i>Clostridium</i>
49	Willmar woodchips	6.84	39.64	0.00	103.17	<i>Clostridium</i>
53	Willmar woodchips	0.83	58.21	0.00	843.64	<i>Clostridium</i>
66	Willmar woodchips	5.03	45.13	0.00	112.09	<i>Clostridium</i>
76	Willmar woodchips	-1.62	44.38	0.00	147.01	<i>Clostridium</i>
80	Willmar woodchips	5.87	49.82	0.00	603.18	<i>Clostridium</i>
81	Willmar woodchips	4.09	47.52	0.00	0.34	<i>Clostridium</i>
91	Willmar woodchips	6.97	38.73	0.00	169.69	unclassified <i>Deltaproteobacteria</i>
94	Willmar woodchips	6.45	49.16	0.00	115.98	<i>Cellulomonas</i>
102	Willmar woodchips	2.51	60.29	0.00	-267.82	<i>Cellulomonas</i>
104	Willmar woodchips	73.11	29.12	0.00	994.87	<i>Cellulomonas</i>
ID 2A1	Willmar bioslime	72.98	62.74	0.00	259.04	<i>Bacillus</i>
ID 2A1.1	Willmar bioslime	65.87	59.16	0.00	168.22	<i>Aeromonas</i>
ID 2B3	Willmar bioslime	38.84	59.27	0.00	837.29	<i>Lelliottia</i>
ID 6A1	Willmar bioslime	58.39	32.23	0.00	1247.67	<i>Bacillus</i>
ID 6B1	Willmar bioslime	60.34	40.41	0.00	1908.73	<i>Enterobacter</i>

Table 3 (continued)

Isolate ID	Source	%N to ammonium	% Nitrate reduced	%N to nitrite	N ₂ O (ppm)	Identification
IDBA1.12	Lamberton bioslime	25.36	49.36	0.00	620.31	<i>Escherichia</i>
IDBA1.2	Lamberton bioslime	46.07	42.78	0.00	453.32	<i>Lelliottia</i>
IDBA1.3	Lamberton bioslime	54.45	49.51	0.00	299.32	<i>Raoultella</i>
IDBA2.2	Lamberton bioslime	63.42	45.84	0.00	439.85	<i>Raoultella</i>
IDBB1.1	Lamberton bioslime	49.40	64.73	0.00	57.82	<i>Raoultella</i>
IDBB1.2	Lamberton bioslime	47.77	102.29	0.00	1231.27	<i>Microvirgula</i>
IDBB1.3	Lamberton bioslime	6.77	21.05	0.00	73.89	<i>Lactococcus</i>
IDBB2.1	Lamberton bioslime	35.76	43.12	0.00	509.27	<i>Lelliottia</i>
IDBB2.2	Lamberton bioslime	54.43	20.43	0.00	459.65	<i>Lelliottia</i>
H6	Dodge County bioslime	9.17	6.20	0.00	739.35	<i>Mariniluteicoccus</i>
H13	Dodge County bioslime	13.09	-22.76	2.18	832.28	<i>Bacillus</i>
H16	Dodge County bioslime	8.40	-10.81	2.09	2292.20	<i>Bacillus</i>
H20	Dodge County bioslime	9.64	-7.19	2.15	941.83	<i>Bacillus</i>
H25	Dodge County bioslime	7.02	5.02	1.84	908.86	<i>Bacillus</i>
H26	Dodge County bioslime	6.13	3.36	0.82	878.60	<i>Bacillus</i>
H29	Dodge County bioslime	8.39	-3.21	1.79	1060.61	unclassified <i>Bacillales</i>
H30	Dodge County bioslime	8.45	27.29	0.53	884.89	<i>Bacillus</i>
H31	Dodge County bioslime	4.35	18.15	0.16	1019.25	<i>Clostridium</i>
H32	Dodge County bioslime	4.96	3.65	1.82	685.91	<i>Bacillus</i>
H33	Dodge County bioslime	8.77	-7.63	1.34	935.31	<i>Bacillus</i>
H34	Dodge County bioslime	-5.04	50.74	2.03	641.78	<i>Bacillus</i>
H37	Dodge County bioslime	-2.04	32.63	1.47	1102.62	<i>Bacillus</i>
H41	Dodge County bioslime	17.77	29.56	17.54	1181.89	<i>Bacillus</i>
H43	Dodge County bioslime	4.42	10.54	3.92	1120.13	<i>Bacillus</i>
H45	Dodge County bioslime	-6.91	41.89	1.21	634.97	<i>Bacillus</i>

4.1.2. Denitrification rates

Seven potential denitrifiers were selected to be tested for aerobic and anaerobic denitrification rates using ¹⁵N-labeled nitrate. Five originated from the BE bioreactor, including *Buttiauxella*, *Raoultella*, *Delftia*, *Microvirgula* and *Clostridium*, and two from the WB bioreactor woodchips, including *Cellulomonas* and *Clostridium*. Two other potential denitrifiers were identified based on our criteria, one additional *Clostridium* from the WB bioreactor and one *Raoultella* from the BE bioreactor, but these were excluded due to repetition.

The denitrification rates were calculated based on the slope of the trend line during the time that ³⁰N₂ gas was produced (Table 4). Rates were measured both under aerobic and anaerobic conditions to see if some strains can reduce nitrate in the presence of oxygen (i.e., aerobic denitrification).

Based on the data presented in Table 3 and 4, we selected *Raoultella* sp. strains BE2.1 (= a fast growing nitrate reducer), *Microvirgula* sp. strain BE2.4 (= aerobic denitrifying bacteria), and *Cellulomonas* sp. strain WB94 (= strain capable of reducing nitrate as well as degrading cellulose) as the candidates for bioaugmentation.

Table 4. The denitrification rate for each sample and the time points that $^{30}\text{N}_2$ gas was produced.

Sample	Hours N2 produced	pmol/cell/hour
WB94 aerobic	0-168	5.00E-08
WB94 anaerobic	0-168	4.00E-08
BE2.4 aerobic	0-336	1.00E-08
BE2.4 anaerobic	0-336	9.00E-09
BE1.2 aerobic	0-336	4.00E-21
BE1.2 anaerobic	0-168	8.00E-07
BE2.1 aerobic	0-48	2.00E-07
BE2.1 anaerobic	0-48	1.00E-08
BE2.6 aerobic	24-48	9.00E-07
BE2.6 anaerobic	0-48	2.00E-07
BE3.11 anaerobic	48-336	2.00E-08
WB53 anaerobic	24-72	3.00E-07

4.13. Gene abundance

The abundance of *nosZ* gene encoding nitrous-oxide reductase (N_2O to N_2) in DNA was determined in water samples collected from the woodchip bioreactors before treatments (May 8, 2017) and one week after the treatments (May 15, 2017) using SYBR quantitative PCR (qPCR) technology (Fig. 5). The Bio-augmentation treatment did not increase the *nosZ* abundance, but the Bio-stimulation treatment showed positive effects. There was a tendency for the *nosZ* gene copy number to be higher at Port 4 than at Port 3, no matter which bioreactor was tested, before or after the treatment.

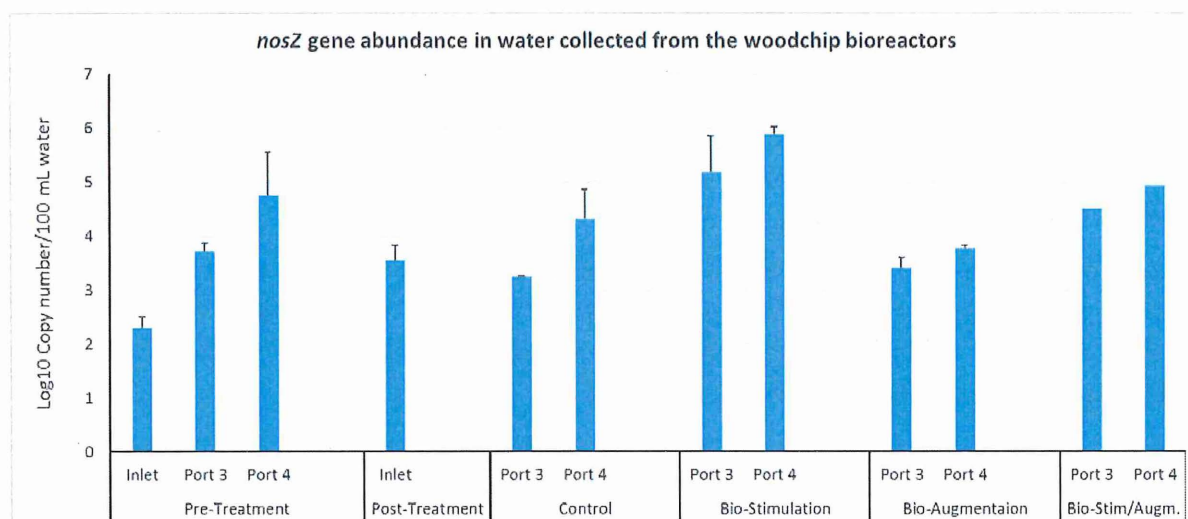


Fig. 5. qPCR results from Spring 2017 campaign.

Total DNA was extracted from each woodchip sample collected from the bioreactors; DNA concentration of 49 woodchip DNA samples was measured. The abundance of 16S rRNA v4 region, *nirS/nirK* genes, structurally different but functionally equivalent single-copy genes coding for nitrite reductases (NO_2^- to NO), a key enzyme of the denitrification process) in water DNA samples; the above genes plus *nosZ* gene, encoding nitrous-oxide reductase (N_2O to N_2) in woodchip DNA samples were also estimated using SYBR qPCR technology. The results showed that the addition of acetate as the bio-stimulant really increased the abundance of denitrifiers in the water (Fig. 6), but its stimulation is not obvious in woodchip samples collected in one week after the acetate addition (Fig. 7). The inoculation of the isolated denitrifier strains to the bioreactors did not show the bio-augmentation effects.

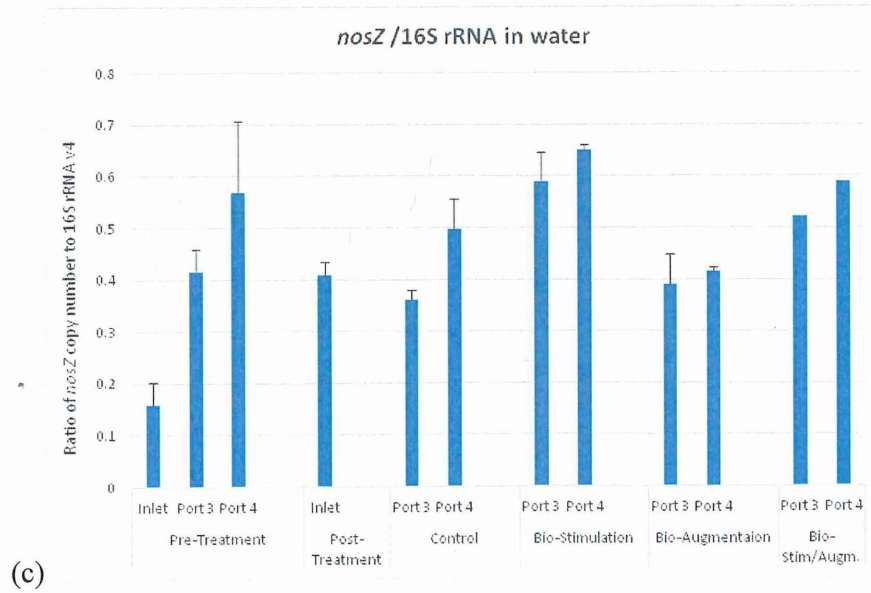
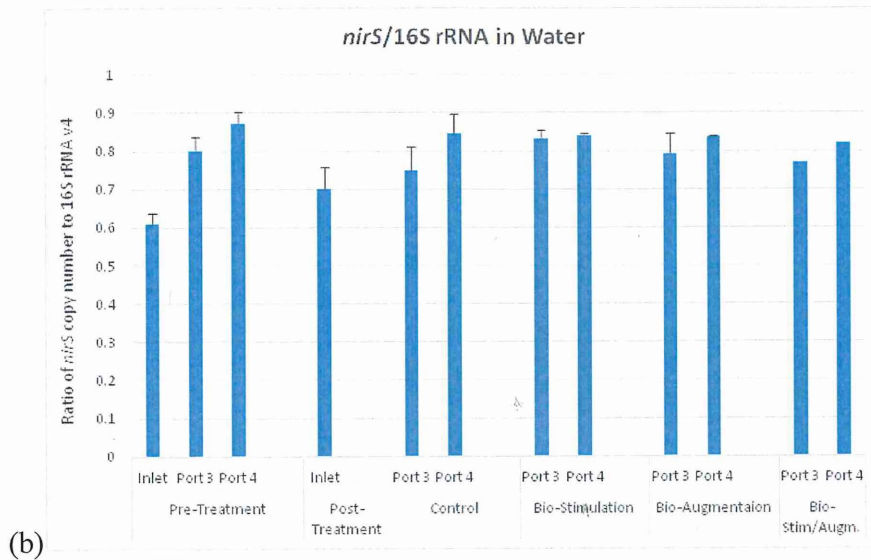
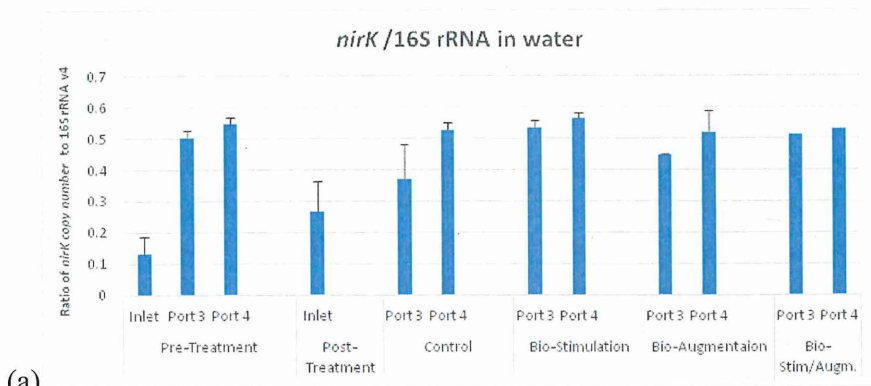


Fig. 6. Gene copy ratios for water samples for (a) *nirK*, (b) *nirS*, and (c) *nosZ*. Samples were collected 15 May 2017, one week after inoculation.

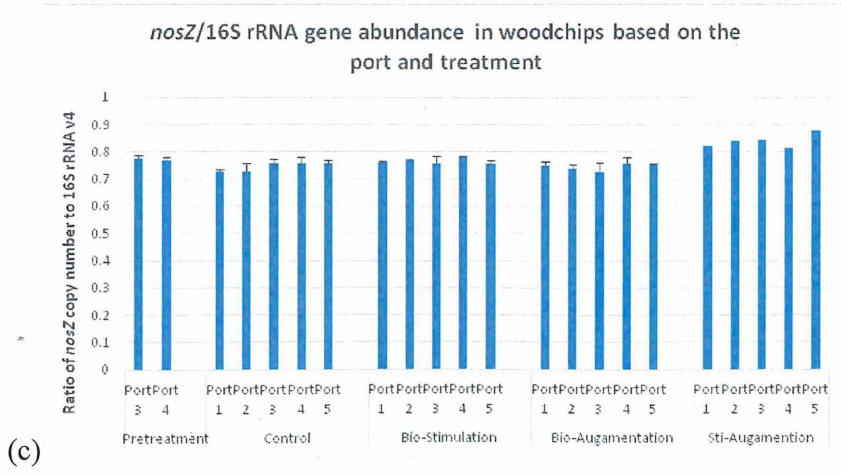
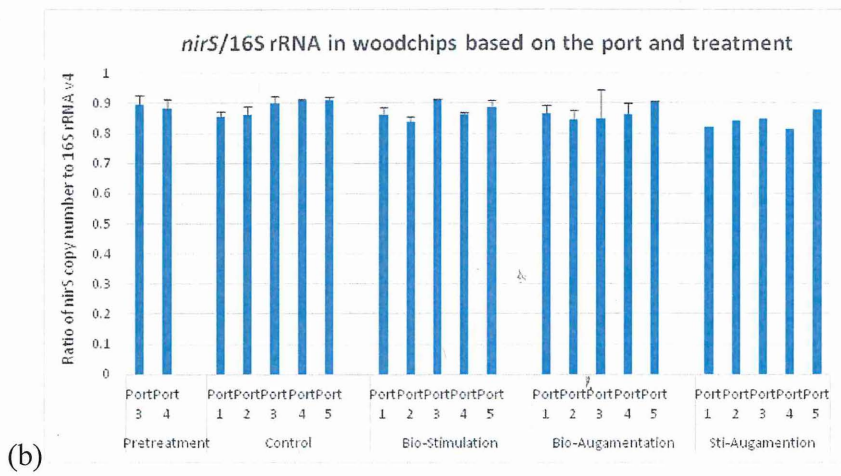
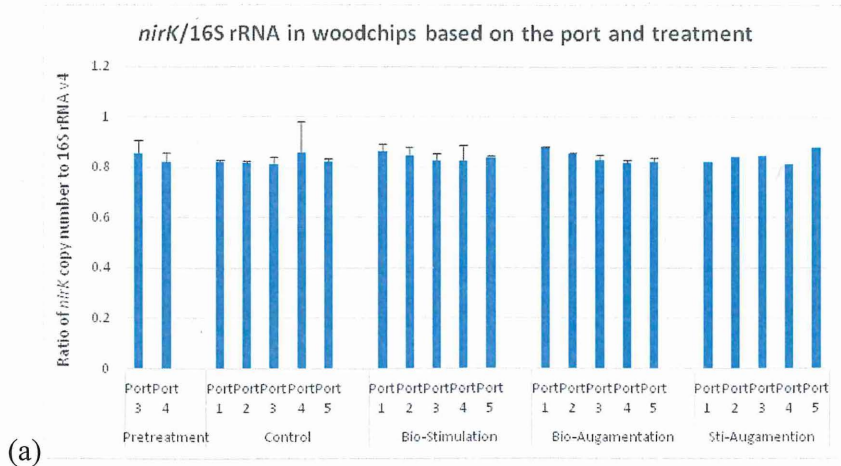


Fig. 7. Gene copy ratios for woodchip samples for (a) *nirK*, (b) *nirS*, and (c) *nosZ*. Samples were collected 15 May 2017, one week after inoculation.

4.2 Nutrient Removal Results and Discussion

4.2.1 Experimental conditions – Hydrology and water temperature

Hydraulic residence times for fall 2016 and spring and fall 2017 are shown in Table 5 below. The greater HRT for the control resulted in more time for denitrification for this treatment and potentially a higher percent reduction in concentration. However, within the relatively narrow range of HRTs of this campaign, nitrate removal rates (NRR) would be expected to be similar. Thus, treatment effects would be expected to be observed in NRR, which normalizes by mass removal per time (day).

Table 5. Hydraulic residence times for bioreactor treatments for the Fall 2016 and Spring and Fall 2017 campaigns.

Time Period	Exp (Bed 2)	Control	Bio Augmentation	Bio Stimulation
	----- (hr) -----			
Fall 2016	7.1 ± 0.1	9.3 ± 0.6	7.2 ± 0.9	7.6 ± 0.4
Spring 2017 10 May – 24 June	-	7.8 ± 0.3	8.3 ± 0.7	8.8 ± 0.6
Fall 2017 31 Oct – 4 Dec	-	7.7 ± 0.6	7.4 ± 1.7	8.6 ± 0.2

Water temperature during the fall 2016 campaign (18 October to 21 November) remained in a tight range, from 13.7 to 13.5°C (data not shown). The inlet supply tank water temperature for 2017 is shown in Fig. 8.

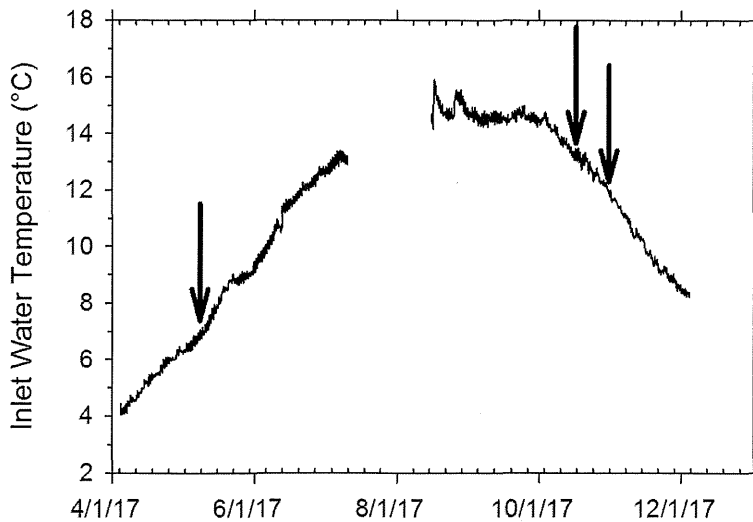


Fig. 8. 2017 hourly drainage water temperature during periods of flow. Arrows indicate inoculation dates.

4.2.2 Nitrogen

4.2.2.1 Nitrate concentration

Bioreactor inlet nitrate-N concentrations and treatment outlet average nitrate-N concentrations from automated daily sample collection for Fall 2016 are shown in Fig. 9. Neither bioaugmentation nor biostimulation resulted in reductions compared to the control. Over the period from 25 October through 7 November 2017, inlet concentration averaged 19.4 ± 0.6 mgN/L and the control, bioaugmentation, and biostimulation concentrations averaged 14.3 ± 0.4 , 14.9 ± 0.3 , and 14.9 ± 0.4 mgN/L, respectively. The average percentage concentration reductions were 26, 23, and 23%, for these respective treatments. The lack of effect for the bioaugmentation treatment may be related to the selection of the bacteria and/or the technique used during inoculation. In the laboratory, flow is typically halted during inoculation for one or two days. In the 2016 field inoculation, the microbes were poured into the inlets without change to the flow rate. Carbon addition to the biostimulation treatments was purposefully kept low (C:N of 0.15) to avoid bioclogging. The results suggest that the amount of C added was insufficient to noticeably improve denitrification. The learnings from the fall 2016 campaign informed changes for spring 2017.

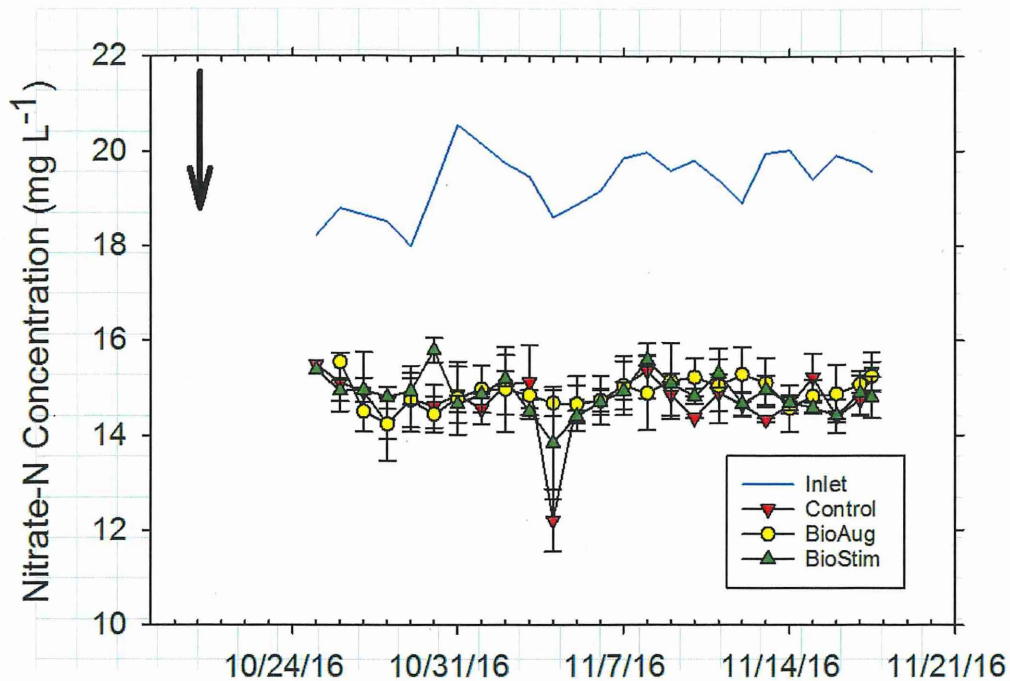


Fig. 9. Fall 2016 nitrate-N concentrations. Treatment data are averages; error bars denote standard errors ($n=2$). Data represent one-day time-based automated sampling concentrations. The arrow indicates the date at which inoculation occurred and biostimulation began.

The beds were operated under similar conditions from 21 April 2017 until treatments were applied on 8 May 2017 (Fig. 10). Outlet concentrations from the biostimulation beds dropped quickly and dramatically after introduction of acetate. However, approximately six weeks later, flow through the beds receiving acetate was restricted by extracellular polymeric substance (EPS) (Fig. 11). Acetate flow was cut off for two weeks to unclog the beds and then re-introduced in early July until drainage flow halted. Bioaugmentation appeared to have reduced nitrate-N concentrations with respect to the control treatment beginning 17 May for nine days. However, the effect was short-lived, suggesting that the microbial community reverted to its original state.

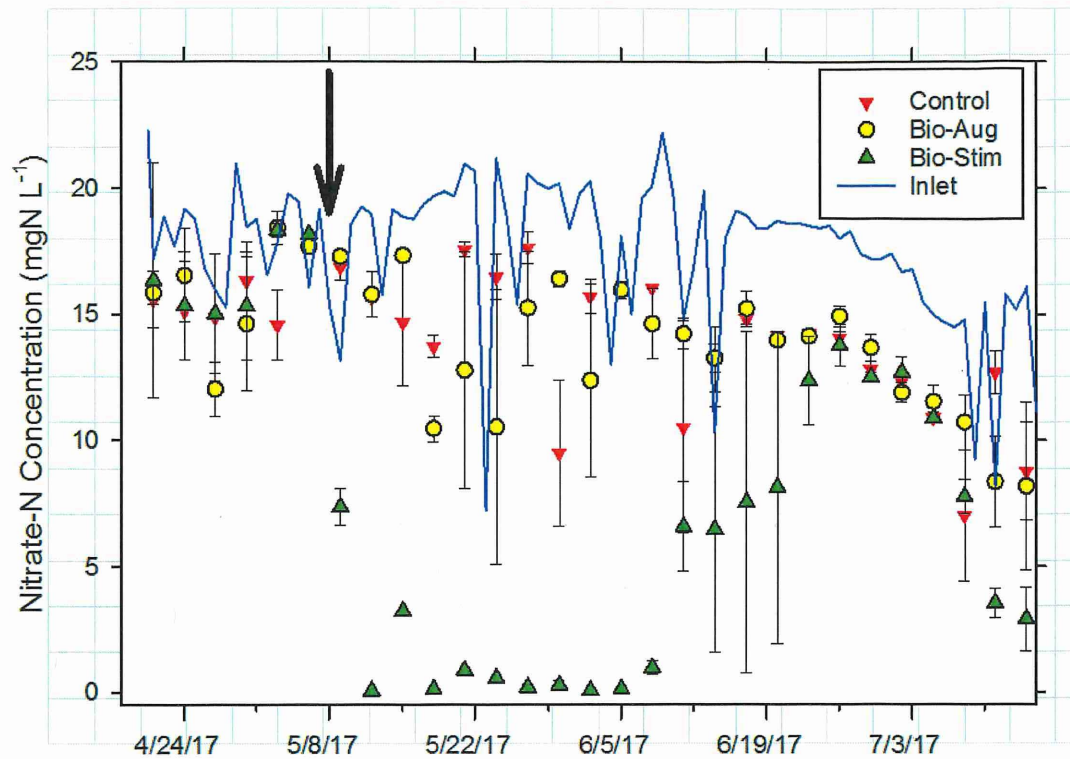


Fig. 10. Spring 2017 nitrate-N concentrations. Data represent three-day time-based automated sampling concentrations. Error bars denote standard error ($n=2$). The arrow indicates the date at which inoculation occurred and biostimulation began.

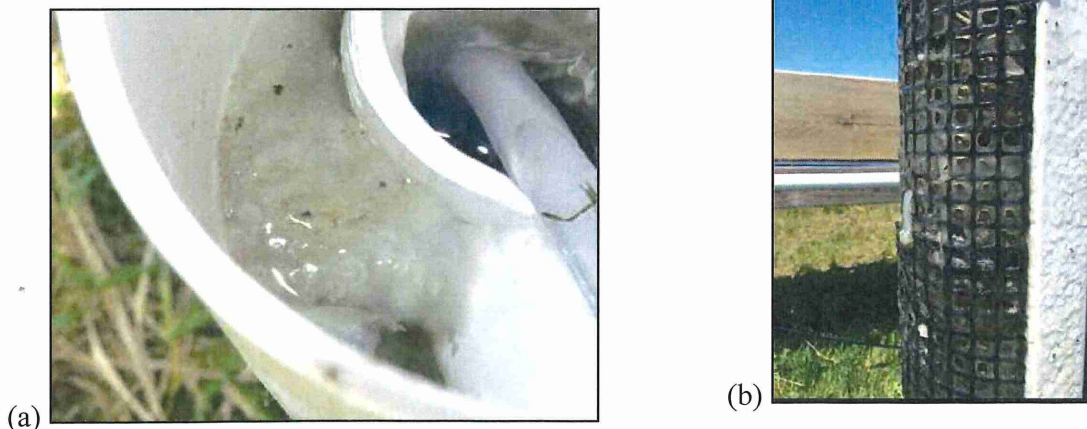


Fig. 11. Extracellular polymeric substance (EPS) formed after introduction of acetate causing blockage of flow; (a) in bed inlet pipe; (b) on port basket containing woodchip balls.

Drainage flow re-started in late August. Changes were made to the acetate delivery in an attempt to overcome bioclogging. The design C:N ratio was reduced from the Spring, 2.5:1, to 0.6:1. New pump heads were installed that reduced the acetate flow rate sufficiently to permit continuous pumping (The initial pumps were cycled on for 21 sec each five minutes). A control system was implemented that sensed a water level rise at the bed inlet and cut off acetate addition until the water level receded. In addition to the biostimulation changes, adjustments were made to the inoculation strategy. In an effort to improve the longevity of the inoculated bacteria, two inoculations were conducted two weeks apart, 17 and 31 October.

Reduction in nitrate-N concentrations was observed for a short time after inoculation of two microbial strains (Fig. 12). Bed flow rate, which was reduced in the bioaugmentation treatment beds to improve inoculation, was inadvertently left low for one week, creating artificially low concentrations indicated by the gray circle symbols in Fig. 12. Again, gains were temporary and bioaugmentation concentrations were slightly above the control until winter forced a shutdown of the system for the season. Although acetate addition was sporadic during the Fall campaign, the biostimulation treatment outlet concentrations were again less than those of the control treatment for several days. The system was shutdown for a few days at the end of October in order to winterize the equipment, which enabled operation through sub-freezing days in the first half of November.

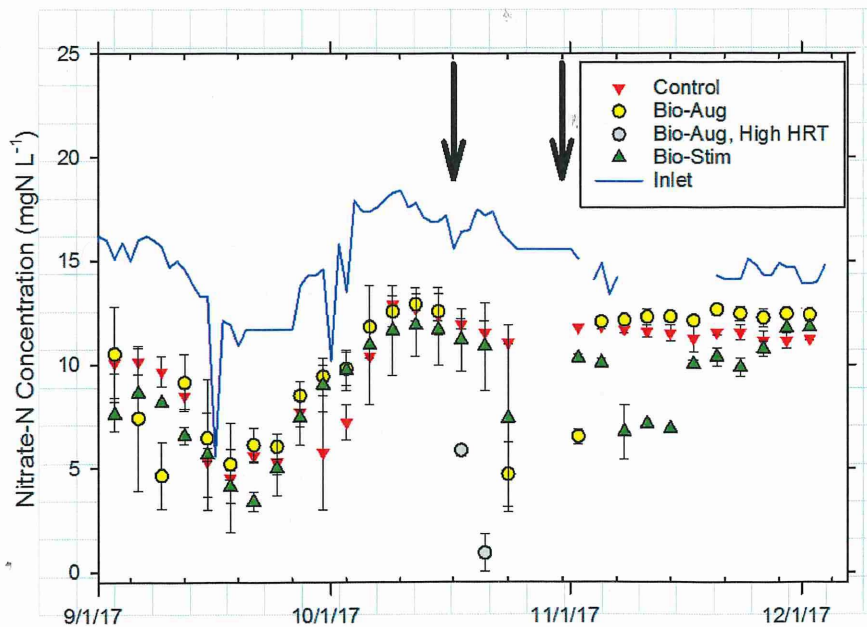


Fig. 12. Fall 2017 nitrate-N concentrations. Data represent three-day time-based automated sampling concentrations. Error bars denote standard error ($n=2$). The arrows indicate inoculation dates.

4.2.2.2 Nitrate loads and removal rates

Nitrate load reductions for spring and fall 2017 are given in Table 6. The biostimulation treatment removed nearly all available nitrate until bioclogging forced cut back in acetate additions. Although bioclogging continued to hamper progress in the fall 2017 campaign, the biostimulation treatment continued to show improvement over the control and bioaugmentation treatments.

Table 6. Nitrate removal as a percentage difference in the sum of nitrate-N mass into and out of each treatment for the time periods shown.

Time Period	Control	Bio Augmentation	Bio Stimulation
	----- (%) -----		
Spring 2017 10 May – 24 June	21	22	82
Fall 2017 31 Oct – 4 Dec	20	26	36

Nitrate removal rates were similar, $\approx 6 \text{ g N m}^{-3} \text{ d}^{-1}$, for the treatments for the fall 2016 campaign (Table 7). This is within the typical range reported for denitrifying woodchip bioreactors, 2 to 22 $\text{g N m}^{-3} \text{ d}^{-1}$ (Addy et al., 2016). Carbon additions to the biostimulation treatment were conservative (C:N = 0.15:1) which did not improve nitrate removal from a standard woodchip bed. Given the lack of improvement with the first inoculation, laboratory screening of denitrifiers continued and additional strains were used for the remaining campaigns.

For the spring 2017 campaign, nitrate removal rates for biostimulation were considerably greater than for control and bioaugmentation (Table 7, Fig. 13). Prior to problems with bioclogging, the nitrate removal rate for the biostimulation treatment approached $30 \text{ g N m}^{-3} \text{ d}^{-1}$, which was essentially an upper limit given that outlet nitrate concentration was near 0 (Fig. 10). During the end-of-May period, when bioaugmentation outlet nitrate-N concentrations were lower than for the control, nitrate removal rates for bioaugmentation were correspondingly greater than for the control (Fig. 13). However, as mentioned previously, this effect was short-lived and the average nitrate removal rates over the 7-week period for these two treatments were similar (Table 7).

Nitrate removal rates for the fall 2017 period are shown in Fig. 14. Subfreezing weather hampered automated sampling efforts, reducing the number of data points and causing gaps in the record. However, for a portion of the period, biostimulation nitrate removal rates were greater than the other two treatments. The initial elevated rate for biostimulation (1 November) may be influenced by the longer HRT purposely used during inoculation.

Table 7. Nitrate removal rates for bioreactor treatments for the Fall 2016 and Spring and Fall 2017 campaigns.

Time Period	Exp (Bed 2)	Control	Bio Augmentation	Bio Stimulation
	----- (g N m ⁻³ d ⁻¹) -----			
Fall 2016	7.1 ± 1.8	5.8 ± 0.9	6.5 ± 1.2	6.4 ± 1.1
Spring 2017 8 May – 24 June	-	5.2 ± 4.4	5.6 ± 3.9	17.1 ± 8.1
Fall 2017 31 Oct – 4 Dec	-	4.1 ± 0.7	5.5 ± 4.2	5.4 ± 2.2

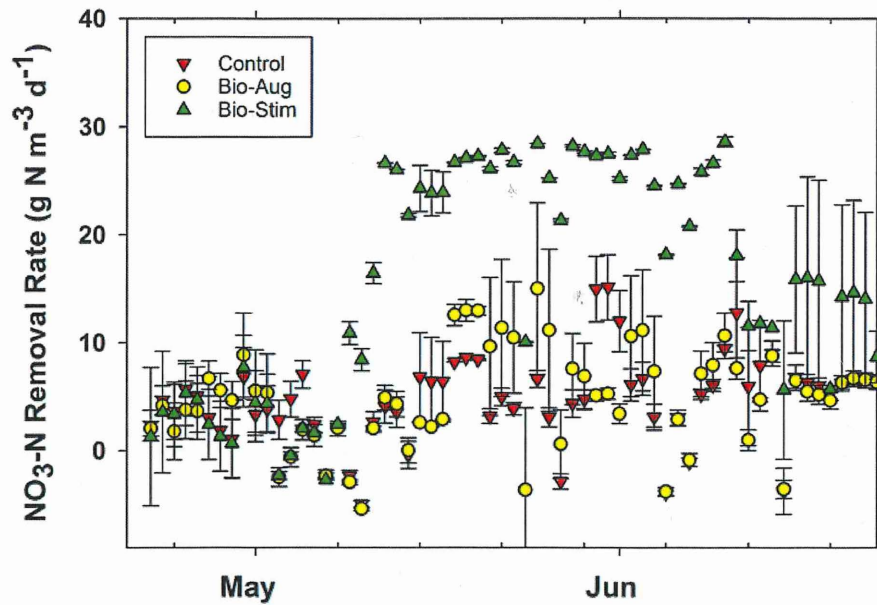


Fig. 13. Spring 2017 nitrate-N removal rates (NRR) based on automated sampling regime. Inoculation occurred and addition of acetate began on 8 May 2017. Error bars denote standard error ($n=2$).

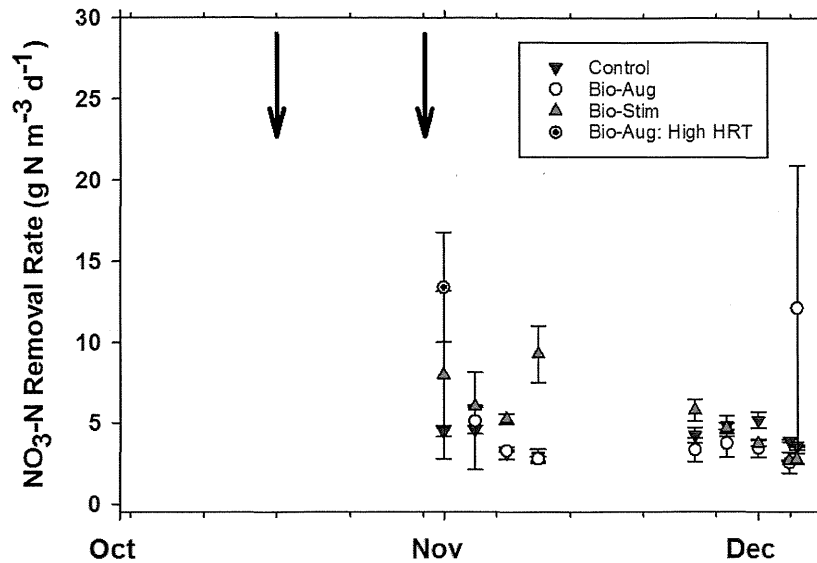


Fig. 14. Fall 2017 nitrate-N removal rates (NRR) based on automated sampling regime. Error bars denote standard error ($n=2$). The arrows indicate inoculation dates. Sampling was suspended between inoculation dates because of freezing weather.

4.2.2.4 Ammonium concentration

Inlet ammonium-N concentrations averaged 0.07 ± 0.10 and 0.13 ± 0.12 mg N/L for the spring and fall 2017 timeframes, respectively (Table 8, Fig. 15). Treatment ammonium-N concentrations were elevated with respect to the inlet over the same time periods. During the spring while acetate was being added, the treatment concentrations were generally ordered Bio-Aug > Control > Bio-Stim. When bioclogging prohibited acetate addition, the control treatment tended to have the lowest concentration. The greater ammonium-N concentrations of the bioaugmentation treatment appears to be related to the biological activity generated by microbial inoculation. The fall results were less distinct. Influent and effluent concentrations were similar with no clear trends among them. Generally, ammonium-N concentrations increased from spring to summer and decreased from late summer to late fall, suggesting a temperature relationship.

Table 8. Ammonium-N concentrations of inlet water and effluent from bioreactor treatments for the Spring and Fall 2017 campaigns.

Time Period	Inlet	Control	Bio Augmentation	Bio Stimulation
	----- (mg NH ₄ -N L ⁻¹) -----			
Spring 2017	0.07 ± 0.10	0.17 ± 0.10	0.20 ± 0.07	0.13 ± 0.08
Fall 2017	0.13 ± 0.12	0.16 ± 0.11	0.18 ± 0.15	0.17 ± 0.11

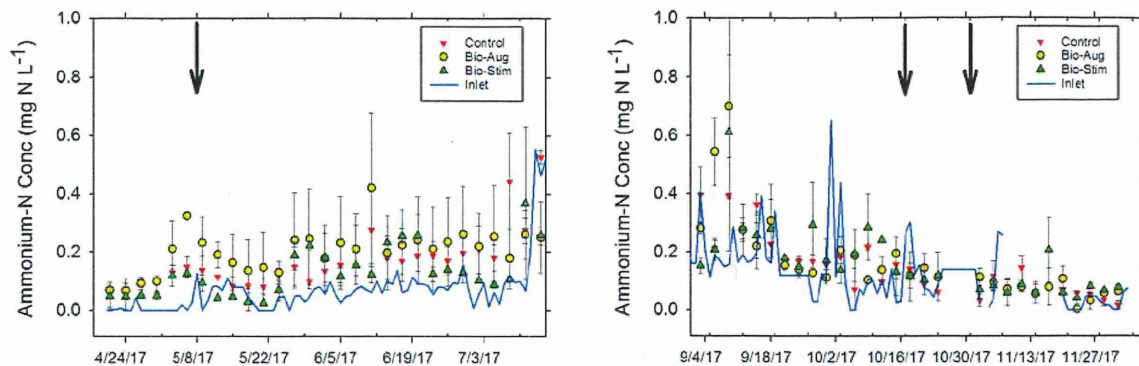


Fig. 15. Spring and fall 2017 ammonium-N concentrations. Data represent three-day time-based automated sampling concentrations. Error bars denote standard error (n=2). The arrows indicate inoculation dates.

4.2.3 Phosphorus

4.2.3.1 Total phosphorus concentration

Inlet TP concentrations averaged 0.084 ± 0.025 and 0.073 ± 0.023 mgP/L for the spring and fall 2017 timeframes, respectively (Table 9, Figs. 16 and 17). Treatment TP concentrations were well below the inlet over the same time periods. This represents average reductions of TP by all treatments of 62 and 57% for the spring and fall periods, respectively. As was the case with ammonium-N, there appears to be an increasing trend in the bioreactor outlet concentrations from spring to summer, but the trend is reversed from late summer to fall. The cause of P removal in the present study was not determined. Potential mechanisms are biological uptake and chemical sorption.

Table 9. Total P concentrations of inlet water and effluent from bioreactor treatments for the Spring and Fall 2017 campaigns.

Time Period	Inlet	Control	Bio Augmentation	Bio Stimulation
	----- (mg P L ⁻¹) -----			
Spring 2017	0.084 ± 0.025	0.035 ± 0.015	0.032 ± 0.009	0.026 ± 0.009
Fall 2017	0.073 ± 0.023	0.028 ± 0.010	0.039 ± 0.038	0.027 ± 0.012

Of note is the relatively low drainage TP concentration coming from the neighboring fields despite having been fertilized with poultry manure for many years (Ghane et al., 2016). The calcareous soil at the site complexes P from the soil solution and restricts movement of P to the subsurface drains. Also, these fields have no surface inlets; therefore, P-carrying sediment transport to the subsurface drains is limited. Others have noted that P can be released from woodchip bioreactors (David et al., 2016); however, to our knowledge no peer-review published research has shown a net P reduction in woodchip bioreactors. Current thinking is that any P storage within a bioreactor is subject to subsequent release, much like within a wetland. We have seen this behavior at the bioreactor near Blue Earth, Minnesota.

The Willmar beds are unique in that flow is controlled and constant. The supply tank acts as surge protection from sudden increases or decreases in flow rate associated with larger precipitation events. The automated sampling strategy used in the experiment should have detected any releases of P, which tend to be short-lived. We conclude that building storage prior to bioreactors so that an even flow rate may be maintained could have benefit in terms of net P removal from source waters.

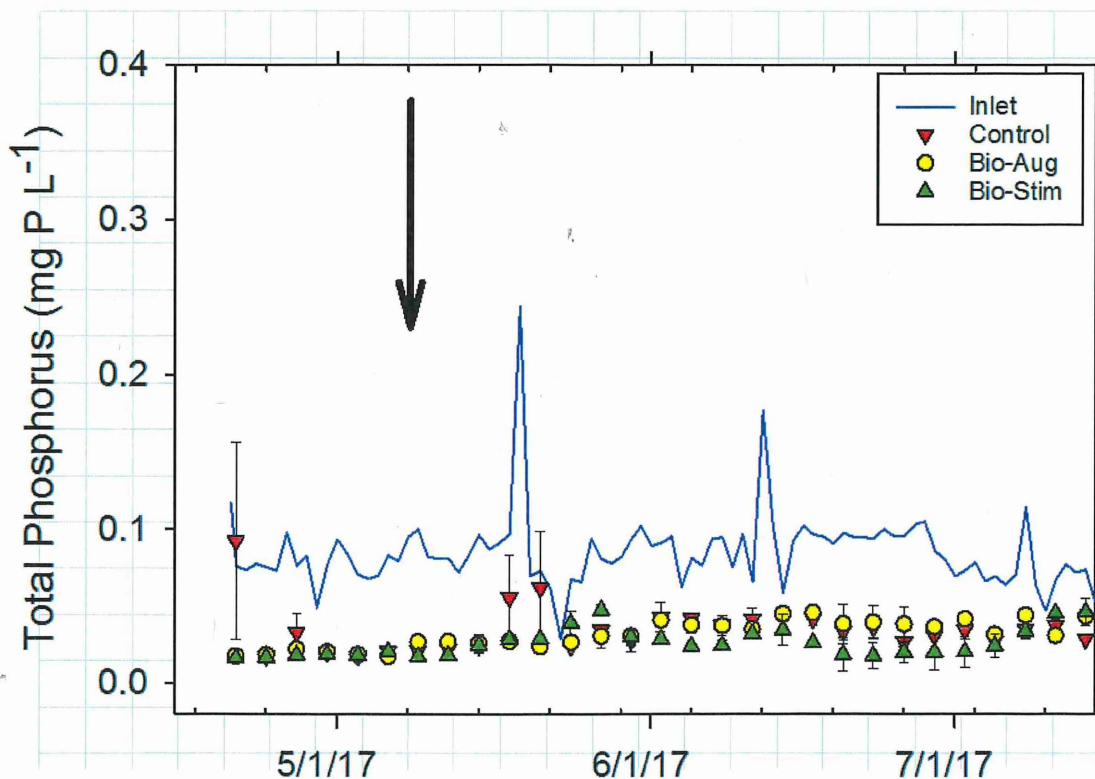


Fig. 16. Spring 2017 total P concentrations. Data represent three-day time-based automated sampling concentrations. Error bars denote standard error ($n=2$). The arrow indicates inoculation date.

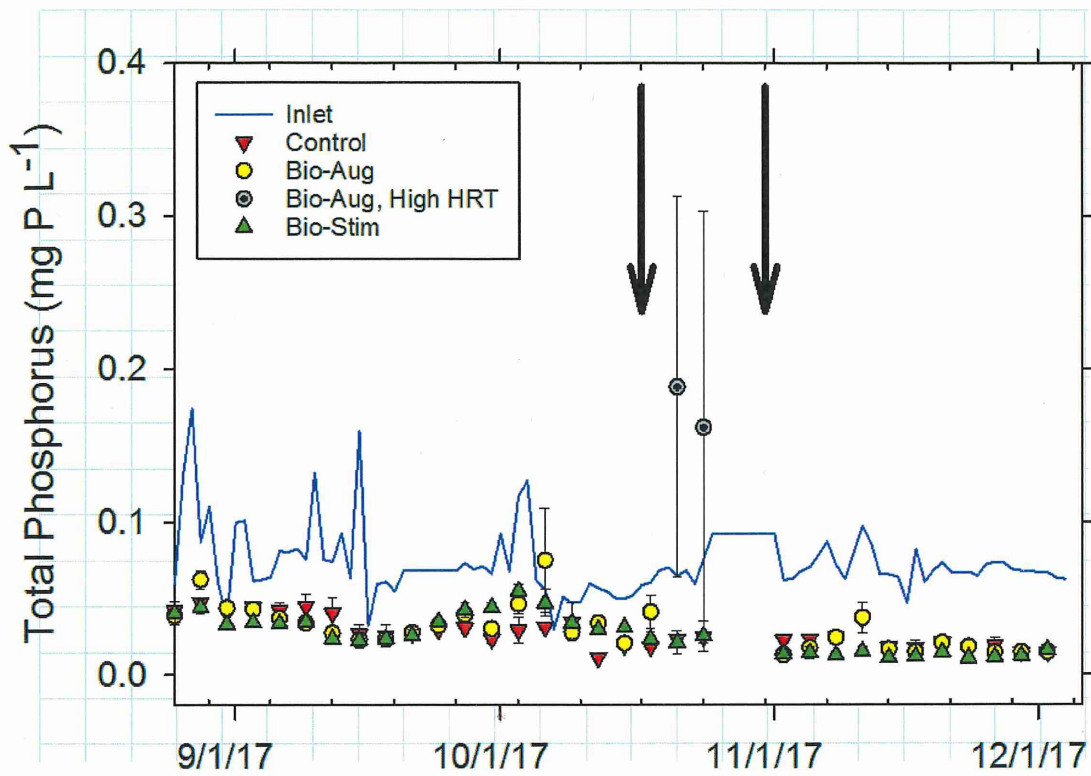


Fig. 17. Fall 2017 total P concentrations. Data represent three-day time-based automated sampling concentrations. Error bars denote standard error ($n=2$). The arrows indicate inoculation dates.

5.0 Education and Outreach Summary

We gave an oral presentation of our work on September 8th, 2016, at the International Drainage Symposium held in Minneapolis.

We conducted a field day on September 9th, 2016, in conjunction with the International Drainage Symposium. Participants (24) included attendees from the Netherlands, Finland, Germany, Sweden, and Denmark.

We presented a poster entitled “Nitrate removal from agricultural runoff using woodchip bioreactors” at the University of Minnesota Water Resources Center's Year of Water Action event “Shared Water, Shared Responsibility: Engaging Minnesota’s Communities, Students, & Policy-Makers” on March 23, 2017, in Minneapolis, MN. There were approximately 25 poster presentations and 70-80 participants in this event.

Emily Anderson,* Jeonghwan Jang, Ehsan Ghane, Gary Feyereisen, Carl Rosen, Mike Sadowsky, Satoshi Ishii. 2017. Nitrate removal from agricultural runoff using woodchip bioreactors. WRC's Year of Water Action –Shared Water, Shared Responsibility: Engaging Minnesota’s Communities, Students, & Policy-Makers, Minneapolis, MN. March 23, 2017.

Pioneer Public TV broadcast a documentary segment on the Willmar bioreactor project on April 9th, 2017. The segment can be accessed at: <http://www.pioneer.org/season-8.html> , PRSP8007, "Plunging through the ice to clear water," beginning at 20:35. MDA appears in the credits.

We included the project in an oral presentation to 65 people at the NCERA-217 “Drainage Design and Management Practices to Improve Water Quality” multi-state research coordinating committee’s annual meeting on March 29, 2017, in Champaign, IL. We presented a lightning talk “Optimizing denitrification beds to reduce N and P in subsurface drainage water” at the University of Minnesota Biotechnology Institute event with Barr Engineering held at Barr’s Bloomington, MN, facility on April 25, 2017. There were approximately 50 – 60 participants.

We held a field day on Friday, November 10, 2017. The information presented was well-received; however, unfortunately, due to cold weather attendance was limited to 13 brave souls.

Jeonghwan Jang, Emily Anderson,* Rodney T. Venterea, Satoshi Ishii. 2018. Cold-adapted denitrifiers in woodchip bioreactors. Water Resources Assembly and Research Symposium, St. Paul, MN. Jan. 19, 2018. (poster presentation)

On April 11, 2018, we gave an oral presentation to students, agency personnel and industry as part of a MnDRIVE Environment Symposium entitled "Optimizing Bioreactors to Reduce Nitrate Losses from Tile Drainage Water." There were approximately 50 people in attendance. Based on this presentation we have been invited to present it again at the MPCA in September, 2018.

Satoshi Ishii.* 2018. Identification and isolation of cold-adapted denitrifiers for bioremediation of nitrate in agricultural environments. MnDRIVE Environment Symposium. St. Paul, MN. April 11, 2018.

Jeonghwan Jang, Emily Anderson,* Rodney T. Venterea, Satoshi Ishii. 2018. Cold-adapted denitrifiers in woodchip bioreactors. ASM Microbe 2018 Meeting, Atlanta, GA. May 7-11, 2018. (poster presentation)

The following are a list of outreach events to the local public:

Bioreactors to Improve Water Quality, Minneapolis Midtown Farmers Market, July 30, 2016 (at Market Science booth)

Bioreactors to Improve Water Quality, Minnesota State Fair, Aug. 29, 2016 (at CFANS booth)

Bioreactors to Improve Water Quality, Minneapolis Northeast Open Streets, Aug. 6, 2017 (at Market Science booth)

Bioreactors to Improve Water Quality, Minnesota State Fair, Aug. 27, 2017 (at DNR stage)

We are also scheduled to give presentations based on our research at the following outreach scientific meetings:

- American Society of Agricultural and Biological Engineers, August 1, 2018
- Gorans Discovery Farm - Field day for AFREC board. August 16, 2018
- MN Water Resources Conference St. Paul, October 16, 2018
- American Society of Agronomy - Baltimore, November 6, 2018

6.0 References

- Addy, K., Gold, A. J., Christianson, L. E., David, M. B., Schipper, L. A., & Ratigan, N. A. (2016). Denitrifying bioreactors for nitrate removal: A meta-analysis. *J. Environ. Qual.* 45(3):873-881.
- Bednarek, A., Szklarek, S., Zalewski, M., 2014. Nitrogen pollution from areas of intensive farming—comparison of various denitrification biotechnologies. *Ecohydrol. Hydrobiol.* 14, 132–141.
- Brauer, N., Maynard, J.J., Dahlgren, R.A., O’Geen, A.T., 2015. Fate of nitrate in seepage from a restored wetland receiving agricultural tailwater. *Ecol. Eng.* 81, 207–217.
- Bru et al. 2011.
- Choudhury, T., Robertson, W.D., Finnigan, D.S., 2015. Suspended sediment and phosphorus removal in a woodchip filter system treating agricultural washwater. *J. Environ. Qual.* In Press.
- Chen, J., & Strous, M. (2013). Denitrification and aerobic respiration, hybrid electron transport chains and co-evolution. *Biochimica et Biophysica Acta - Bioenergetics*, 1827(2), 136–144. <https://doi.org/10.1016/j.bbabi.2012.10.002>
- Christianson, L.E., Bhandari, A., Helmers, M.J., 2012. A practice-oriented review of woodchip bioreactors for subsurface agricultural drainage. *Appl. Eng. Agric.* 28, 861–874.
- Christianson, L.E., Helmers, M.J., Bhandari, A., Moorman, T.B., 2013. Internal hydraulics of an agricultural drainage denitrification bioreactor. *Ecol. Eng.* 52, 298–307.
- Clesceri, L.S., A.E. Greenburg, and D.A. Eaton, editors. 1998. Standard methods for the examination of water and wastewater. 20th ed. Am. Public Health Assoc., Washington, DC.
- David, M.B., Gentry, L.E., Cooke, R.A., Herbstritt, S.M., 2015. Temperature and substrate control woodchip bioreactor performance in reducing tile nitrate loads in east-central Illinois. *J. Environ. Qual.* doi:10.2134/jeq2015.06.0296
- Feyereisen, G.W., Moorman, T.B., Christianson, L.E., Venterea, R.T., Coulter, J.A., Tschirner, U.W., 2016. Performance of Agricultural Residue Media in Laboratory Denitrifying Bioreactors at Low Temperatures. *J. Environ. Qual.* doi:10.2134/jeq2015.07.0407
- Ghane, E., G.W. Feyereisen, C.R. Rosen, and U.W. Tschirner. 2018. Carbon quality of four-year-old woodchips in a denitrification bed treating agricultural drainage water. *Trans. ASABE* 61(3):995-1000. doi.org/10.13031/trans.12642
- Ghane, E., Fausey, N.R., Brown, L.C., 2015. Modeling nitrate removal in a denitrification bed. *Water Res.* 71, 294–305.
- Heiskary, S.A., Lindon, M.J., Anderson, J., 2014. Summary of microcystin concentrations in Minnesota lakes. *Lake Reserv. Manage.* 30, 268–272.
- Huffman, R.L., D.D. Fangmeier, W.J. Elliot, S.R. Workman, and G.O. Schwab. 2013. Soil and water conservation engineering. American Society of Agricultural and Biological Engineers. St. Joseph. MI.
- Krause Camilo, B., 2016. Bioreactor reduces atrazine and nitrate in tile drain waters. *Ecol. Eng.*

86, 269–278.

- MPCA. 2014. The Minnesota nutrient reduction strategy. Minnesota Pollut. Control Agency. <https://www.pca.state.mn.us/sites/default/files/wq-s1-80.pdf> (accessed 27 July 2018).
- Mississippi River/Gulf of Mexico Watershed Nutrient Task Force. 2008. Gulf hypoxia action plan 2008 for reducing, mitigating, and controlling hypoxia in the Northern Gulf of Mexico and improving water quality in the Mississippi River Basin, Mississippi River/Gulf of Mexico Watershed Nutr. Task Force, Washington, DC.
- Patton and Kryskalla. 2003. USGS, Water Investigations Report 03-4174.
- Ranaivoson, A.Z., Moncrief, J.F., Venterea, R., Rice, P., Dittrich, P., 2012. Report: Anaerobic woodchip bioreactor for denitrification, herbicide dissipation, and greenhouse gas mitigation. Minnesota Department of Agriculture.
- Petersen et al. 2012.
- Roser, M.B., G.W. Feyereisen, K.A. Spokas, D.J. Mulla, J.S. Strock, and J. Gutknecht. 2018. Carbon dosing increases nitrate removal rates in denitrifying bioreactors at low-temperature high-flow conditions. *J. Environ. Qual.* 47(4): 856-864. doi:10.2134/jeq2018.02.0082
- Schipper, L.A., W.D. Robertson, A.J. Gold, D.B. Jaynes, and S.C. Cameron. 2010. Denitrifying bioreactors-an approach for reducing nitrate loads to receiving water. *Ecological Engineering.* 36, 1532–1543.
- Takaya, N., Catalan-sakairi, M. A. B., Sakaguchi, Y., Kato, I., Zhou, Z., & Shoun, H. (2003). Aerobic Denitrifying Bacteria That Produce Low Levels of Nitrous Oxide Aerobic Denitrifying Bacteria That Produce Low Levels of Nitrous Oxide. *Appl. Environ. Microbiol.*, 69(6), 3152–3157. <https://doi.org/10.1128/AEM.69.6.3152>
- Tiedje, J. (1994) Denitrifiers. In *Methods of Soil Analysis Part 2: Microbiological and Biochemical Properties*. Weaver R.R., Angel, S., Bottomley, P., Bezdiecek, D., Smith, S., Tabatabai, A., Wollum, A. et al. (eds) Madison, WI: Soil Science Society of America, pp. 245-267.
- USEPA., 2013. Reassessment 2013: Assessing progress made since 2008. Mississippi River Gulf of Mexico Watershed Nutrient Task Force. United States Environmental Protection Agency, Washington, DC, USA.
- Wang, P., Li, X., Xiang, M., & Zhai, Q. (2007). Characterization of Efficient Aerobic Denitrifiers Isolated from Two Different Sequencing Batch Reactors by 16S-rRNA Analysis. *Journal of Bioscience and Bioengineering*, 103(6), 563–567.
- Ward, A.D., Trimble, S.W., Burkhard, S.R., Lyon, J.G., 2016. *Environmental Hydrology*. CRC Press, Boca Raton, FL, USA.
- Warneke, S., Schipper, L.A., Bruesewitz, D.A., Baisden, W.T., 2011. A comparison of different approaches for measuring denitrification rates in a nitrate removing bioreactor. *Water Res.* 45, 4141–4151.

7.0 Peer-reviewed Publications Based on this Project

Abstracts for peer-reviewed publications based on this project follow. The first and second are in preparation for submission. The third is currently in the review process. The abstract for a fourth paper has been accepted to go through the review process for a special collection in the Journal of Environmental Quality on agricultural water quality under cold conditions. The contents of the first, second and third manuscripts are included in the Appendices.

7.1 *Efficacy of bromide tracers for evaluating the hydraulic performance of denitrification beds*

Authors: Ehsan Ghane^{a,*}, Gary W. Feyereisen^b, Carl J. Rosen^c

^a Department of Biosystems and Agricultural Engineering, Michigan State University, East Lansing, MI 48824, USA

^b Soil and Water Management Research Unit, USDA Agricultural Research Service, Saint Paul, MN 55108, USA

^c Department of Soil Water and Climate, University of Minnesota, Saint Paul, MN 55108, USA

Abstract:

One biotechnology that can reduce nitrate concentration in subsurface drainage water is called a denitrification bed. Bromide tracer testing is used to evaluate the internal hydraulics of these systems to be used in design and modeling, but efficacy of bromide tracers has not been investigated. The objectives of this study were to determine if bromide is a suitable tracer for woodchip media based on laboratory sorption experiments and based on field tracer tests. To achieve this goal, we conducted bromide sorption experiments in the laboratory and bromide tracer tests in seven denitrification beds near Willmar, Minnesota, USA. We did not find sorption (neither adsorption nor absorption) of bromide to woodchips in our laboratory sorption experiments. In contrast, bromide tracer tests showed an average bromide recovery of 82%, revealing that bromide was retarded in the woodchip denitrification beds. Thus, bromide did not meet the conservancy requirement of a tracer test. To the best of our knowledge, our experiment is the first study to estimate the in-situ effective porosity (average of 0.61) of a field-scale bed (i.e., with a non-point source inflow and outflow) using a tracer test. Also, a more accurate estimate of the actual hydraulic residence time (HRT) can be obtained by using the in-situ effective porosity rather than total porosity. In conclusion, our laboratory experiment did not show any sorption of bromide to woodchips, but in contrast and for unclear reasons, our field tracer testing showed bromide retardation.

7.2 Comparison of the denitrifying microbial communities between four woodchip bioreactors in Minnesota

Authors: Emily L. Anderson^{1,2}, et al.

¹BioTechnology Institute, University of Minnesota, St. Paul, MN

²Land and Atmospheric Sciences Graduate Program, Department of Soil, Water, and Climate, University of Minnesota, St. Paul, MN

Abstract:

Woodchip bioreactors are a feasible strategy to prevent nitrate in agricultural wastewater from reaching bodies of water and causing eutrophication. These systems rely on denitrification, a microbial respiration in which nitrate is reduced to dinitrogen gas. Under cold temperatures, bioreactor efficiency is low due to inhibited microbial activity. This study employed a culture-dependent approach to isolate and characterize low temperature-adapted denitrifying microorganisms from four different bioreactors in Minnesota with the purpose of selecting a cold-adapted denitrifier for use in bioaugmentation. A total of 207 bacteria were isolated from both submerged woodchips and from biofilms causing clogging in bioreactor pipes, 79 of which were able to reduce nitrate. Denitrification potential was determined based on nitrate-N reduction and conversion of nitrate-N to ammonium-N using segmented flow analysis, and N₂O production using gas chromatography. The denitrification rate of seven potential denitrifiers was measured using ¹⁵N-labelled nitrate. Two isolates, *Cellulomonas* isolate WB94 and *Microvirgula* isolate BE2.4, demonstrated promising nitrate reduction and a consistent denitrification rate. No potential denitrifiers were isolated from the biofilm samples and it is likely that these biofilms clogging woodchip bioreactors are composed mostly of microbes performing dissimilatory nitrate reduction to ammonium. Between the bioreactors, the composition of the isolated denitrifiers varied. *Microvirgula*, an aerobic denitrifier, made up the majority of the isolates from the newly established woodchip bioreactor, while *Clostridium*, an obligate anaerobe, made up the majority of the isolates from the woodchip bioreactor established four years prior to sampling, indicating that age may play a role in bioreactor denitrifier community.

7.3 Cold-Adapted Denitrifying Bacteria in Woodchip Bioreactors

Authors: Jeonghwan Jang¹, Emily L. Anderson², Rodney T. Venterea^{2,3}, Michael J. Sadowsky^{1,2}, Carl Rosen², Gary W. Feyereisen³, Satoshi Ishii^{1,2}

¹BioTechnology Institute, University of Minnesota, St. Paul, MN

²Department of Soil, Water, and Climate, University of Minnesota, St. Paul, MN

³USDA-ARS, Soil and Water Management Research Unit, St. Paul, MN

Abstract:

Woodchip bioreactor technology removes nitrate from agricultural subsurface drainage by using denitrifying microorganisms. Although woodchip bioreactors have demonstrated success in many field locations, low water temperature can significantly limit bioreactor efficiency and performance. To improve bioreactor performance, it is important to identify the microbes responsible for nitrate removal under low temperature conditions. Therefore, in this study, we identified and characterized low temperature-adapted denitrifiers by using culture-independent and -dependent approaches. By comparative 16S rRNA (gene) analysis and culture isolation technique, *Pseudomonas* spp., *Polaromonas* spp., and *Cellulomonas* spp. were identified as being important bacteria responsible for denitrification in woodchip bioreactor microcosms under low temperature conditions (15°C). Genome analysis of *Cellulomonas* sp. strain WB94 confirmed the presence of nitrite reductase gene *nirK*. Transcription levels of this *nirK* were significantly higher in the denitrifying microcosms than in the non-denitrifying microcosms. Strain WB94 was also capable of degrading cellulose and other complex polysaccharides. Taken together, our results suggest that *Cellulomonas* sp. denitrifiers could degrade woodchips to provide C source and electron donors to themselves and other denitrifiers in woodchip bioreactors. By inoculating these cold-adapted denitrifiers (i.e., bioaugmentation), it might be possible to increase the nitrate removal rate of woodchip bioreactors under cold temperature conditions.

7.4 Carbon supplementation and bioaugmentation to improve denitrifying woodchip bioreactor performance under cold conditions

Authors: Gary Feyereisen¹, Satoshi Ishii^{2,3}, Ping Wang^{2,3}, Emily Anderson^{2,3}, Jeonghwan Jang³, Ehsan Ghane⁴, Scott Schumacher³, Carl Rosen³, and Michael J. Sadowsky^{2,3}

¹ USDA-ARS Soil and Water Management Research Unit, 1991 Upper Buford Circle, 439 Borlaug Hall, St. Paul, MN 55108

² BioTechnology Institute, University of Minnesota, 140 Gortner Lab, 1479 Gortner Ave., St. Paul, MN 55108

³ Department of Soil, Water, and Climate, University of Minnesota, 1991 Upper Buford Circle, 439 Borlaug Hall, St. Paul, MN 55108

⁴ Department of Biosystems and Agricultural Engineering, Michigan State University, 524 S. Shaw Lane, 220 Farrall Hall, East Lansing, MI 48824

Abstract:

By-pass flow and cold temperatures limit nitrate load reductions of woodchip bioreactors in northern climates. A multi-year field study was conducted to improve bioreactor performance during cool, springtime temperatures by addition of cold-adapted bacterial denitrifier strains (bioaugmentation) or a readily available C source (biostimulation). These effects were

investigated at a replicated bioreactor site on a farm near Willmar, Minnesota. Results from 2017 showed that biostimulation dramatically reduced nitrate concentrations at the outlet, confirming earlier laboratory findings, but stimulated biofouling of the bed, which restricted flow. Nitrate removal corresponded to an increase in *nosZ* gene abundance for the biostimulation treatment. Bioaugmentation with two locally-isolated denitrifier bacterial strains introduced in 2017 was moderately successful for nitrate removal. Laboratory selection of improved denitrifier bacterial strains continued and another inoculation campaign is being conducted in spring/early summer 2018. The anticipated outcome of this research is a technology that substantially improves the nitrate removal effectiveness of woodchip bioreactors at low-temperatures and high-flow conditions.

Appendix A.

Efficacy of Bromide Tracers for Evaluating the Hydraulic Performance of Denitrification Beds

Research Paper; Ecological Engineering

Ehsán Ghane^{a,*}, Gary W. Feyereisen^b, Carl J. Rosen^b

^a Department of Biosystems and Agricultural Engineering, Michigan State University, East Lansing, MI 48824, USA

^b Department of Soil Water and Climate, University of Minnesota, Saint Paul, MN 55108, USA

^c Soil and Water Management Research Unit, USDA Agricultural Research Service, Saint Paul, MN 55108, USA

Corresponding author e-mail address: ghane@msu.edu

Abstract

One biotechnology that can reduce nitrate concentration in subsurface drainage water is called a denitrification bed. Bromide tracer testing is used to evaluate the internal hydraulics of these systems to be used in design and modeling, but efficacy of bromide tracers has not been investigated. The objectives of this study were to determine if bromide is a suitable tracer for woodchip media based on laboratory sorption experiments and based on field tracer tests. To achieve this goal, we conducted bromide sorption experiments in the laboratory and bromide tracer tests in seven denitrification beds near Willmar, Minnesota, USA. We did not find sorption (neither adsorption nor absorption) of bromide to woodchips in our laboratory sorption experiments. In contrast, bromide tracer tests showed an average bromide recovery of 82%, revealing that bromide was retarded in the woodchip denitrification beds. Thus, bromide did not meet the conservancy requirement of a tracer test. To the best of our knowledge, our experiment is the first study to estimate the in-situ effective porosity (average of 0.61) of a field-scale bed (i.e., with a non-point source inflow and outflow) using a tracer test. Also, a more accurate estimate of the actual HRT can be obtained by using the in-situ effective porosity rather than total porosity. In conclusion, our laboratory experiment did not show any sorption of bromide to woodchips, but in contrast and for unclear reasons, our field tracer testing showed bromide retardation.

Keywords: denitrifying bioreactor, hydraulic retention time, sodium chloride, tile drainage, woodchip bioreactor

1. Introduction

When elevated concentrations of nitrate flows into surface water, it can cause deleterious effects on the environment. While nitrate is transported via the pathway of subsurface drainage (Ghane et al., 2016b), a denitrification bed (also known as a woodchip bioreactor) can reduce nitrate concentration before it enters surface water (Bednarek et al., 2014; Schipper et al., 2010). In this system (hereafter referred to as bed), denitrification is the main mechanism for nitrate removal (Warneke et al., 2011) and woodchips are the most common media used. As this system is relatively new, there is a need to evaluate its internal hydraulics using tracer tests under field conditions, if we are to successfully design and model the flow through these beds. Tracer testing can also be used to determine the in-situ properties of woodchip beds that can be used in the design of these systems.

One important property of woodchip beds is the in-situ effective porosity, which is determined from tracer testing. Effective porosity is the interconnected (active) pore volume that contribute to transmitting water (Fetter, 2001; Sen, 2015), and it is used for estimating the actual hydraulic retention time (actual HRT) in design and modeling of beds (Kadlec and Wallace, 2009). However, we did not find any study that had estimated the in-situ effective porosity of a field-scale bed (with a non-point source inflow and outflow setting) using a tracer test. A non-point source inflow and outflow is the common design for beds treating drainage water in the Midwest USA, and it includes collector and distributor pipes that extend across the entire width of a bed. Therefore, a need exists to determine the in-situ effective porosity of typical beds using tracer tests.

Bromide is a common chemical for tracer testing of beds and column bioreactors with woodchip media, since it has long been assumed to be an inert chemical. Ghane et al. (2015) found retardation of bromide in a tracer test of a denitrification bed, but sorption of bromide to woodchips has not been shown in laboratory sorption experiments. Although bromide occurs at low natural concentrations, it should not be sorbed (i.e., neither adsorption nor absorption) by woodchips, and it should also be conserved to be a suitable tracer (Denbigh and Turner, 1984; Kadlec and Wallace, 2009; Levenspiel, 2012; Metcalf and Eddy, 2014). Therefore, verification of whether bromide is retained by woodchip media is needed using laboratory and field tracer testing.

A review of the literature shows that there is a need to assess the efficacy of bromide tracer in evaluating the hydraulic performance of denitrification beds. In this study, we compared the hydraulic performance of eight denitrification beds that will be used in an upcoming replicated experiment involving the enhancement of nitrate removal under cold temperatures. The objectives of this study were to (1) determine if bromide is a suitable tracer for woodchip media based on laboratory sorption experiments, (2) determine the suitability of bromide based on field tracer testing of denitrification beds (i.e., evaluating the hydraulic terms), and (3) determine the hydraulic performance of eight denitrification beds.

2. Materials and methods

2.1. Site description

In November 2010, a plastic-lined bed (106.4 m long and 1.49 to 1.86 m wide) was installed on a private farm near Willmar, Minnesota, USA (Ghane et al., 2017). In October 2014, we retrofitted that plastic-lined bed into eight smaller beds (Supplementary Video 1) (Fig. 1). During the retrofitting, woodchip media along the bed length were collected and combined to yield a composite sample (i.e., representing the entire bed) for laboratory sorption experiments (section 2.2.).

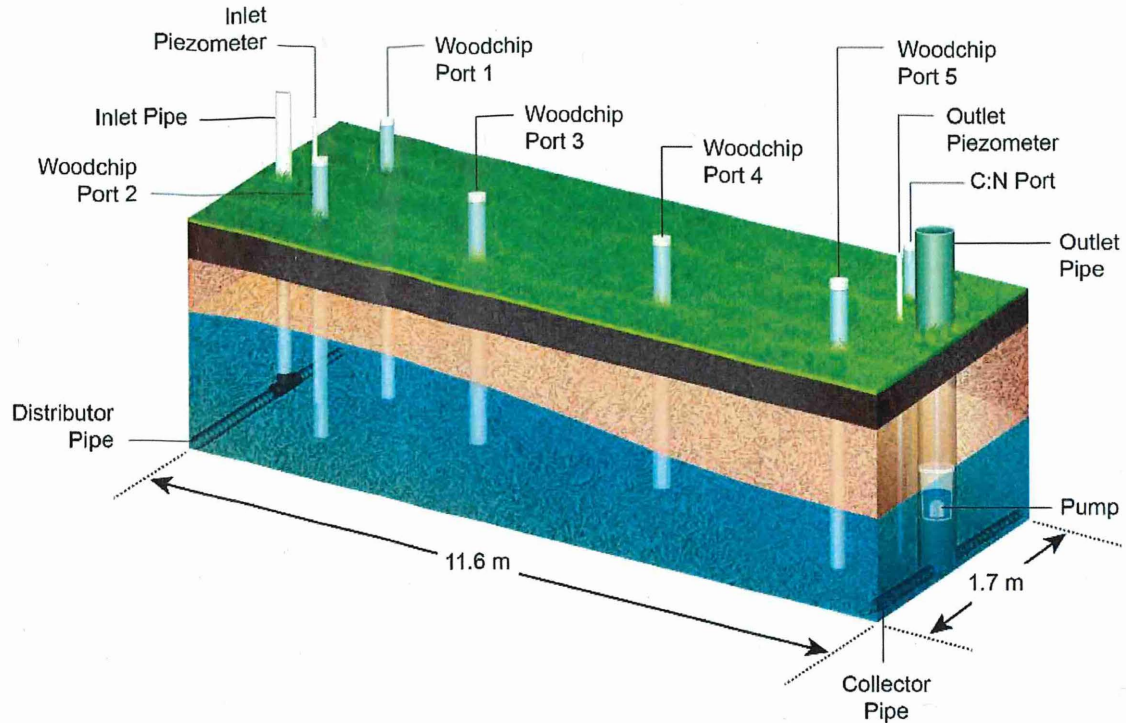


Fig. 1. Diagram of the denitrification beds near Willmar, Minnesota, USA. The dimensions shown are for bed 3.

Retrofitting the original bed resulted in eight plastic-lined beds with lengths ranging from 11.51 to 11.67 m, widths ranging from 1.49 to 1.86 m (Table 1), and they had a soil cover ranging from about 0.1 to 0.6 m. Each of the eight beds were separated from one another using a compacted soil berm with an average length of 1.83 m. Plastic sheets (13-mm thick) were inserted before and after the soil berms to prevent water movement between beds (Supplementary Image 1). All the vertical pipes were PVC, and were laid on the bottom of each bed except Woodchip Ports 3 and 4 (Fig. 1). Geotextile fabric was laid on top of the woodchips at the inlet and outlet ends of each bed (i.e., vicinity of Inlet and Outlet Pipe) to separate the woodchips from the soil, and the fabric was covered with soil up to the ground surface (Supplementary Image 2). A plan view of a bed can be found in Supplementary File 1.

Table 1

Summary of the denitrification beds dimensions located near Willmar, Minnesota, USA.

Bed Number	Bed length (m)	Mean bed width \pm SD (m)	Mean bed height (m)
1	11.51	1.58 \pm 0.098	0.72
2	11.61	1.49 \pm 0.106	0.96
3	11.67	1.70 \pm 0.092	0.96
4	11.66	1.86 \pm 0.117	1.01
5	11.67	1.63 \pm 0.109	1.05
6	11.58	1.80 \pm 0.110	1.00
7	11.58	1.62 \pm 0.112	1.07
8	11.61	1.67 \pm 0.085	1.01

Subsurface drainage water flowed into a sump from which the water was pumped into an 11,355-L tank ([Supplementary Image 3](#)). Excess drainage water above the capacity of the tank was pumped into an adjacent wetland. The water head in the tank forced gravity flow of water through a manifold for distributing water to each bed. From the manifold, water flowed through a globe valve, which was used to adjust the flow rate of each bed. A paddlewheel flow sensor (model FP-5300, Omega, Stamford, Connecticut, USA) was used to measure the inflow rate of each bed ([Supplementary Image 4](#)).

Following the paddlewheel, water was conveyed via a pipe (40-mm diameter PVC) to the inlet pipe (100-mm diameter PVC) of each bed ([Supplementary Image 5](#)). From the inlet pipe, water entered the bed via a distributor pipe, and then was collected inside the outlet pipe (350-mm diameter PVC) via a collector pipe. The collector and distributor pipes were placed at the bottom of the beds and were made of corrugated plastic tubing while extending across the entire width of each bed. Water inside the outlet pipe was collected inside a bucket, from which it was pumped (Model 2VAN7, Dayton Electronics Manufacturing Co., Niles, Illinois, USA) through a

paddlewheel flow sensor to measure the outflow rate of each bed. After the paddlewheel, water was transported to an adjacent wetland via a PVC pipe (40 mm diameter).

The Inlet and Outlet Piezometers (50-mm diameter PVC) were used to measure the height of water at the inlet and outlet of each bed, respectively (Fig. 1). Water heights were measured using a meter stick and water finding paste (Kolor Kut Products, Houston, Texas). We used the water heights to calculate the saturated volume (V_s) of each bed.

2.2. Laboratory sorption experiments

To verify if bromide is a suitable tracer for woodchip media, two bromide sorption processes were investigated, adsorption and absorption. Adsorption by formation of a bond between bromide and C of the organic compounds of wood, and absorption when bromide diffuses into the interior pores of woodchips (physical entrapment) (Strawn et al., 2015). To investigate these two processes, we conducted three laboratory sorption experiments. The first sorption experiment was conducted on ground old woodchips (unwashed) to evaluate adsorption on November 4, 2016. The second and third experiments were conducted on unwashed and washed old woodchips, respectively, to evaluate the combined effect of absorption and adsorption on December 12, 2016.

2.2.1. Experiment 1 (ground woodchips)

For sorption experiment 1, we mixed the air-dried composite woodchips (that had fine wood and sediments) in a tray and took a representative sample for grinding (Wiley Mill, Standard Model 3, Thomas Scientific, Swedesboro, New Jersey, USA). Then, the wood particles were further ground using another grinder to obtain particles size of <1 mm (Supplementary Image 6). We poured a known mass of the ground woodchips into seven 500-ml bottles (i.e., six test bottles plus one control).

We then prepared varying initial bromide concentrations by measuring six different quantities of potassium bromide (KBr) in cups and emptying the KBr granulates from the measuring cups into 1000-ml bottles. The measuring cups were rinsed with deionized water into the 1000-ml bottles to capture the entire KBr. Then, we added agricultural drainage water (collected from the site described in section 2.1) to the 1000-ml bottles. After shaking the 1000-ml bottles for 5 min, we took water samples from it to analyze for the initial bromide concentration.

The sorption experiment was initiated by pouring the seven bromide solutions from the 1000-ml bottles into the six 500-ml bottles containing woodchips and one 500 ml bottle without wood chips which served as a control. Subsequently, we measured the mass of water in the 500-ml bottles and then placed them on a reciprocal shaker (Model E6005, Eberbach Corp. Ann Arbor, MI, USA) to shake for 5 h at room temperature. After the shaking process, the solutions were poured in centrifuge tubes (SARSTEDT, Nümbrecht, Germany) and were centrifuged at 15°C and 5,000 rpm for 5 min. Following the centrifugation, we collected the filtered solutions using a

0.45- μm sterile syringe filter (VWR, Radnor, Pennsylvania, USA). Filtered solutions were kept in a cooler at 4°C until analysis for equilibrium bromide concentration.

2.2.2. Experiments 2 and 3 (woodchips)

For the second sorption experiment, we poured a known mass of the air-dried composite old woodchips (that had fine wood and sediments) into seven 500-ml bottles (i.e., six test bottles plus one control) ([Supplementary Image 7](#)). We then prepared six initial bromide concentrations in 1000 ml bottles (i.e., independent from experiment 1) using the procedure described in [section 2.2.1](#). After shaking the 1000-ml bottles for 5 min, we took water samples to analyze for the initial bromide concentration. Then, we added agricultural drainage water (i.e., from a drainage system near Blue Earth, MN) to the 1000-ml bottles. Subsequently, the sorption experiment was initiated and the 500-ml bottles were shaken for 1 h, and the samples were centrifuged and filtered as described in [section 2.2.1](#) to obtain the filtered solutions. Filtered solutions were kept in a cooler at 4°C until analysis for equilibrium bromide concentration.

We conducted the third experiment simultaneously with the second experiment using the same initial bromide solutions with the only difference that the old composite woodchips were washed with drainage water to remove sediments and fine wood particles. The washed composite woodchips were then air dried for the third experiment ([Supplementary Image 8](#)).

2.2.3. Sorption calculation

The amount of bromide retained by woodchips, x , (mg kg^{-1}) is calculated as

$$x = (C_i - C_e) \frac{V_w}{m_{wc}} \quad (1)$$

where C_i and C_e is the concentration in the initial and equilibrium solutions (mg L^{-1}), respectively, V_w is the volume of water (L), and m_{wc} is the mass of air-dried ground-woodchips or woodchips (kg) (Strawn et al., 2015).

2.2.4. Water analysis for sorption experiments

To determine the initial bromide and filtered-solution concentrations, the solutions were analyzed for bromide within 11 days by colorimetry (Lachat QuikChem 8500 Flow Injection Analysis, Hack Co., Loveland, CO, USA) based on the QuikChem method 10-135-21-2-B. We made standard bromide concentrations using the yellow-colored drainage water that had been in contact with woodchips to check the concentration results. After checking the results, we found that the yellow color of the filtered solutions interfered with the measurements ([Supplementary Image 9](#)), and caused the colorimetry method to underestimate the bromide concentrations. Consequently, we used ion chromatography to determine the bromide concentrations.

Initial bromide solutions and filtered solutions were analyzed for bromide within 44 days using ion chromatography (Thermo Scientific, Dionex Integrion HPIC, San Jose, CA, USA). The ion chromatography instrument was able to measure up to 100 mg L⁻¹ of bromide based on standard calibration, so our samples did not need dilution as they were below 100 mg L⁻¹. Finally, we measured the pH of the initial bromide and equilibrium solutions for all three sorption experiments using a benchtop meter (Model SB90M5, VWR sympHony, Radnor, PA, USA).

For the sorption experiments, bottles without bromide addition (i.e., control) were used to determine the background concentration of bromide in the wood. Sampling the control bottles after shaking showed that the natural background concentrations of bromide in the wood were undetectable (Table 2). To our knowledge, our study is the first to report on the adsorption and absorption processes pertaining to the suitability of bromide as a tracer for woodchip medium.

2.3. Bromide tracer field test

We dissolved 400 g of potassium bromide (265.9 g of Br⁻) in about 10 L of water, and poured the solution into the inlet pipe of each bed in less than 30 seconds. Subsequently, samples were collected from the outlet pipe of each bed using two auto-samplers (6700 series Teledyne ISCO, Lincoln, Nebraska, USA) beginning with 10 min intervals during the rise of the hydrograph, 5 min at the peak, and increased to 10 and 30 min during the fall of the hydrograph. Flow rate was adjusted using a globe valve, and was kept relatively constant by maintaining a constant water level in the tank. A measured porosity of 0.85 for old woodchips from Ghane et al. (2014) was used to calculate the theoretical (nominal) retention time. Bed number 1 was found to have a major leak that resulted in considerable loss of inflow, so we did not conduct a tracer test for this bed.

Water samples from the tracer tests were kept in a cooler at 4°C until analyzed for bromide within 6 weeks by colorimetry (Lachat QuikChem 8500 Flow Injection Analysis, Hack Co., Loveland, CO, USA) based on the QuikChem method 10-135-21-2-B. As we had clear water samples (i.e., no yellow-colored water), we did not encounter interferences with the bromide measurements.

2.4. Hydraulic terms

2.4.1. Mean tracer residence time

The mean tracer residence time (actual HRT in hours) is the first moment of the residence time distribution (RTD) curve (i.e., centroid of the area under RTD curve). At steady-state flow, the mean tracer residence time (\bar{t}) is estimated as

$$\bar{t} \approx \frac{\sum t_i C_i \Delta t_i}{\sum C_i \Delta t_i} \quad (2)$$

where t_i is the time (h) at the i th sample, C_i is the outlet bromide concentration (mg L^{-1}), and Δt_i is the time interval (h) between sampling (Metcalf and Eddy, 2014).

2.4.2. Tracer recovery

The percent bromide recovery was calculated as the ratio of the mass of bromide recovered at the outlet (M_{out}) to the mass of bromide injected into the inlet of the bed (M_{in}). The mass of bromide recovered (in milligrams) is the zeroth moment of the RTD curve, and it is estimated as

$$M_{\text{out}} \approx \sum 60Q_i C_i \Delta t_i \quad (3)$$

where Q_i is the outflow rate at the i th sample (L min^{-1}), C_i is the outlet bromide concentration (mg L^{-1}), and Δt_i is the time interval (h) between sampling (Kadlec and Wallace, 2009).

2.4.4. Theoretical hydraulic retention time

For water flow through porous media (e.g., denitrification beds), the nominal (theoretical) retention time (in hours) is calculated as

$$t_n = \frac{V_s n}{60Q_{\text{ave}}} \quad (4)$$

where V_s is the saturated volume of the bed (L), n is porosity (a.k.a. total porosity) of the media, and Q_{ave} is approximated as the average of the inflow and outflow rates of the bed (L min^{-1}). The approximation of Q_{ave} is good at a 4% accuracy, if the water recovery fraction ($R = \text{outflow/inflow}$) is $0.5 < R < 2.0$ (Kadlec and Wallace, 2009). When variation in flow rate from the inflow to outflow is negligible (i.e., under minimal leaks), the outflow rate can be used in the calculation of t_n . We also calculated t_n based on the outflow rate so that it may be compared with those studies that used the outflow rate (Supplementary File 2). Porosity (n) is the ratio of void volume to total volume of woodchips that is equal to the sum of specific yield (drainable porosity) and specific retention (internal porosity) (Sen, 2015; Ward et al., 2016).

To compare various tracer tests from the same denitrification bed or between different beds, we used the plot of temporally normalized RTD versus normalized time (Metcalf and Eddy, 2014). The normalized time (θ) is calculated as the ratio of t_i over the theoretical hydraulic retention time (t_n), and the normalized RTD at the i th sample and at steady-state is calculated as

$$E(\theta) = \frac{60Q_{\text{ave}} C_i}{M_{\text{out}}} \times t_n \quad (5)$$

where M_{out} is the total mass of bromide recovered (mg) (Eq. (3)), and t_n is the nominal (theoretical) hydraulic retention time (h) (Eq. (6)).

2.4.3. Volumetric efficiency

Thackston et al. (1987) defined volumetric efficiency (e_v) as

$$e_v = \frac{\bar{t}}{t_n} \quad (6)$$

A volumetric efficiency of 1 indicates full use of the reactor total pore volume, a value less than 1.0 indicates the flow distribution is not uniform (i.e., due to dead zones), and a value greater than 1 indicates physical/chemical retardation (Kadlec and Wallace, 2009). The volumetric efficiency can be used to correct the theoretical hydraulic retention time to yield the actual hydraulic retention time (AHRT) as

$$\text{AHRT} = e_v \times t_n \quad (7)$$

2.4.5. In-situ effective porosity

After calculating the mean tracer residence time (\bar{t}) from the tracer tests, the in-situ effective porosity of the beds is estimated as

$$n_e = \frac{60Q_{ave} \bar{t}}{V_s} \quad (8)$$

2.4.6. Actual hydraulic retention time

The AHRT is appropriate for design and modeling of denitrification beds, since it provides the actual time it takes for water to travel in the media. By combining Eqs. (5) and (6), we can calculate the actual hydraulic retention time as

$$\text{AHRT} = e_v \times \frac{V_s n}{60Q_{ave}} \quad (9)$$

By substituting $n_e = n \times e_v$ in Eq. (9), the above equation shrinks to

$$\text{AHRT} = \frac{V_s n_e}{Q_{ave}} \quad (9)$$

where n_e is the in-situ effective porosity of the woodchip media. Therefore, if we have the effective porosity of a denitrification bed, we can calculate its AHRT.

2.4.7. Morrill dispersion index

The Morrill Dispersion Index (MDI) is an indicator of mixing, which is written as

$$\text{MDI} = \frac{t_{90}}{t_{10}} \quad (10)$$

where t_{10} and t_{90} are the times at which 10% and 90% of the tracer is recovered (Metcalf and Eddy, 2014). An MDI of 1.0 indicates ideal plug-flow reactor, and when $1.0 < \text{MDI} \leq 2.0$ is considered an effective plug-flow reactor, and MDI of 22.0 is indicative of a complete-mix bioreactor.

3. Results and discussion

3.1. Laboratory bromide sorption experiments

In a typical sorption experiment, the solid to solution ratio ranges from 0.005 to 0.5 to allow for uniform mixing of the suspension (Strawn et al., 2015). Thus, we conducted sorption experiment 1 such that the ground wood to water ratio ranged from 0.17 to 0.18 g ml⁻¹ (Table 2). For sorption experiments 2 and 3, the wood to solution ratio (i.e., 0.32-0.35 g ml⁻¹) was selected to represent the wood and water matrix in a denitrification bed under field conditions as closely as possible (Table 2).

Measurements of pH for sorption experiments 1, 2, and 3 (Supplementary File 3) show that the pH of the equilibrium solutions (i.e., ranging from 6.8 to 7.1) was close to the range of 6.7 to 7.1 reported for bed outflows treating drainage water and greenhouse effluent (Ghane et al., 2015; Warneke et al., 2011). This range is within the optimum range of 6.0 to 8.0 for denitrifying organisms (Pierzynski et al., 2005).

3.1.1. Bromide sorption experiment 1 (ground woodchips)

The purpose of experiment 1 was to evaluate adsorption, which is the formation of a bond between bromide and C of the organic compounds of wood (Strawn et al., 2015). Bromide has been reported to not adsorb (i.e., by electrostatic attraction) to clay minerals in temperate regions due to the mineral's negative surface charge (Gilley et al., 1990; Korom, 2000; Levy and Chambers, 1987), but more recently, it has been shown that bromide adsorbs to temperate soils at a pH below 7 (Goldberg and Kabengi, 2010). Furthermore, bromide can become oxidized and form a bond with C during bromination (i.e., transformation from inorganic to organic) and this form has been found to be reactive with organic matter (Leri and Ravel, 2015). Woodchips have lignin, an aromatic compound that is a good substrate for bromination reactions (Leri and Ravel, 2015). Furthermore, fresh plant materials (e.g., woodchips) are more vulnerable to bromination than decomposed organic material (e.g., humus) due to the presence of a labile (or fast) pool of organic compounds (Leri and Ravel, 2015).

Having explained the potential for bromination in experiment 1, Table 2 and Fig. 2 show that the concentration of bromide did not reduce after being in contact with ground woodchips. Based on experiment 1, we found no clear trend of adsorption of bromide to ground woodchips (Table 3). Nonetheless, we suggest investigating the presence of organobromine in ground woodchips that

have been in contact with bromide in case our sorption experiment was unable to detect any bromide concentration difference (Leri and Ravel, 2015).

Table 2

Summary of the bromide sorption experiments 1, 2, and 3.

Sample number	Experiment 1 (ground woodchips)		Experiment 2 (woodchips)		Experiment 3 (washed woodchips)	
	Wood to solution ratio (g ml ⁻¹)	Bromide retained by ground wood, x (mg kg ⁻¹)	Wood to solution ratio (g ml ⁻¹)	Bromide retained by woodchips, x (mg kg ⁻¹)	Wood to solution ratio (g ml ⁻¹)	Bromide retained by woodchips, x (mg kg ⁻¹)
1	0.18	0.3	0.32	2.2	0.34	-1.2
2	0.18	1.6	0.33	3.3	0.35	-3.1
3	0.18	2.3	0.33	0.9	0.35	-6.7
4	0.18	-2.8	0.33	-2.8	0.35	-7.5
5	0.18	5.7	0.32	-3.4	0.34	-7.3
6	0.17	2.3	0.32	-4.7	0.35	-10.1
Control	0.18	0.0	0.32	0.0	0.35	0.0

3.1.2. Bromide Sorption Experiments 2 and 3 (woodchips)

The purpose of experiments 2 and 3 was to evaluate the combined effect of adsorption and absorption. Since experiment 1 showed that adsorption was not present ([section 3.1.1.](#)), the primary purpose of experiments 2 and 3 was to evaluate absorption, which occurs when bromide diffuses into the interior pores of woodchips (physical entrapment) (Strawn et al., 2015). Based on experiments 2 and 3, we did not find any clear trend of bromide absorption to woodchips ([Table 2](#)), which is opposite of what we expected due to the porous property of woodchips. Nevertheless, we recommend others to investigate sorption of bromide to woodchips as it could be a reason for low bromide recovery.

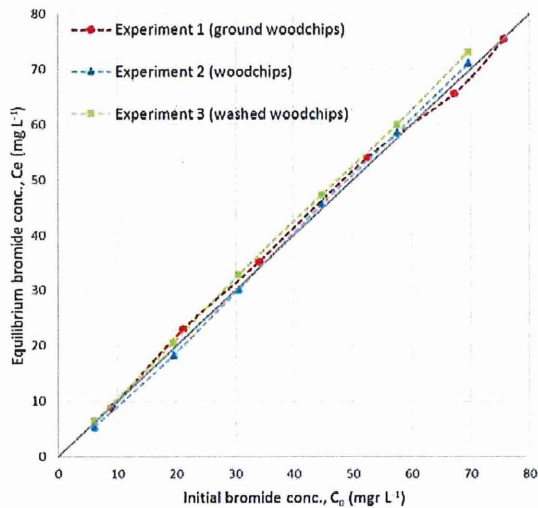


Fig. 2. The relationship between the initial and equilibrium bromide concentration for sorption experiments 1 (ground woodchips), 2 (woodchips), and 3 (washed woodchips). The solid gray line is the 1:1 line.

3.2. Bromide tracer testing of denitrification beds

3.2.1. Tracer residence time distribution curve

Our temporally normalized RTD curves show that the peak concentrations have been included in the sampling due to the presence of a short plateau, consisting of two or more points with similar concentrations that are close in time, as opposed to a sharp peak where the peak concentration may have been missed (Fig. 3). This will be important in calculating the hydraulic term that relies on the time of the peak. Furthermore, the variable water sampling (section 2.3.) at the bed outlets provided a high-resolution curve for more accurate evaluations. The plot of bromide concentration versus time can be found in [Supplementary File 4](#).

The comparison of the temporally normalized RTD curves shows that the hydraulic behavior of the bromide tracer was very similar for beds 4, 5, 6, and 8, whereas the hydraulic behavior for beds 3 and 7 slightly varied from the other beds (Fig. 3). However, bed 2 showed a very different pattern than all other beds. The general similarity of the curves for beds 3 to 8 can be explained by their similar dimension (Table 1) as well as their similar d_{50} (i.e., diameter at which 50% of particles are finer) according to the companion study of Ghane et al. (2018). These minor variations can be explained by minor differences in dimension (Table 1) and bottom elevation ([Supplementary File 5](#)). For Bed 2, the bell-shaped pattern is not a typical response curve that one would expect from a tracer test. More investigation is needed to determine the reason for the anomaly of the normalized RTD curve of bed 2.

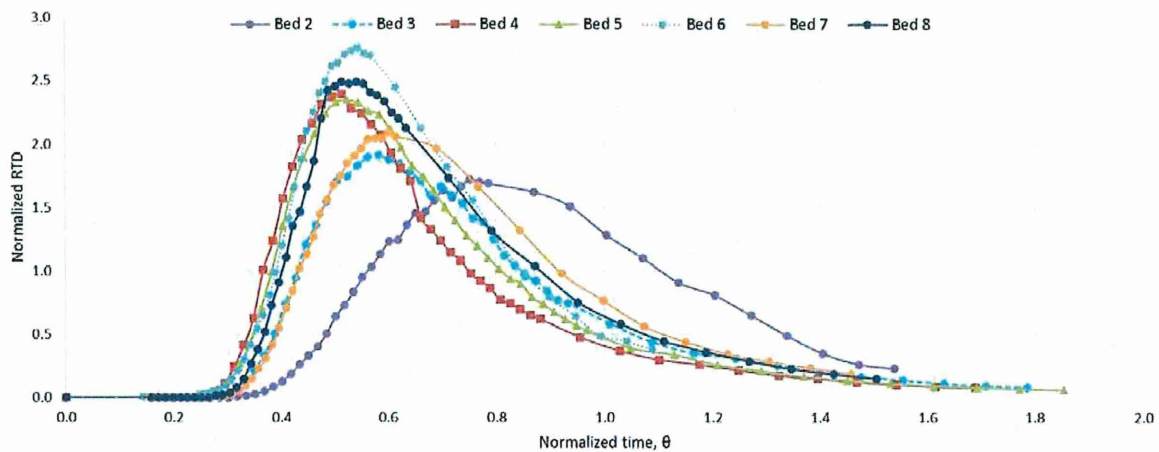


Fig. 3. Temporally normalized residence time distribution (RTD) curve for the bromide tracer tests.

3.2.2. Bromide recovery

Tracer recovery near 100% is important for validating the conservancy of the tracer used (Kadlec and Wallace, 2009; Metcalf and Eddy, 2014). In general, since denitrification beds are commonly installed with a plastic liner and they have non-point source inflow and outflow (section 3.3.), we expect recovery of an inert tracer near 100%. In our tracer experiments, we calculated a wide range of bromide mass recovery from 76.4% to 95.8% with an average of 82% \pm 13.3% (Table 3).

The average bromide recovery of 82% reveals that approximately 18% of the bromide was retarded in the woodchip bed. In contrast, we did not find sorption of bromide to woodchips in our laboratory sorption experiments (section 3.1). Perhaps other processes under field conditions are responsible for the retardation of bromide in the woodchip beds that we could not fully simulate in our laboratory sorption experiments. One possible explanation for the retardation could be that biofilm and bacteria played a part in sorbing bromide in addition to woodchips sorbing bromide under field conditions. Therefore, there is a need to ascertain the cause of bromide retardation in woodchip beds. Overall, bromide did not meet the conservancy requirement for tracer testing of beds filled with woodchips.

Other studies have also reported bromide tracer recoveries as low as 40% for a pilot-scale laboratory bioreactor made from silicone-sealed plywood (Christianson et al., 2011b), as low as 17% for a pilot-scale bed lined with polyethylene tarpaulin (Christianson et al., 2011a), as low as 60% for an unlined woodchip bed that allowed seepage (Christianson et al., 2013), 84% in a pilot-scale upward flow bioreactor made in a polyethylene tank (Jaynes et al., 2016), and an average 77% for pilot-scale concrete denitrification beds (Hoover et al., 2017). One possible cause for these low bromide recoveries could be retardation due to sorption to biofilm and bacteria as well as woodchips, which needs to be investigated. For unlined beds, another reason

for low bromide recovery can be loss of bromide with seepage. For the beds with point-source outflow in Hoover et al. (2017), another reason could be entrapment of bromide in the dead zones that have stagnant water (Fig. 4b).

Table 3

Summary of the bromide tracer tests for beds 2 to 8.

Bed Number	Injection date in 2016	Outflow rate, (L min ⁻¹)	Average flow rate, Q _{ave} (L min ⁻¹)	Water recovery fraction, R	Peak concentration in outflow (mg L ⁻¹)	Recovery (%)
2	July 8	7.5	8.4	0.81	48.1	76
3	July 18	11.3	11.7	0.93	56.1	96
4	July 18	11.7	11.7	1.00	59.7	90
5	July 18	11.5	12.2	0.89	58.8	88
6	July 8	7.0	7.9	0.78	44.4	57
7	June 30	9.1	9.1	0.98	68.6	92
8	June 30	10.2	10.3	0.97	59.2	76

3.2.3. Bromide mean residence time

For beds 2 to 8, the mean tracer residence times ranged from 8.84 to 13.61 hours (Table 4). However, the low bromide recoveries (section 3.2.2.) suggest retardation of bromide in the bed. When retardation is present in a tracer test, mean tracer residence times will be overestimated. As a result, we will take caution in evaluating the hydraulic performance (e.g., dispersion, short-circuiting, and efficiency) of each bed using the hydraulic terms, but we can still compare the beds to each other as the effect of bromide retardation is expected to be similar across beds.

Some studies have used bromide as a tracer to calculate the tracer residence time in laboratory columns (Healy et al., 2015). Others have used bromide tracer to evaluate the hydraulics of woodchips in laboratory columns (Hoover et al., 2016), in pilot-scale beds (Christianson et al., 2011a), and in an unlined bed (Christianson et al., 2013). Caution is advised when interpreting hydraulic indices from bromide tracer results, since we showed bromide did not meet the conservancy requirement of an inert tracer (section 3.2.2.). Therefore, this is an area that needs further investigation.

3.2.4. Theoretical HRT from bromide tracer

For beds 2 to 8, the theoretical HRT ranged from 12.30 to 19.81 hours (Table 4) based on a porosity of 0.85. It is important to note that t_n (and n_e) should be compared with that from other denitrification beds that were calculated using the same flow rate, i.e., either average of the inflow and outflow rates, or only outflow rate when bed leakage is negligible. In our study, we also calculated the hydraulic terms (i.e., t_n , e_v , and n_e) based on the outflow rate

([Supplementary File 2](#)) for comparison with an unlined bed that used the outflow rate for their calculations (Christianson et al., 2013). Based on our data, lower values of outflow than average flow rate (i.e., due to possible leakage) for beds 2, 3, 5, 6, 7, and 8 induced t_n to be higher (and n_e to be lower) than those based on the average flow rate ([Supplementary File 2](#)) ([Table 4](#)). This shows that the choice of the flow rate substantially affects t_n (and n_e), when beds have considerable leakage due to being unlined or having major punctures in their plastic liner. Furthermore, t_n is dependent on the value of porosity used in its calculation, so t_n calculated based on a porosity of 0.85 should not be compared to that of an assumed 0.70. Overall, we advise caution when comparing these hydraulic terms to other studies.

In terms of the calculation of theoretical HRT, some studies have reported the theoretical HRT of a denitrification bed (Christianson et al., 2013) and laboratory bioreactors (Pluer et al., 2016) based on the saturated woodchip volume. Other studies have calculated the theoretical HRT by including the unsaturated woodchip pore volume (Christianson et al., 2011b; Porter et al., 2015), and without including the porosity of woodchips (David et al., 2016 Per. Comm.; Liang et al., 2015).

Table 4

Summary of the hydraulic terms for beds 2 to 8.

Bed Number	Saturated volume, V_s (m^3)	Mean tracer residence time, \bar{t} (h)	Theoretical retention time, t_n (h)	Volumetric efficiency, e_v	Effective porosity, n_e	Morrill dispersion index, MDI
2	8.49	13.55	14.32	0.95	0.80	2.2
3	10.18	9.96	12.30	0.81	0.69	2.6
4	11.26	9.29	13.65	0.68	0.58	2.6
5	10.91	8.84	12.62	0.70	0.60	2.6
6	11.10	13.61	19.81	0.69	0.58	2.1
7	8.73	10.00	13.54	0.74	0.63	2.3
8	10.03	9.19	13.76	0.67	0.57	2.4

3.2.5. Volumetric efficiency from bromide tracer

Results of the bromide tracer tests indicate very similar volumetric efficiencies (e_v) for beds 4, 5, 6, and 8 (i.e., 0.68 ± 0.013), whereas e_v for beds 3 and 7 (i.e., 0.77 ± 0.051) slightly varied from the former-mentioned beds (Table 4). However, bed 2 showed a very different e_v than other beds. These results are consistent with the differences in their temporally normalized RTD curves (Fig. 3). Explanation of possible reasons for their differences is in section 3.2.1.

We did not find volumetric efficiencies greater than one in any of the tracer tests that would have been one indicator of physical or chemical retardation. However, Ghane et al. (2015) found volumetric efficiency greater than one indicating retardation of bromide to woodchips in a tracer test of a denitrification bed. Based on the bromide tracer test data published in Christianson et al. (2011a), we were able to calculate volumetric efficiencies greater than one for all of their pilot-scale beds. In another study, Christianson et al. (2011b) used the unsaturated woodchip volume to calculate t_n , and when we used the saturated woodchip volume from their data, we were able to calculate e_v greater than one for all six of their pilot-scale beds. Cameron and Schipper (2012) also reported a volumetric efficiency greater than one while injecting 99% of the bromide tracer into their woodchip columns over a 4.5 h period rather a short period of time. The previously reported retardations (i.e., volumetric efficiency greater than one) are consistent with our finding of low bromide recovery from tracer testing (section 3.2.2.).

It is important to note that interpretation of the hydraulic performance of woodchip beds based on volumetric efficiency should be done with caution. In a steady-state porous system without dead zones, the entire porosity is involved in the active flow of water ($n = n_e$), and thereby, the

mean tracer residence time is equal to the theoretical HRT ($e_v = 1$) (Kadlec and Wallace, 2009). However, the theoretical HRT is calculated using porosity that includes non-active pore volumes (i.e., dead end pore volumes) internal to woodchips. This causes the theoretical HRT to normally be greater than the tracer residence time ($e_v < 1$), since effective porosity is smaller than porosity of woodchips. Therefore, volumetric efficiency lower than one may not necessarily indicate non-uniform flow. Furthermore, volumetric efficiency is dependent on the value of porosity used in its calculation. Therefore, various assumptions of porosity will result in different volumetric efficiencies.

3.2.6. *In-situ effective porosity from bromide tracer testing*

Based on the bromide tracer tests, the in-situ effective porosity ranged from 0.57 to 0.80 (Table 4). Results indicate very similar effective porosity (n_e) for beds 4, 5, 6, and 8 (i.e., 0.58 ± 0.011), whereas n_e for beds 3 and 7 had effective porosity (0.66 ± 0.043) close to other beds. However, bed 2 showed a very different n_e than other beds. These results are consistent with the differences in their temporally normalized RTD curves (Fig. 3). Explanation of possible reasons for their differences is in section 3.2.1.

An in-situ effective porosity is useful for estimating the actual hydraulic retention time (AHRT) (Eq. (9)) for design and modeling of beds (Kadlec and Wallace, 2009). Even though the average in-situ effective porosity was 0.610 ± 0.045 for beds 3 to 8, it was lower than porosity values of 0.65 to 0.84 (Christianson et al., 2017; Law et al., 2018; Lepine et al., 2016; Woli et al., 2010) used to estimate the actual HRT. We advise caution in using overly large porosities, since it may result in overestimation of the actual HRT. To the best of our knowledge, our experiment is the first study to estimate the in-situ effective porosity of a typical bed (i.e., with a non-point source inflow and outflow) using a tracer test under field conditions.

The lower effective porosity (i.e., 0.61 ± 0.045 for beds 3 to 8) than total porosity (i.e., assumed 0.85) of woodchip media is evidence that the entire porosity of woodchips does not contribute to the active flow of water in a bed (Ghane et al., 2016a). Specific retention is the water volume retained against gravity, which describes the water content held inside woodchip particles. Since this water is held inside woodchip pores, its content has been determined from drying of gravity-drained woodchips using a fume hood and an oven (Ghane et al., 2014; Robertson, 2010). Therefore, using large effective porosity values (i.e., > 0.65) can result in overestimation of the actual HRT. In-situ drainable porosity values close to 0.40-0.45 have been reported (Ghane et al., 2016a, 2014) to yield the actual HRT for beds under field conditions when effective porosity was unavailable from tracer testing.

Based on a literature review, bromide has been used as a tracer to calculate the effective porosity of woodchips in laboratory columns (Healy et al., 2012). Some studies have provided rough estimates of *in-situ* effective porosity based on sodium chloride (NaCl) tracer tests for a bed with a point source inflow (see section 3.4.). Van Driel et al. (2006) provided a rough estimate of 0.7

for the in-situ effective porosity of a lateral flow denitrification bed, which was based on an assumption of 90% of flow through the coarse woodchip layer. Later, Robertson et al. (2009) conducted another tracer test on the same bed and reported a rough estimate of 0.7 for the in-situ effective porosity in which they used an assumption of 100% after year 3 of their experiment. However, we could not find the reason for their assumptions and its variation over time. The suitability of NaCl tracer for woodchips is discussed in [section 3.4](#).

3.2.7. Morrill dispersion index of bromide tracer

The Morrill Dispersion Index (MDI) for beds 2 to 8 ranged from 2.1 to 2.6 ([Table 4](#)). When $1.0 < \text{MDI} \leq 2.0$, it is considered that we have an effective plug-flow reactor. Our MDI values show that there is some mixing taking place in the beds with the higher value showing more mixing than the lower value. Our values show relatively better plug-flow characteristics than other bromide tracer tests. Christianson et al. (2013) reported an MDI of 3.2 and 4.2 for an unlined denitrification bed (Christianson et al., 2013). Based on the data published in Ghane et al. (2015), we calculated an MDI of 2.7 for that denitrification bed in Ohio.

3.3. Effective porosity of non-point source inflow and outflow

It is important to note that an in-situ effective porosity determined for a bed with a point source inflow and outflow does not represent a bed with a non-point source inflow and outflow. A non-point source inflow and outflow is the common design for beds treating drainage water in the Midwest USA, and it includes collector and distributor pipes that extend across the entire width of a bed ([Fig. a](#)). In the case of a point-source inflow/outflow, dead zones (i.e., stagnant water pockets) will develop within the bed that will not mix with the incoming water (Metcalf and Eddy, 2014) ([Fig. b](#)). Consequently, effective porosity (from tracer testing) will incorporate the effect of the dead zones whereas the effective porosity from a common bed will not. In other words, for a commonly-designed bed with isotropic and homogeneous woodchips that has uniform bottom slope and width along its length, when there are no dead zones ([Fig. 4a](#)), other than the non-active pore volume internal to woodchips, drainable porosity will be close to effective porosity (Sen, 2015). Therefore, we advise against using the in-situ effective porosity from beds with non-point and point source designs interchangeably. This concept also applies to laboratory experiments with a point source inflow and outflow.

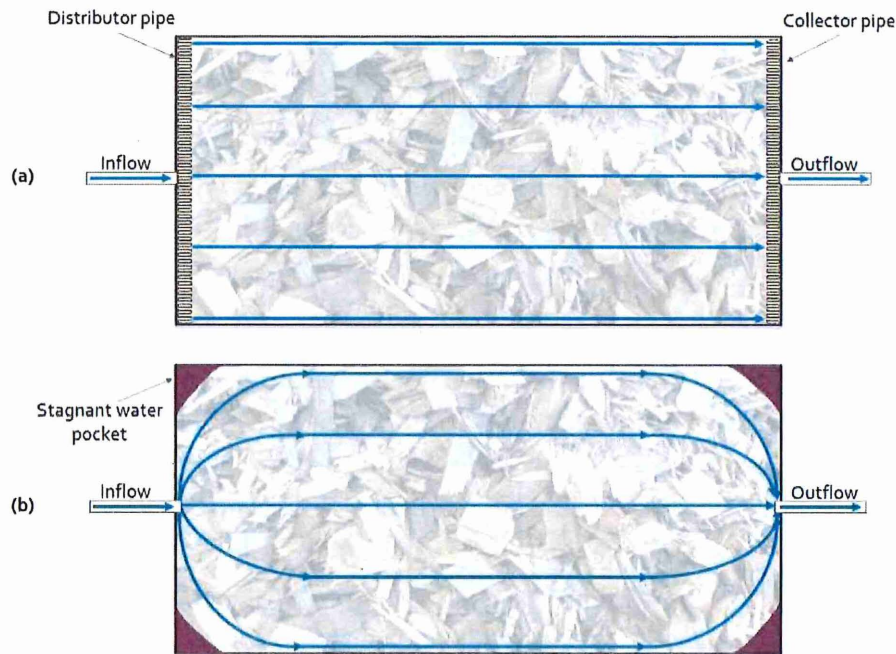


Fig. 4. Plan view of a denitrification bed when (a) distributor and collector pipes are placed on an impervious layer, and pipes extend across the entire width, and (b) there is a point source inflow and outflow. The bed has uniform bottom slope along its length, and the woodchips are assumed isotropic and homogeneous.

3.4. Is NaCl a suitable tracer?

In addition to the three bromide sorption experiments, we conducted a chloride sorption experiment using the same procedure as sorption experiment 2 with the only difference of using deionized water instead of drainage water. However, chloride concentrations were detected in the control test, so results from the chloride sorption experiment were inconclusive. Chloride has been reported as an ineffective tracer in soil-water studies due to high natural background concentration (Bero et al., 2016; Levy and Chambers, 1987), though its suitability as a tracer for woodchip media has not been investigated.

As an alternative to measuring the concentration of chloride in the outflow of a denitrification bed, an electrical conductivity (EC) meter to measure salt has been used to conduct tracer tests. In these studies, NaCl has been used as a tracer for bark mulch chips in laboratory columns (Krause Camilo et al., 2013), a pilot-scale bed (Krause Camilo, 2016), a lateral flow denitrification bed (Robertson et al., 2009; Van Driel et al., 2006), and a pilot-scale laboratory bioreactor (Christianson et al., 2016). Robertson (2010) also used water with high salt concentration to conduct a tracer test for woodchip media in laboratory columns. Although calculation of the NaCl tracer recovery is possible based on converting EC units of dS m^{-1} to ppm, the above mentioned authors did not verify its conservancy requirement. Due to the inherent porous property of woodchips, NaCl may be absorbed to woodchips due to the

molecular diffusion process and violate the tracer non-absorption requirement (Denbigh and Turner, 1984; Levenspiel, 2012). In this regard, Christianson et al. (2016) found a volumetric efficiency greater than one indicating retardation of NaCl. Therefore, we recommend investigating the suitability of NaCl as a tracer for woodchip media.

4. Conclusions

Bromide tracer testing of seven denitrification beds showed an average bromide recovery of 82%, revealing that bromide was retarded in the woodchip media and did not meet the conservancy requirement of a tracer test. Therefore, there is a need to ascertain the cause of low bromide recovery in beds as it could result in error in hydraulic performances. This is an important question because retardation of bromide in denitrification beds can result in overestimation of the mean residence time, volumetric efficiency, and in-situ effective porosity.

Even though the average in-situ effective porosity for beds 3 to 8 was 0.61, it was lower than those with greater values (> 0.65) that were used to estimate the actual HRT. Therefore, a more accurate estimate of the actual HRT can be obtained by using a more realistic effective porosity than those with much greater values. In addition, the in-situ effective porosity determined from a tracer test for a bed with a point source inflow and outflow should not be used for a bed with a non-point source inflow and outflow.

In conclusion, there is a need for further investigation about using a bromide tracer for evaluating the hydraulic performance of denitrification beds as it may provide misleading conclusions. We recommend either accounting for possible retardation of bromide to woodchips, or using non-sorbing and conservative tracers to investigate the internal hydraulics. Beds 3 to 8 showed similar hydraulic behavior based on the temporally normalized RTD curves, and they showed generally similar effective porosity.

Acknowledgments

We express gratitude to Scott Schumacher, Edward Dorsey, Todd Schumacher, Jacob Mattson, Connor Hagen, and Brendan McShane for their assistance.

Role of funding source

Funding of this research was provided in part by Minnesota Discovery, Research and Innovation Economy, and Minnesota Department of Agriculture Clean Water Fund. The funding sources were not involved in the study design, collection, analysis, interpretation of data, and preparation of the manuscript. Mention of trade names or commercial products in this publication is solely for the purpose of providing specific information and does not imply recommendation or endorsement by the U.S. Department of Agriculture.

Supplementary material

Supplementary data associated with this article can be found, in the online version, at. These data include a Google map, videos, files, and images.

References

- Bednarek, A., Szklarek, S., Zalewski, M., 2014. Nitrogen pollution removal from areas of intensive farming-comparison of various denitrification biotechnologies. *Ecohydrol. Hydrobiol.* 14, 132–141.
- Bero, N.J., Ruark, M.D., Lowery, B., 2016. Bromide and chloride tracer application to determine sufficiency of plot size and well depth placement to capture preferential flow and solute leaching. *Geoderma* 262, 94–100.
- Cameron, S.G., Schipper, L.A., 2012. Hydraulic properties, hydraulic efficiency and nitrate removal of organic carbon media for use in denitrification beds. *Ecol. Eng.* 41, 1–7.
- Christianson, L., Helmers, M., Bhandari, A., Moorman, T., 2013. Internal hydraulics of an agricultural drainage denitrification bioreactor. *Ecol. Eng.* 52, 298–307.
- Christianson, L.E., Bhandari, A., Helmers, M.J., 2011a. Pilot-Scale Evaluation of Denitrification Drainage Bioreactors: Reactor Geometry and Performance. *J. Environ. Eng.* 137, 213–220.
- Christianson, L.E., Hanly, J.A., Hedley, M.J., 2011b. Optimized denitrification bioreactor treatment through simulated drainage containment. *Agric. Water Manag.* 99, 85–92.
- Christianson, L.E., Lepine, C., Sharrer, K.L., Summerfelt, S.T., 2016. Denitrifying bioreactor clogging potential during wastewater treatment. *Water Res.* 105, 147–156.
- Christianson, L.E., Lepine, C., Sibrell, P.L., Penn, C., Summerfelt, S.T., 2017. Denitrifying woodchip bioreactor and phosphorus filter pairing to minimize pollution swapping. *Water Res.* 121, 129–139. <https://doi.org/10.1016/j.watres.2017.05.026>
- David, M.B., Gentry, L.E., Cooke, R.A., Herbstritt, S.M., 2016. Temperature and Substrate Control Woodchip Bioreactor Performance in Reducing Tile Nitrate Loads in East-Central Illinois. *J. Environ. Qual.* 45, 822–829.
- Denbigh, K.G., Turner, J.C.R., 1984. *Chemical Reactor Theory*. Cambridge University Press, Cambridge, NY, USA.
- Fetter, C.W., 2001. *Applied Hydrogeology*. Prentice Hall, Inc., Upper Saddle River, NJ, USA.
- Ghane, E., Fausey, N.R., Brown, L.C., 2015. Modeling nitrate removal in a denitrification bed. *Water Res.* 71, 294–305.
- Ghane, E., Fausey, N.R., Brown, L.C., 2014. Non-Darcy flow of water through woodchip media. *J. Hydrol.* 519, 3400–3409.

- Ghane, E., Feyereisen, G.W., Rosen, C.J., 2016a. Non-linear hydraulic properties of woodchips necessary to design denitrification beds. *J. Hydrol.* 542, 463–473.
- Ghane, E., Feyereisen, G.W., Rosen, C.J., Tschirner, U.W., 2018. Carbon quality of four-year-old woodchips in a denitrification bed treating agricultural drainage water 61, 995–1000.
- Ghane, E., Ranaivoson, A.Z., Feyereisen, G.W., Rosen, C.J., Moncrief, J.F., 2016b. Comparison of Contaminant Transport in Agricultural Drainage Water and Urban Stormwater Runoff. *PLoS One* 11, e0167834.
- Gilley, J.E., Finkner, S.C., Doran, J.W., Kottwitz, E.R., 1990. Adsorption of Bromide Tracers onto Sediment. *Appl. Eng. Agric.* 6, 35–38.
- Goldberg, S., Kabengi, N.J., 2010. Bromide Adsorption by Reference Minerals and Soils. *Vadose Zo. J.* 9, 780. <https://doi.org/10.2136/vzj2010.0028>
- Healy, M.G., Barrett, M., Lanigan, G.J., Joao Serrenho, A., Ibrahim, T.G., Thornton, S.F., Rolfe, S.A., Huang, W.E., Fenton, O., 2015. Optimizing nitrate removal and evaluating pollution swapping trade-offs from laboratory denitrification bioreactors. *Ecol. Eng.* 74, 290–301.
- Healy, M.G., Ibrahim, T.G., Lanigan, G.J., Joao Serrenho, A., Fenton, O., 2012. Nitrate removal rate, efficiency and pollution swapping potential of different organic carbon media in laboratory denitrification bioreactors. *Ecol. Eng.* 40, 198–209.
- Hoover, N.L., Bhandari, A., Soupir, M.L., Moorman, T.B., 2016. Woodchip Denitrification Bioreactors: Impact of Temperature and Hydraulic Retention Time on Nitrate Removal. *J. Environ. Qual.* 45, 803–812.
- Hoover, N.L., Soupir, M.L., Vandepol, R.D., Goode, T.R., Law, J.Y., 2017. Pilot-Scale Denitrification Bioreactors for Replicated Field Research. *Appl. Eng. Agric.* 33, 83–90. <https://doi.org/10.13031/aea.11736>
- Jaynes, D.B., Moorman, T.B., Parkin, T.B., Kaspar, T.C., 2016. Simulating Woodchip Bioreactor Performance Using a Dual-Porosity Model. *J. Environ. Qual.* 45, 830–838.
- Kadlec, R.H., Wallace, S.D., 2009. *Treatment Wetlands*, 2nd ed. CRC Press, Boca Raton, FL, USA.
- Korom, S.F., 2000. An adsorption isotherm for bromide. *Water Resour. Res.* 36, 1969–1974.
- Krause Camilo, B., 2016. Bioreactor reduces atrazine and nitrate in tile drain waters. *Ecol. Eng.* 86, 269–278.
- Krause Camilo, B., Matzinger, A., Litz, N., Tedesco, L.P., Wessolek, G., 2013. Concurrent nitrate and atrazine retention in bioreactors of straw and bark mulch at short hydraulic residence times. *Ecol. Eng.* 55, 101–113.
- Law, J.Y., Soupir, M.L., Raman, D.R., Moorman, T.B., Ong, S.K., 2018. Electrical stimulation for enhanced denitrification in woodchip bioreactors : Opportunities and challenges 110,

38–47. <https://doi.org/10.1016/j.ecoleng.2017.10.002>

- Lepine, C., Christianson, L.E., Sharrer, K.L., Summerfelt, S.T., 2016. Optimizing Hydraulic Retention Times in Denitrifying Woodchip Bioreactors Treating Recirculating Aquaculture System Wastewater. *J. Environ. Qual.* 45, 813–821.
- Leri, A.C., Ravel, B., 2015. Abiotic Bromination of Soil Organic Matter. *Environ. Sci. Technol.* 49, 13350–13359.
- Levenspiel, O., 2012. *Tracer Technology Modeling the Flow of Fluids*. Springer, New York, NY, USA.
- Levy, B.S., Chambers, R.M., 1987. Bromide as a conservative tracer for soil-water studies. *Hydrol. Process.* 1, 385–389. <https://doi.org/10.1002/hyp.3360010406>
- Liang, X., Lin, L., Ye, Y., Gu, J., Wang, Z., Xu, L., Jin, Y., Ru, Q., Tian, G., 2015. Nutrient removal efficiency in a rice-straw denitrifying bioreactor. *Bioresour. Technol.* 198, 746–754.
- Metcalf, Eddy, 2014. *Wastewater Engineering: Treatment and Resource Recovery*. McGraw-Hill, New York, NY, USA.
- Pierzynski, G.M., Vance, G.F., Sims, J.T., 2005. *Soils and Environmental Quality*. CRC Press, Boca Raton, FL, USA.
- Pluer, W.T., Geohring, L.D., Steenhuis, T.S., Walter, M.T., 2016. Controls Influencing the Treatment of Excess Agricultural Nitrate With Denitrifying Bioreactors. *J. Environ. Qual.* 45, 772–778.
- Porter, M.D., Andrus, J.M., Bartolerio, N.A., Rodriguez, L.F., Zhang, Y., Zilles, J.L., Kent, A.D., 2015. Seasonal Patterns in Microbial Community Composition in Denitrifying Bioreactors Treating Subsurface Agricultural Drainage. *Microb. Ecol.* 70, 710–723.
- Robertson, W.D., 2010. Nitrate removal rates in woodchip media of varying age. *Ecol. Eng.* 36, 1581–1587.
- Robertson, W.D., Ptacek, C.J., Brown, S.J., 2009. Rates of nitrate and perchlorate removal in a 5-year-old wood particle reactor treating agricultural drainage. *Gr. Water Monit. Remediat.* 29, 87–94.
- Schipper, L.A., Robertson, W.D., Gold, A.J., Jaynes, D.B., Cameron, S.G., 2010. Denitrifying bioreactors-An approach for reducing nitrate loads to receiving waters. *Ecol. Eng.* 36, 1532–1543.
- Sen, Z., 2015. *Practical and Applied Hydrogeology*. Elsevier Inc., Amsterdam, The Netherlands.
- Smith, S.J., Davis, R.J., 1974. Relative movement of bromide and nitrate through soils. *J. Environ. Qual.* 3, 152–155.
- Strawn, D.G., Bohn, H.L., O'Connor, G.A., 2015. *Soil Chemistry*. John Wiley & Sons, Ltd,

West Sussex, UK.

- Thackston, E.L., Shields Jr., F.D., Schroeder, P.R., 1987. Residence time distributions of shallow basins 113, 1319–1332.
- Van Driel, P.W., Robertson, W.D., Merkley, L.C., 2006. Denitrification of Agricultural Drainage Using Wood-Based Reactors. *Trans. ASABE* 49, 565–573.
- Ward, A.D., Trimble, S.W., Burckhard, S.R., Lyon, J.G., 2016. *Environmental Hydrology*. CRC Press, Boca Raton, FL, USA.
- Warneke, S., Schipper, L. a., Bruesewitz, D. a., McDonald, I., Cameron, S., 2011. Rates, controls and potential adverse effects of nitrate removal in a denitrification bed. *Ecol. Eng.* 37, 511–522.
- Woli, K.P., David, M.B., Cooke, R.A., McIsaac, G.F., Mitchell, C.A., 2010. Nitrogen balance in and export from agricultural fields associated with controlled drainage systems and denitrifying bioreactors. *Ecol. Eng.* 36, 1558–1566.

Appendix B.

Comparison of the denitrifying microbial communities between four woodchip bioreactors in Minnesota

INTRODUCTION

Increasing nitrate pollution from agricultural runoff has had detrimental impacts on water quality, as evidenced by the hypoxic zone in the Gulf of Mexico. To mitigate this, the United States Environmental Protection Agency (USEPA) called for a minimum of 45% reduction in total nitrogen (N) load in the Mississippi River. As Minnesota is one of the major contributors of nutrients to the Mississippi River, the Minnesota Pollution Control Agency has also set reduction goals of 45% for N and phosphorus (P) loads to the Mississippi River. Woodchip bioreactors are one approach to achieve this goal, and are becoming an increasingly common method for reducing the flow of nitrate from agricultural wastewater to surface waters (Gilbert et al. 2008; Schipper et al. 2010b). In a woodchip bioreactor, water diverted from an agricultural field flows through a below-ground bioreactor filled with woodchips. Nitrate in the water is reduced to dinitrogen (N_2) gas by denitrification, a microbial respiration in which nitrate is used as the terminal electron acceptor (Seitzinger et al. 2006; Rivett et al. 2008). The woodchips in woodchip bioreactors provide a C source and an electron donor to denitrifiers (Gilbert et al. 2008). Woodchip bioreactors have been successful at removing nitrate, with almost 100% nitrate load reductions reported in some cases (Gilbert et al. 2008; Christianson et al. 2012). However, under cold temperatures, bioreactor performance decreases due to inhibited microbial activity (Schipper et al. 2010a; Warneke et al. 2011; Ghane et al. 2015; Hartz et

al. 2017; Husk et al. 2017). This is a concern in Minnesota where average temperatures are low and spring melt contributes large quantities of runoff when the water temperature is still very low. It is believed that supplementing the woodchips with a more readily available C source would enhance microbial denitrification (Feyereisen et al. 2016). However, doing so risks clogging the bioreactor inlet and outlet pipes as biofilms accumulate, a common problem among field woodchip bioreactors (Gilbert et al. 2008; Christianson et al. 2016; Husk et al. 2017). It is unknown whether these commonly found biofilms are composed of denitrifying microorganisms or how they play a role in denitrification in woodchip bioreactors. Gaining a better understanding of denitrifying microorganisms and biofilms may help enhance bioreactor efficiency, particularly under cold conditions.

Additionally, most comparative studies on nitrate-removing practices have focused on design and management of the bioreactor, rather than the microorganisms present. In two meta-analyses of woodchip bioreactors, Christianson et al. (2012) and Addy et al. (2016) compare different woodchip bioreactors based on factors such as retention time, influent and effluent nitrate-N concentrations, and wood source. These factors are important in establishing a bioreactor and determining its success, but do not consider the microbial contribution and differences in community structure between sites. In a lab-based study, Griebmeier et al. (2017), set up bioreactors using nitrate-contaminated drainage water and fresh woodchips to analyze the microbial composition under different nitrate load concentrations. In analyzing the relative abundance of bacterial and archaeal operational taxonomic units (OTUs), Griebmeier et al. (2017) found differences in the microbial community structure with *Pseudomonadales* being a

relevant denitrifier at low nitrate concentrations and *Rhodocyclales* and *Rhizobiales* predominating at higher nitrate conditions. However, there have not been any studies to date that have compared the denitrifying microorganisms present between bioreactors in the field. It is possible that the successfulness of different bioreactors could be a result of the microorganisms present and their relative abundance. Therefore, the purpose of this study was to: 1) isolate denitrifying bacteria from four different bioreactors in Minnesota; 2) compare common denitrifiers between sites; and 3) determine whether any denitrifiers perform better than others and identify those that could be useful in enhancing field bioreactor performance.

METHODS

Sites and sample collection

Denitrifying microorganisms were isolated from either biofilms or woodchips in four existing woodchip bioreactors located in Willmar (bioreactor WB), Blue Earth (bioreactor BE), Olmsted County (bioreactor DC) and Lamberton (bioreactor LB), Minnesota. The ages of the woodchip bioreactors varied from 2 months (bioreactor BE) to 6 years (bioreactor WB). Woodchips were collected from submerged areas of the bioreactors and were immediately placed in a cooler. Clogging as a result of biofilm formation occurred in three of the woodchip bioreactors (see photos below). Bioreactor DC which contained fine wood pieces and green cuttings; bioreactor WB which contained only soft hardwood woodchips, but was supplemented with acetate through the warming spring and summer months; and bioreactor LB which contained a mix of material including corn cobs and woodchips and was also supplemented with acetate. The

biofilm samples from bioreactors WB and LB were collected from inlet tubing where the acetate and drainage water converged and the biofilm samples collected from bioreactor



b) LB were collected at the clogged outlet pipe. Samples were frozen for further use.

Descriptions of each of the bioreactors are presented in **Table 3-1**.



Photos of biofilm clogging woodchip bioreactors. a) biofilm inside the woodchip sampling port. b) biofilm accumulation at the inlet pipe and acetate injection site.

Table 3-1: Descriptions of the four bioreactors from which denitrifying bacteria were isolated

Bioreactor ID	DC	BE	WB	LB
Location of bioreactor	Olmsted County, MN	Blue Earth, MN	Willmar, MN	Lamberton, MN
	43°59'46.70"N	43°41'42.25"N	45° 3'0.17"N	44°14'35.83"N
	92°17'10.67"W	94° 7'21.52"W	95° 0'6.64"W	95°18'16.01"W
Date	Built: May 2016 Start up: July 2016	Built: Dec 2015 – Mar 2016	Built: Fall 2010 Re-built: Fall 2014	Built April 2016 Start up: May 2016
	Sampled: Sept. 2016	Start up: April 2016	Experimental Flow: Fall 2015	Sampled: June 2017

		Sampled	Sampled: November 2016	
Size	1 bed: 20' x 100' x 4.2'	3 beds: 25' x 135' x 5'	Original: 1 bed 5.5' x 350' x 4.5' Rebuilt 8 beds: 5.5' x 38' x 3'	Cube nominal size: 275 gal; avg dimension of materials layers in cubes: L 3.8' x W 3.15' x H 2.55'
Bed Materials	During sampling, appeared to contain twigs, bark, green cuttings, fines.	Bed 3: finely ground cottonwood; small particle size Bed 2: similar to bed 3, but mixed with large woodchips Bed 1: filled last; composed of large, clean uniform woodchips	Mixed hardwood and softwood chips; not many fines	2 – 3" Phosphorous- sorbing material (crushed limestone; steel slag; crushed concrete) 8" Corn Cobs 8" Woodchips 3 – 4 " Lava Rock
Flow rate	6 – 11 gal/min	130 gal/min	2.5 gal/min	1 gal/min
HRT	50 – 90 hours	≈6 hours	9 – 10 hours	3 – 4 hours
Influent NO ₃ - N concentration (mg N L ⁻¹)	17 - 18	15 - 25	15 - 20	2016: 15 - 23.4 2017: 17.15 - 17.72
Effluent NO ₃ - N concentration (mg N L ⁻¹)	0.1	12 – 16	0.2 – 0.4	2016: 3.6 – 17.2 2017: 12.2 - 17.2
Inlet pH	6.31	7.2 – 8.0	7.56	7.38 average (2016-17)

Outlet pH	6.05	7.2 – 7.9	7.51	5.96 – 7.44 (2016) 6.79 – 8.88 (2017)
Inlet TC/TOC	0.1	5 – 11 (DOC)	3 (DOC)	NA
Outlet TC/TOC	50	6 – 9 (DOC)	4 (DOC)	NA
Acetate Added?	No	No	Yes	Yes
Acetate Rate	n/a	n/a		72 mL/min
Acetate C concentration (g C L ⁻¹)				12.5 g C/L
≈C:N ratio				
Type of sample collected	Biofilm	Woodchips	Woodchips and biofilm	Biofilm Sampled in the inlet pipe prior to reaching the bioreactor cubes.

Isolation

Denitrifying microorganisms were isolated at 15°C according to the methods outlined in Chapter 2. Briefly, woodchip and biofilm samples were suspended in phosphate buffered saline (PBS, pH 7.4) and then plated on R2A agar containing 5 mM nitrate and 10 mM acetate (R2A-NA). Plates were incubated anaerobically at 15°C using an AnaeroPak system (Mitsubishi Gas Chemical) and continually restreaked until individual colonies appeared. Denitrification potential was confirmed for all isolates using the acetylene inhibition method which prevents the final step in denitrification from N₂O to N₂ gas so that N₂O gas can be measured (Yoshinari and Knowles 1976). In order

to differentiate between denitrification and dissimilatory nitrate reduction to ammonium (DNRA), we also measured concentrations of nitrate, nitrite and ammonium by using the SEAL AA3 HR AutoAnalyzer to confirm nitrate-reduction.

Identification

All nitrate-reducing microorganisms were identified based on 16S rRNA gene sequencing. First, DNA was extracted by heating cells at 95°C for 15 min and then diluted 10-fold for PCR. The reaction mixture (50 µl) contained 1x Ex Taq buffer (Takara Bio, Otsu, Japan), 0.2 µM of each primer (27F and 1492R; ref), 0.2 mM of each dNTP, 1 U of Ex Taq DNA polymerase (Takara Bio), and 2 µl of DNA template. PCR was performed using a Veriti Thermal Cyclers (Life Technologies) and the following conditions: initial annealing at 95°C for 5 min, followed by 30 cycles of 95°C for 30 s, 55°C for 30 s and 72°C for 1.5 min, and one cycle of 72°C for 7 min. Amplification was confirmed using agarose gel electrophoresis and PCR products were purified using AccuPrep PCR Purification Kit (Bioneer) and then quantitated using PicoGreen dsDNA quantitation assay (Thermo Scientific). The purified PCR products were bidirectionally sequenced using the Sanger method by at the University of Minnesota Genomics Center. The resulting forward (27F) and reverse (1492R) reads were aligned using the phred, phrap, consed software (Ewing et al. 1998) and strain identity was determined using Naïve Bayesian classifier (Wang et al. 2007).

Denitrification rate measurement

Potential cold-adapted denitrifiers chosen for further testing were selected based on the following criteria: greater than 49% nitrate-N was reduced, less than 10% N was converted to ammonium, and no nitrite-N was produced.

Denitrification rates were measured using ^{15}N -labeled nitrate and a gas chromatograph-mass spectrometer (GC-MS). Having confirmed that these strains are capable of reducing nitrate, the ^{15}N -labeled nitrogenous gases would allow us to track nitrate through the denitrification process, showing whether or not complete denitrification is occurring. In brief, denitrifying bacteria grown in R2A-NA broth under anaerobic conditions were washed in piperazine-N, N'-bis (PIPES) buffer (pH 7.4). Denitrifying bacteria were incubated at 15°C in triplicate 50 ml PIPES buffer (pH 7.4) containing 10 mM acetate and 5 mM ^{15}N -labeled nitrate in 160 ml airtight bottles. The gas phase was exchanged for He. 10 μl gas samples were taken at hours 0, 24, 48, 72 and 1 week and 2 weeks and immediately analyzed using a GCMS-QP2010 SE (Shimadzu) equipped with Rt-Q-BOND column ($30\text{ m} \times 0.32\text{ mm} \times 10\text{ }\mu\text{m}$; Restek) to measure the absorbance values of $^{30}\text{N}_2$ and $^{46}\text{N}_2\text{O}$. A standard curve was created by injecting different volumes of $^{30}\text{N}_2$ gas and comparing absorbance values to known concentrations. Data was analyzed according to this standard curve and results were calculated as pmol-N $^{46}\text{N}_2\text{O}$ and $^{30}\text{N}_2$ produced per cell, based on OD_{600} values. The denitrification rate was calculated as pmol-N/cell/hour for $^{30}\text{N}_2$ gas based on the slope of the trendline where $^{30}\text{N}_2$ gas was produced linearly.

Aerobic denitrification confirmation

While denitrification is thought to be an anaerobic process, some microorganisms have recently been identified that are capable of aerobic denitrification (Takaya et al. 2003) and explanations for compatible aerobic respiration and denitrification have been hypothesized (Chen and Strous 2013). Aerobic denitrification would serve an important role in wastewater treatment, particularly in woodchip bioreactors where fluctuating water depth corresponds to a fluctuation in oxygen levels. To test for aerobic denitrification, potential denitrifying bacteria were incubated under the same conditions as the denitrification rate test except the gas phase was not exchanged. Gas samples were taken at the same time intervals.

Statistical analysis

The PAST software was used to perform one-way ANOVA tests to analyze statistical differences between samples and a p-value of ≤ 0.05 was used to indicate statistically significant differences (Hammer et al. 2001).

RESULTS

Isolated potential denitrifying bacteria

A total of 207 microorganisms were isolated under cold temperatures from woodchip or biofilm samples from four woodchip bioreactors in Minnesota. Of these, 79 were identified as cold-adapted nitrate-reducers. **Table 3-2** shows the identity and denitrification potential of all isolates across all sites. While nitrate reduction and ammonium production varied widely, overall little to no nitrite was produced. As shown

in **Figure 3-1**, the composition of the nitrate-reducing isolates varied widely across sites. From the bioreactor BE woodchip samples, a total of 25 bacteria were isolated, all of which were confirmed nitrate reducers and many potential denitrifiers. The isolated nitrate-reducers from this site belonged mostly to the genera *Microvirgula* and *Enterobacter*. Six isolated bacteria were considered to be potential denitrifiers (>49% nitrate reduced, <10% ammonium produced) and belonged to a more diverse group of genera, including *Microvirgula*, *Delftia*, *Raoultella*, *Clostridium* and *Buttiauxella*.

Table 3-2: Nitrate-reducing bacteria isolated from woodchip bioreactors in Minnesota and their N transformations

<u>Isolate ID</u>	<u>Source</u>	<u>%N to ammonium</u>	<u>% Nitrate reduced</u>	<u>%N to nitrite</u>	<u>GC (ppm)</u>	<u>Identification</u>	<u>Accession number</u>
BE1.1	BE woodchips	32.73	100.00	0.00	2020.21	<i>Enterobacter</i>	
BE 1.2	BE woodchips	7.95	69.84	0.00	1532.52	<i>Delftia</i>	
BE 1.3	BE woodchips	27.30	99.85	0.00	3348.41	<i>Enterobacter</i>	
BE 1.4	BE woodchips	34.33	100.00	0.00	2786.80	<i>Microvirgula</i>	
BE 1.5	BE woodchips	21.57	81.02	0.00	2695.12	<i>Microvirgula</i>	
BE1.6	BE woodchips	48.00	87.50	0.00	1861.03	<i>Kosakonia</i>	
BE 1.7	BE woodchips	29.51	74.58	0.00	17.97	<i>Enterobacter</i>	
BE 2.1	BE woodchips	6.82	70.09	0.00	1815.50	<i>Raoultella</i>	
BE 2.2	BE woodchips	14.89	73.63	0.00	2072.18	<i>Clostridium</i>	
BE 2.3	BE woodchips	33.49	99.80	0.00	3693.00	<i>Microvirgula</i>	
BE 2.4	BE woodchips	-0.23	62.05	0.00	2072.18	<i>Microvirgula</i>	
BE2.5	BE woodchips	7.78	66.83	0.00	316.15	<i>Raoultella</i>	
BE 2.6	BE woodchips	-0.30	62.12	0.00	88.76	<i>Buttiauxella</i>	
BE2.7	BE woodchips	21.84	78.40	0.00	1898.18	<i>Enterobacter</i>	
BE 3.1	BE woodchips	18.12	74.79	0.00	2111.09	<i>Serratia</i>	
BE3.2	BE woodchips	36.77	99.89	0.00	939.63	<i>Enterobacter</i>	
BE 3.3	BE woodchips	16.46	73.87	0.00	1567.94	<i>Microvirgula</i>	
BE 3.4	BE woodchips	35.22	100.00	0.00	2919.65	<i>Raoultella</i>	
BE 3.5	BE woodchips	33.60	49.99	0.00	917.43	<i>Lelliottia</i>	
BE 3.6	BE woodchips	26.66	60.11	0.00	2073.42	<i>Enterobacter</i>	
BE 3.7	BE woodchips	73.59	100.00	0.00	3504.32	<i>Microvirgula</i>	
BE 3.8	BE woodchips	66.17	99.92	0.00	3706.89	<i>Microvirgula</i>	
BE 3.9	BE woodchips	39.12	56.90	0.00	1668.99	<i>Enterobacter</i>	
BE 3.10	BE woodchips	74.68	100.00	0.00	3333.53	<i>Microvirgula</i>	
BE 3.11	BE woodchips	4.83	62.38	0.00	64.93	<i>Clostridium</i>	
WB17	WB woodchips	40.88	98.31	0.00	1401.13	<i>Microvirgula</i>	
WB18	WB woodchips	44.86	98.30	0.00	1479.26	<i>Microvirgula</i>	
WB19	WB woodchips	4.06	-6.92	0.00	63.11	<i>Clostridium</i>	

<u>Isolate ID</u>	<u>Source</u>	<u>%N to ammonium</u>	<u>% Nitrate reduced</u>	<u>%N to nitrite</u>	<u>GC (ppm)</u>	<u>Identification</u>	<u>Accession number</u>
WB21	WB woodchips	5.78	-12.89	0.00	224.02	<i>Clostridium</i>	
WB22	WB woodchips	42.11	98.41	0.00	1496.52	<i>Microvirgula</i>	
WB23	WB woodchips	6.96	-16.99	0.00	9.45	<i>Clostridium</i>	
WB24	WB woodchips	7.26	-15.18	0.00	7.11	<i>Clostridium</i>	
WB26	WB woodchips	-7.50	33.45	0.00	2.45	<i>Clostridium</i>	
WB29	WB woodchips	-6.47	31.96	0.00	1.26	<i>Clostridium</i>	
WB39	WB woodchips	7.12	39.44	0.00	68.83	<i>Clostridium</i>	
WB40	WB woodchips	2.04	3.77	0.00	5.12	<i>Clostridium</i>	
WB49	WB woodchips	6.84	39.64	0.00	103.17	<i>Clostridium</i>	
WB53	WB woodchips	0.83	58.21	0.00	843.64	<i>Clostridium</i>	
WB66	WB woodchips	5.03	45.13	0.00	112.09	<i>Clostridium</i>	
WB76	WB woodchips	-1.62	44.38	0.00	147.01	<i>Clostridium</i>	
WB80	WB woodchips	5.87	49.82	0.00	603.18	<i>Clostridium</i>	
WB81	WB woodchips	4.09	47.52	0.00	0.34	<i>Clostridium</i>	
						<i>unclassified_Deltaprote</i>	
WB91	WB woodchips	6.97	38.73	0.00	169.69	<i>obacteria</i>	
WB94	WB woodchips	6.45	49.16	0.00	115.98	<i>Cellulomonas</i>	
WB102	WB woodchips	2.51	60.29	0.00	-267.82	<i>Cellulomonas</i>	
WB104	WB woodchips	73.11	29.12	0.00	994.87	<i>Cellulomonas</i>	
2A1	WB biofilm	72.98	62.74	0.00	259.04	<i>Bacillus</i>	
2A1.1	WB biofilm	65.87	59.16	0.00	168.22	<i>Aeromonas</i>	
2B3	WB biofilm	38.84	59.27	0.00	837.29	<i>Lelliottia</i>	
6A1	WB biofilm	58.39	32.23	0.00	1247.67	<i>Bacillus</i>	
6B1	WB biofilm	60.34	40.41	0.00	1908.73	<i>Enterobacter</i>	
BA1.12	LB biofilm	25.36	49.36	0.00	620.31	<i>Escherichia</i>	
BA1.2	LB biofilm	46.07	42.78	0.00	453.32	<i>Lelliottia</i>	
BA1.3	LB biofilm	54.45	49.51	0.00	299.32	<i>Raoultella</i>	
BA2.2	LB biofilm	63.42	45.84	0.00	439.85	<i>Raoultella</i>	
BB1.1	LB biofilm	49.40	64.73	0.00	57.82	<i>Raoultella</i>	
BB1.2	LB biofilm	47.77	102.29	0.00	1231.27	<i>Microvirgula</i>	

<u>Isolate ID</u>	<u>Source</u>	<u>%N to ammonium</u>	<u>% Nitrate reduced</u>	<u>%N to nitrite</u>	<u>GC (ppm)</u>	<u>Identification</u>	<u>Accession number</u>
BB1.3	LB biofilm	6.77	21.05	0.00	73.89	<i>Lactococcus</i>	
BB2.1	LB biofilm	35.76	43.12	0.00	509.27	<i>Lelliottia</i>	
BB2.2	LB biofilm	54.43	20.43	0.00	459.65	<i>Lelliottia</i>	
H6	DC biofilm	9.17	6.20	0.00	739.35	<i>Mariniluteicoccus</i>	
H13	DC biofilm	13.09	-22.76	2.18	832.28	<i>Bacillus</i>	
H16	DC biofilm	8.40	-10.81	2.09	2292.20	<i>Bacillus</i>	
H20	DC biofilm	9.64	-7.19	2.15	941.83	<i>Bacillus</i>	
H25	DC biofilm	7.02	5.02	1.84	908.86	<i>Bacillus</i>	
H26	DC biofilm	6.13	3.36	0.82	878.60	<i>Bacillus</i>	
H29	DC biofilm	8.39	-3.21	1.79	1060.61	<i>unclassified_bacillales</i>	
H30	DC biofilm	8.45	27.29	0.53	884.89	<i>Bacillus</i>	
H31	DC biofilm	4.35	18.15	0.16	1019.25	<i>Clostridium</i>	
H32	DC biofilm	4.96	3.65	1.82	685.91	<i>Bacillus</i>	
H33	DC biofilm	8.77	-7.63	1.34	935.31	<i>Bacillus</i>	
H34	DC biofilm	-5.04	50.74	2.03	641.78	<i>Bacillus</i>	
H37	DC biofilm	-2.04	32.63	1.47	1102.62	<i>Bacillus</i>	
H41	DC biofilm	17.77	29.56	17.54	1181.89	<i>Bacillus</i>	
H43	DC biofilm	4.42	10.54	3.92	1120.13	<i>Bacillus</i>	
H45	DC biofilm	-6.91	41.89	1.21	634.97	<i>Bacillus</i>	

From bioreactor WB, a total of 104 and 16 bacterial strains were isolated under denitrifying conditions from the woodchips and biofilm, respectively. Of these, 21 isolates from woodchips and five isolates from biofilm were confirmed nitrate-reducers and both samples contained unique microorganisms. A total of three potential denitrifiers were identified from the WB woodchips, two of which belonged to the genus *Clostridium* and one to *Cellulomonas*. Of the five nitrate-reducers isolated from the biofilm, many demonstrated relatively high nitrate reduction (32- 62%), but correspondingly high ammonium concentrations, indicating that these strains are likely performing DNRA.

A total of nine nitrate-reducing bacteria were isolated from the LB bioreactor biofilm, none of which were identified as potential denitrifiers. Similarly, no potential denitrifiers were isolated from the DC woodchip bioreactor, which belonged almost exclusively to the genus *Bacillus*. The isolated nitrate-reducers from the DC biofilm produced little ammonium, but the presence of nitrite was detected in all but one sample.

Denitrification rate

Seven potential denitrifiers were selected to be tested for aerobic and anaerobic denitrification rates using ¹⁵N-labeled nitrate. Five originated from the BE bioreactor, including *Buttiauxella*, *Raoultella*, *Delftia*, *Microvirgula* and *Clostridium*, and two from the WB bioreactor woodchips, including *Cellulomonas* and *Clostridium*. Two other potential denitrifiers were identified based on our criteria, one additional *Clostridium* from the WB bioreactor and one

Raoultella from the BE bioreactor, but these were excluded due to repetition. Most of the results showed some increase in $^{30}\text{N}_2$, but had too great a variation to conclude whether denitrification was occurring, particularly for the aerobic conditions (Figure 3-2,a-g). Isolate BE2.4, belonging

to

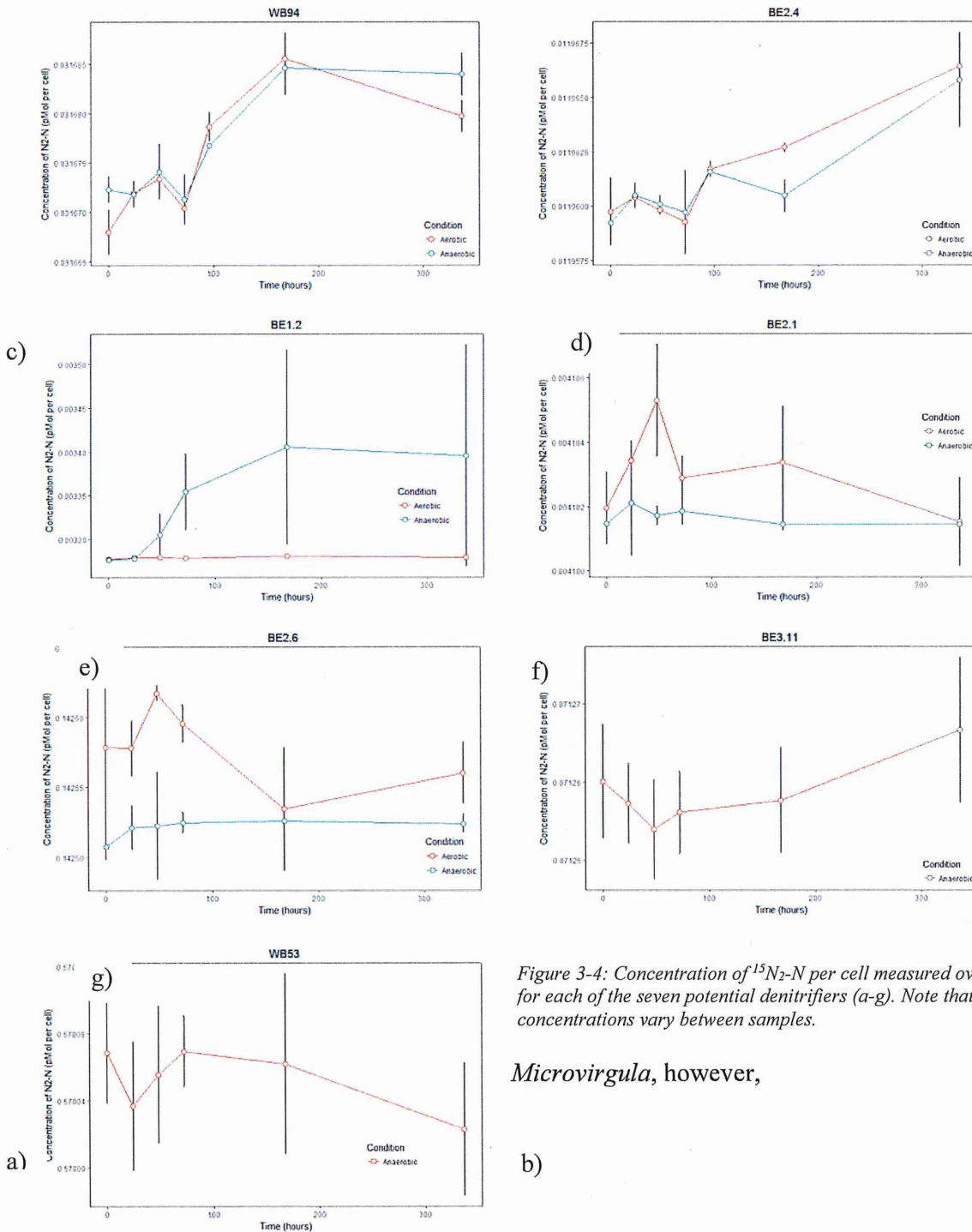


Figure 3-4: Concentration of $^{15}\text{N}_2\text{-N}$ per cell measured over time for each of the seven potential denitrifiers (a-g). Note that the concentrations vary between samples.

Microvirgula, however,

showed significant increases in $^{30}\text{N}_2$ aerobically at each time point following hour 72 (**Figure 3-2b**). Anaerobic $^{30}\text{N}_2$ did not increase significantly until after the first week (hour 168). This suggests that isolate BE2.4 may be a strong aerobic denitrifier. Surprisingly, *Cellulomonas* isolate WB94 also displayed aerobic denitrification, with significant increases in $^{30}\text{N}_2$ between hours 72 to 168 under both aerobic and anaerobic conditions (**Figure 3-2a**). The production of

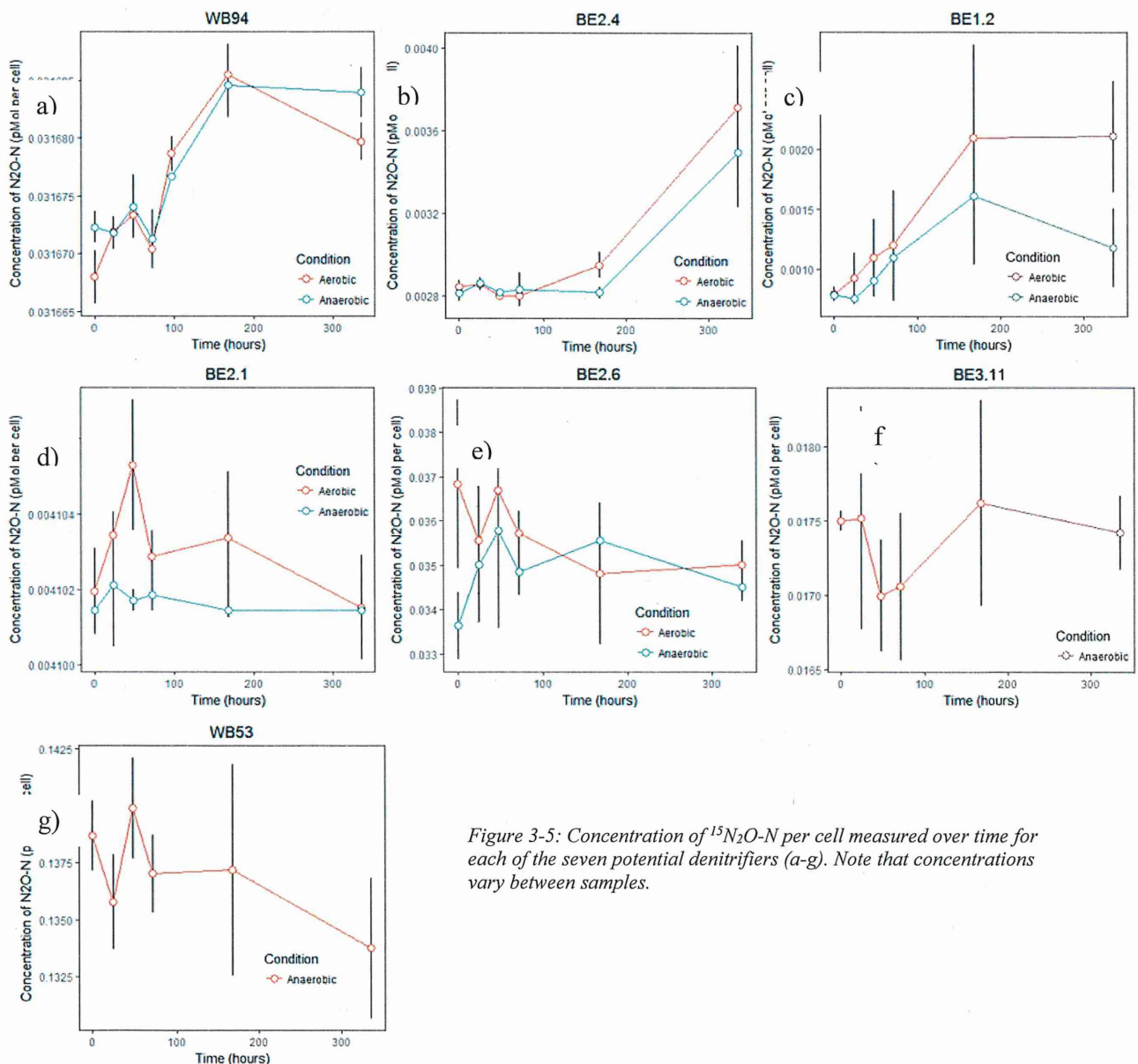


Figure 3-5: Concentration of $^{15}\text{N}_2\text{O-N}$ per cell measured over time for each of the seven potential denitrifiers (a-g). Note that concentrations vary between samples.

$^{46}\text{N}_2\text{O}$ was also measured and is displayed in **Figure 3-3**. There was a significant increase in $^{46}\text{N}_2\text{O}$ aerobically produced by BE2.1 during the first 48 hours. $^{46}\text{N}_2\text{O}$ increased significantly towards the end of the experiment in both the WB94 (**Figure 3-2a**) and BE2.4 (**Figure 3-2b**) aerobic incubations (between 72 and 336 hours for BE2.4 and between 72 and 168 for WB94), and anaerobic conditions (between 168 and 336 hours for BE2.4 and 72 and 168 for WB94). The denitrification rates, based on the slope of the trend line during the time that $^{30}\text{N}_2$ gas was produced, varied between samples and between aerobic and anaerobic conditions. The time range during which $^{30}\text{N}_2$ gas was produced and the rate are shown in **Table 3-3**.

Table 3-3: The denitrification rate for each sample and the time points that $^{30}\text{N}_2$ gas was produced.

Sample	Hours N2 produced	pmol/cell/hour
WB94 aerobic	0-168	5.00E-08
WB94 anaerobic	0-168	4.00E-08
BE2.4 aerobic	0-336	1.00E-08
BE2.4 anaerobic	0-336	9.00E-09
BE1.2 aerobic	0-336	4.00E-21
BE1.2 anaerobic	0-168	8.00E-07
BE2.1 aerobic	0-48	2.00E-07
BE2.1 anaerobic	0-48	1.00E-08
BE2.6 aerobic	24-48	9.00E-07
BE2.6 anaerobic	0-48	2.00E-07
BE3.11 anaerobic	48-336	2.00E-08
WB53 anaerobic	24-72	3.00E-07

DISCUSSION

The majority of the potential denitrifiers were isolated from the BE bioreactor woodchips followed by the WB bioreactor woodchips. The BE bioreactor, which was the newest bioreactor at the time of sampling, contained fresh and uniform soft hardwood woodchips and we isolated a more diverse community of nitrate-reducing bacteria than at the other bioreactor sites. The genus

Microvirgula, which was the dominant taxa at the BE bioreactor, is known to harbor strains capable of denitrification in the presence of oxygen, which may be useful in woodchip bioreactors where fluctuating levels of oxygen are present (Patureau et al. 1998; Patureau et al. 2001; Takaya et al. 2003). Our results were consistent with this as BE2.4 demonstrated ability to reduce nitrate to N₂ gas both aerobically and anaerobically. BE2.4 also produced ³⁰N₂ gas consistently over the two week sampling period at a rate of 1.00E-08 and 9.00E-09 pmol-N/cell/hour aerobically and anaerobically, respectively. While all eight *Microvirgula* isolates from bioreactor BE showed promising nitrate reduction ranging from 62-100%, the remaining seven converted >10% of N to ammonium instead of N₂ gas. Similarly, the *Enterobacter* strains in this study reduced 74-100% nitrate-N, but much of the nitrate-N was converted to ammonium (27-39%). This is unsurprising as *Enterobacter* is a known facultative aerobe capable of nitrate reduction to ammonium (Fazzolari et al. 1990; Tiedje et al. 1988). Isolate BE1.2 belonged to the genus *Delftia*, which has previously demonstrated potential as an efficient denitrifier (Zhang et al. 2016) and may have the ability to denitrify aerobically (Wang et al. 2007). The *Delftia* isolate in this study (BE1.2) was able to denitrify anaerobically at a rate of 8.00E07 pmol-N/cell/hour between hour 0 to one week, but did not demonstrate aerobic denitrification. Three isolates belonged to the genera *Raoultella* and *Buttiauxella*, both of which are known nitrate reducers to ammonium, and seemingly reduced nitrate completely during initial denitrification screening, however neither BE2.1 nor BE2.6 produced a significant amount of N₂ gas, indicating that they are in fact likely carrying out DNRA. While the denitrification rates were higher for BE2.1 and BE2.6, the time points that ³⁰N₂ gas was produced were limited (0-48 hours or 24-48 hours). Other nitrate-reducing bacteria isolated in this study including *Serratia*, *Lelliottia*, *Buttiauxella*,

and *Kosakonia* fall under Enterobacteriaceae, the same family as *Enterobacter*, and are also known to be capable of nitrate reduction to ammonium (Tiedje et al. 1988).

The three biofilm sampling sites contained similar nitrate-reducing bacteria many of which are known dissimilatory nitrate reducers to ammonium, such as *Raoultella*, *Enterobacter*, *Aeromonas* and *Lelliottia*, and our results supported this. One *Microvirgula* strain was isolated from the Lamberton bioreactor biofilm, but it was not classified as a denitrifier according to our definition because it converted >10% N to ammonium-N. *Bacillus* were the most common nitrate-reducing bacteria isolated from both the WB bioreactor biofilm and DC bioreactor biofilm, but despite positive GC results indicating that some of the strains may be potential denitrifiers, the majority of the isolates reduced a negligible amount of nitrate (<10% nitrate-N) or produced significant amounts of nitrite (>3%). This highlights a problem with the acetylene inhibition method which is that it does not distinguish whether a microorganism is capable of carrying out the last step in denitrification reducing N₂O to N₂ gas (Tiedje 1988). Additionally, *Bacillus* is known to harbor many DNRA bacteria (Tiedje 1988). No potential denitrifiers were identified from any of the biofilm samples across the three sites, indicating that biofilms that cause clogging in woodchip bioreactors are likely composed of non-denitrifying microorganisms primarily performing DNRA. This result is consistent with Tiedje (1983), who proposed that a high C/N ratio would select for DNRA bacteria over denitrifying bacteria. A higher ratio of available C (ie. acetate) to electron acceptor (ie. NO₃⁻) is more suitable for DNRA because it allows for an additional three electrons to be accepted compared to denitrification (Tiedje 1983).

The WB bioreactor contained both hardwood and softwood woodchips that had been submerged for 6 years prior to sampling. Three of the 21 isolates from the WB woodchips were identified as *Microvirgula*, although these particular isolates converted 40-44% of the nitrate-N

to ammonium. Interestingly, strains belonging to the genus *Clostridium*, a known obligate anaerobe, made up the majority of the nitrate-reducing woodchip isolates, despite no obligate anaerobe capable of denitrification having been identified previously. While the denitrification rates of BE3.11 and WB53 were comparable to those of the other potential denitrifiers, $^{30}\text{N}_2$ gas increased over a short time period and the results varied too much to confirm complete denitrification to N_2 gas. Nevertheless, *Clostridium* may play an active role in woodchip bioreactors as they are known to be able to degrade wood compounds including hemicellulose, xylan and pectin under anaerobic conditions (Kosugi et al. 2001; Desavaux 2006). An additional three nitrate-reducers from the WB woodchips were identified as *Cellulomonas* which is another genus known for its ability to degrade cellulose (Han et al. 1968; Thayer et al. 1984; Poulsen et al. 2016). This is an important process in woodchip bioreactors as it allows for the breakdown of complex polysaccharides which provide a C source for denitrification. *Cellulomonas* isolate WB94 was tested for aerobic and anaerobic denitrification rates and was shown to produce $^{30}\text{N}_2$ consistently over a one week period both under anaerobic ($5.00\text{E}08$ pmol-N/cell/hour) and aerobic ($4.00\text{E}08$ pmol-N/cell/hour) conditions. While some *Cellulomonas* strains are known to be capable of nitrate reduction to nitric oxide, a full set of denitrification genes have not been found (GenBank: AEE45473.1). It is possible that WB94 may be capable of complete denitrification, however more research is needed to confirm the presence of all denitrification genes and to further confirm whether it has the ability for aerobic denitrification.

The nitrate-reducing communities isolated from the two woodchip sample sites, WB and BE, were distinct from one another, indicating that age of the bioreactor may play a major role in denitrifier community composition. The BE bioreactor, which was the most recently established of the four bioreactors was composed mainly of the aerobic denitrifier, *Microvirgula*, implying

that an anaerobic denitrifying community may not have been established at the time of sampling. The WB woodchip bioreactor, on the other hand, had been in use for six years before sampling and was composed mainly of the obligate anaerobe, *Clostridium*, and the cellulose-degrading *Cellulomonas*. These two genera likely play major roles in long-established bioreactors. Previous studies comparing bioreactor efficiency between variably-aged woodchips show that nitrate removal rates decrease by about 50% during the first year and then become stable for years thereafter (Robertson 2010). It is possible that these two cellulose-degrading genera may play an important role in providing usable C for denitrification in aged woodchip bioreactors that contain little labile C. Additional studies are needed to determine how a denitrifying community changes over time within a bioreactor.

No denitrifiers were isolated from biofilm samples, demonstrating that the clogging due to warming temperatures and readily available C is composed of non-denitrifying microorganisms. From this study, *Cellulomonas* isolate WB94 and *Microvirgula* isolate BE2.4 are the recommended candidates for bioaugmentation in the field due to their potential for aerobic and anaerobic denitrification and the possible ability of WB94 to degrade cellulose in the woodchips. More research is needed to confirm the presence of complete denitrification genes in these two isolates and of any genes involved in the degradation of complex polysaccharides in WB94.

REFERENCES

- Addy, K., Gold, A. J., Christianson, L. E., David, M. B., Schipper, L. A., & Ratigan, N. A. (2016). Denitrifying Bioreactors for Nitrate Removal: A Meta-Analysis. *Journal of Environment Quality*, 45(3), 873. <https://doi.org/10.2134/jeq2015.07.0399>
- Christianson, L. E., Bhandari, A., Helmers, M. J., & Schilfgaard, V. (2012). A PRACTICE-ORIENTED REVIEW OF WOODCHIP BIOREACTORS FOR SUBSURFACE AGRICULTURAL DRAINAGE, 28(3), 861–874.

- Christianson, L. E., Lepine, C., Sharrer, K. L., & Summerfelt, S. T. (2016). Denitrifying bioreactor clogging potential during wastewater treatment. *Water Research*, 105, 147–156. <https://doi.org/10.1016/j.watres.2016.08.067>
- Chen, J., & Strous, M. (2013). Denitrification and aerobic respiration, hybrid electron transport chains and co-evolution. *Biochimica et Biophysica Acta - Bioenergetics*, 1827(2), 136–144. <https://doi.org/10.1016/j.bbabi.2012.10.002>
- Chun, J. A., Cooke, R. A., Eheart, J. W., & Kang, M. S. (2009). Estimation of flow and transport parameters for woodchip-based bioreactors: I. laboratory-scale bioreactor. *Biosystems Engineering*, 104(3), 384–395. <https://doi.org/10.1016/j.biosystemseng.2009.06.021>
- Desvaux, M. (2006). Unravelling carbon metabolism in anaerobic cellulolytic bacteria. *Biotechnology Progress*, 22(5), 1229–1238. <https://doi.org/10.1021/bp060016e>
- Ewing, B., L. Hillier, M. C. Wendl, and P. Green. 1998. Base-calling of automated sequencer traces using phred. I. Accuracy assessment. *Genome Res*.
- Fazzolari, E., Mariotti, A., & Germon, J. C. (1990). Nitrate reduction to ammonia: a dissimilatory process in *Enterobacter amnigenus*. *Canadian Journal of Microbiology*, 36(11), 779–785. <https://doi.org/10.1139/m90-134>
- Feyereisen, G. W., Moorman, T. B., Christianson, L. E., Venterea, R. T., Coulter, J. A., & Tschirner, U. W. (2016). Performance of Agricultural Residue Media in Laboratory Denitrifying Bioreactors at Low Temperatures. *Journal of Environment Quality*, 45(3), 779. <https://doi.org/10.2134/jeq2015.07.0407>
- Ghane, E., Fausey, N. R., & Brown, L. C. (2015). Modeling nitrate removal in a denitrification bed. *Water Research*, 71, 294–305. <https://doi.org/10.1016/j.watres.2014.10.039>
- Gibert, O., Pomierny, S., Rowe, I., & Kalin, R. M. (2008). Selection of organic substrates as potential reactive materials for use in a denitrification permeable reactive barrier (PRB). *Bioresource Technology*, 99(16), 7587–7596. <https://doi.org/10.1016/j.biortech.2008.02.012>
- Grießmeier, V., Bremges, A., McHardy, A. C., & Gescher, J. (2017). Investigation of different nitrogen reduction routes and their key microbial players in wood chip-driven denitrification beds. *Scientific Reports*, 7(1), 1–12. <https://doi.org/10.1038/s41598-017-17312-2>
- Hammer, Ø., Harper, D.A.T., Ryan, P.D. (2001) PAST: Paleontological statistics software package for education and data analysis. *Palaeontologia Electronica* 4: 9.
- Han, Y. W., and V. R. Srinivasan. 1968. Isolation and characterization of a cellulose-utilizing bacterium. *Appl. Microbiol.* 16:1140-1145.
- Hartz T, Smith R, Cahn M, Bottoms T, Bustamante S, Tourte L, Johnson K, Coletti L. 2017. Wood chip denitrification bioreactors can reduce nitrate in tile drainage. *Calif Agr* 71(1):41-47. <https://doi.org/10.3733/ca.2017a0007>.
- Husk, B. R., Anderson, B. C., Whalen, J. K., & Sanchez, J. S. (2017). Reducing nitrogen contamination from agricultural subsurface drainage with denitrification bioreactors and controlled drainage. *Biosystems Engineering*, 153, 52–62. <https://doi.org/10.1016/j.biosystemseng.2016.10.021>

- Kosugi A, Murashima K, Doi RH. Characterization of xylanolytic enzymes in *Clostridium cellulovorans*: expression of xylanase activity dependent on growth substrates. *J Bacteriol.* 2001;183:7037–43.
- Patureau, D., J.-J. Godon, P. Dabert, T. Bouchez, N. Bernet, J. P. Delgenes, and R. Moletta. 1998. *Microvirgula aerodenitrificans* gen. nov., sp. nov., a new gram-negative bacterium exhibiting co-respiration of oxygen and nitrogen oxides up to oxygen saturated conditions. *Int. J. Sys. Bacteriol.* 48:775–782
- Patureau, D., Helloin, E., Rustrian, E., Bouchez, T., Delgenes, J. P., & Moletta, R. (2001). T0518 Combined phosphate and nitrogen removal in sequencing batch reactor using *Microvirgula a.* *Wat. Res.*, 35(1), 189–197.
- Poulsen, H. V., Willink, F. W., & Ingvorsen, K. (2016). Aerobic and anaerobic cellulase production by *Cellulomonas uda*. *Archives of Microbiology*, 198(8), 725–735. <https://doi.org/10.1007/s00203-016-1230-8>
- Rivett, M. O., Buss, S. R., Morgan, P., Smith, J. W. N., & Bemment, C. D. (2008). Nitrate attenuation in groundwater: A review of biogeochemical controlling processes. *Water Research*, 42(16), 4215–4232. <https://doi.org/10.1016/j.watres.2008.07.020>
- Robertson, W. D. (2010). Nitrate removal rates in woodchip media of varying age. *Ecological Engineering*, 36(11), 1581–1587. <https://doi.org/10.1016/j.ecoleng.2010.01.008>
- Schipper, L. A., Robertson, W. D., Gold, A. J., Jaynes, D. B., & Cameron, S. C. (2010a). Denitrifying bioreactors-An approach for reducing nitrate loads to receiving waters. *Ecological Engineering*, 36(11), 1532–1543. <https://doi.org/10.1016/j.ecoleng.2010.04.008>
- Schipper, L. A., Cameron, S. C., & Warneke, S. (2010b). Nitrate removal from three different effluents using large-scale denitrification beds. *Ecological Engineering*, 36(11), 1552–1557. <https://doi.org/10.1016/j.ecoleng.2010.02.007>
- Seitzinger, S., Harrison, J., Bohlke, J., Bouwman, A., Lowrance, R., Peterson, B., ... Van Drecht, G. (2006). Denitrification across landscapes and waterscapes: a synthesis. *Ecological Applications*, 16(6), 2064–2090. [https://doi.org/10.1890/1051-0761\(2006\)016\[2064:DALAWA\]2.0.CO;2](https://doi.org/10.1890/1051-0761(2006)016[2064:DALAWA]2.0.CO;2)
- Smith, M. S., & Zimmerman, K. (1981). Nitrous Oxide Production by Nondenitrifying Soil Nitrate Reducers I. *Soil Science Society of America Journal*, 45(5), 865. <https://doi.org/10.2136/sssaj1981.03615995004500050008x>
- Takaya, N., Catalan-sakairi, M. A. B., Sakaguchi, Y., Kato, I., Zhou, Z., & Shoun, H. (2003). Aerobic Denitrifying Bacteria That Produce Low Levels of Nitrous Oxide Aerobic Denitrifying Bacteria That Produce Low Levels of Nitrous Oxide. *Appl. Environ. Microbiol.*, 69(6), 3152–3157. <https://doi.org/10.1128/AEM.69.6.3152>
- Thayer, D.W., Lowther, S.V., and Phillips, J.G. (1984) Cellulolytic Activities of Strains of the Genus *Cellulomonas*. *International Journal of Systematic and Evolutionary Microbiology* 34: 432-438.
- Tiedje, J. M., Sexstone, A. J., Myrold, D. D., & Robinson, J. A. (1983). Denitrification: ecological niches, competition and survival. *Antonie van Leeuwenhoek*, 48(6), 569–583. <https://doi.org/10.1007/BF00399542>

- Tiedje, J. M. (1988). Ecology of denitrification and dissimilatory nitrate reduction to ammonium. *Environmental Microbiology of Anaerobes*, (April), 179–244.
- Wang, P., Li, X., Xiang, M., & Zhai, Q. (2007). Characterization of Efficient Aerobic Denitrifiers Isolated from Two Different Sequencing Batch Reactors by 16S-rRNA Analysis. *Journal of Bioscience and Bioengineering*, 103(6), 563–567.
- Warneke, S., Schipper, L. A., Matiasek, M. G., Scow, K. M., Cameron, S., Bruesewitz, D. A., & McDonald, I. R. (2011). Nitrate removal, communities of denitrifiers and adverse effects in different carbon substrates for use in denitrification beds. *Water Research*, 45(17), 5463–5475. <https://doi.org/10.1016/j.watres.2011.08.007>
- Yoshinari, T., and R. Knowles. 1976. Acetylene inhibition of nitrous oxide reduction by denitrifying bacteria. *Biochemical and Biophysical Research Communications* 69:705–710.
- Zhang H., Zhou S. (2016) Screening and Cultivation of Oligotrophic Aerobic Denitrifying Bacteria. In: Huang T. (eds) Water Pollution and Water Quality Control of Selected Chinese Reservoir Basins. The Handbook of Environmental Chemistry, vol 38. Springer, Cham

Appendix C.

Cold-Adapted Denitrifying Bacteria in Woodchip Bioreactors

Jeonghwan Jang¹, Emily L. Anderson², Rodney T. Venterea^{2,3}, Michael J. Sadowsky^{1,2}, Carl Rosen², Gary W. Feyereisen³, Satoshi Ishii^{1,2}

¹BioTechnology Institute, University of Minnesota, St. Paul, MN

²Department of Soil, Water, and Climate, University of Minnesota, St. Paul, MN

³USDA-ARS, Soil and Water Management Research Unit, St. Paul, MN

* Corresponding author: Dr. Satoshi Ishii, BioTechnology Institute, University of Minnesota, 1479 Gortner Ave., 140 Gortner Labs, St. Paul, MN. Email: ishi0040@umn.edu

Running title: Denitrifiers in woodchip bioreactor

Originality-Significance statement

This work combined comparative 16S rRNA (gene) sequencing analysis and culture-based methods to identify cold-adapted denitrifiers in woodchip bioreactors, which is used to remove nitrate from subsurface drainage in agricultural fields. Physiological and genome analyses revealed that some novel cold-adapted denitrifiers could break down cellulose and use it for denitrification. This study significantly advances our scientific knowledge in the ecology of denitrifiers, and contributes to improve water quality in agricultural fields.

Summary

Woodchip bioreactor technology removes nitrate from agricultural subsurface drainage by using denitrifying microorganisms. Although woodchip bioreactors have demonstrated success in many field locations, low water temperature can significantly limit bioreactor efficiency and performance. To improve bioreactor performance, it is important to identify the microbes responsible for nitrate removal under low temperature conditions. Therefore, in this study, we identified and characterized low temperature-adapted denitrifiers by using culture-independent and -dependent approaches. By comparative 16S rRNA (gene) analysis and culture isolation technique, *Pseudomonas* spp., *Polaromonas* spp., and *Cellulomonas* spp. were identified as being important bacteria responsible for denitrification in woodchip bioreactor microcosms under low temperature conditions (15°C). Genome analysis of *Cellulomonas* sp. strain WB94 confirmed the presence of nitrite reductase gene *nirK*. Transcription levels of this *nirK* were significantly higher in the denitrifying microcosms than in the non-denitrifying microcosms. Strain WB94 was also capable of degrading cellulose and other complex polysaccharides. Taken together, our results suggest that *Cellulomonas* sp. denitrifiers could degrade woodchips to provide C source and electron donors to themselves and other denitrifiers in woodchip bioreactors. By inoculating these cold-adapted denitrifiers (i.e., bioaugmentation), it might be possible to increase the nitrate removal rate of woodchip bioreactors under cold temperature conditions.

Introduction

Nitrogen (N) and phosphorus (P) are the most important nutrients in fertilizers for agriculture. While some of them are taken up by plants or adsorbed to minerals or organic matter, a proportion of the nutrients can be leached from agricultural fields into rivers, lakes, and oceans, causing eutrophication (USEPA, 2008; MPCA, 2014). Agricultural runoff water from the Upper Midwest States is considered a major cause of the hypoxic zone, also known as the dead zone, in the Gulf of Mexico (USEPA, 2008).

Large amounts of nutrients are released from agricultural fields through subsurface (tile) drainage, which is installed to improve soil conditions for root growth and soil trafficability for timely planting and harvesting (Bhattarai et al., 2005). While artificial subsurface drainage has increased agricultural productivity, it has also increased the amount of nutrients, especially nitrate, released from fields into surrounding waterways (Gentry et al., 1998).

One approach to remove nitrate from subsurface drainage water is to install denitrifying bioreactors at the end of the drainpipes before water is discharged to ditches or streams (Warneke et al., 2011). A woodchip bioreactor is a subsurface trench filled with woodchips through which drainage water passes. The woodchips provide a C and energy source to denitrifying microorganisms (Schipper et al., 2010; Ghane et al., 2015). Although woodchip bioreactors have demonstrated success in nitrate removal in many field locations (Christianson et al., 2012), low water temperature during the cold seasons significantly limits bioreactor performance (Christianson et al., 2012; David et al., 2016), which is likely related to the low metabolic activity of denitrifying microorganisms under low temperatures. In addition to cold temperatures (<5°C) in winter and early spring, water temperature usually ranges only from 10 to 20°C throughout the remainder of the year (Ghane et al., 2015), implying that microorganisms

adapted to low temperatures might play important roles for nitrate removal more generally within woodchip bioreactors.

Previous woodchip bioreactor research has focused largely on the hydrology and engineering aspects of the system (Ghane et al., 2015; Lepine et al., 2016; Sharrer et al., 2016), although microorganisms play key roles in the technology. There have been a few reports on the microbial communities in woodchip bioreactors by using quantitative PCR (qPCR) or restriction fragment length polymorphism (RFLP) targeting denitrification functional genes (Warneke et al., 2011; Hathaway et al., 2015; Healy et al., 2015; Porter et al., 2015). However, it is still unclear which specific microorganisms are responsible for nitrate removal in woodchip bioreactors. This is partly due to difficulties in identifying denitrifying microorganisms. Denitrifying ability is sporadically distributed among taxonomically diverse groups of bacteria, archaea and fungi (Knowles, 1982; Zumft, 1997; Ishii et al., 2009). Both denitrifying and non-denitrifying strains can be present in the same genus; therefore, it is difficult to identify denitrifying organisms based on taxonomic information alone. In addition, denitrifiers in different taxa can have almost identical denitrification functional gene sequences (Philippot, 2002; Jones et al., 2008; Ishii et al., 2011). Therefore, it is also difficult to identify microorganisms based on the denitrification functional gene sequence information.

More recently, comparative 16S rRNA gene sequencing analyses has been successfully used to identify denitrifying microorganisms (Ishii et al., 2009). In this approach, microbial communities under different conditions (i.e., denitrification and non-denitrification conditions) are compared to identify microorganisms that increased their abundance under denitrification conditions. This is based on the assumption that microorganisms that grow or become more active under denitrification conditions are most likely denitrifiers. This assumption was proven

feasible because most denitrifiers identified by the comparative 16S rRNA gene sequencing analysis (Ishii et al., 2009) were later isolated and confirmed as bona fide denitrifiers (Ishii et al., 2011).

In this study, we used the comparative 16S rRNA (gene) sequencing analysis to identify nitrate-reducing and denitrifying microorganisms active at the low temperature conditions found in a woodchip bioreactor. We used both DNA and RNA to identify total and metabolically active microorganisms, respectively (Gremion et al., 2003; Yoshida et al., 2012). In addition, we isolated nitrate-reducing and denitrifying microorganisms from the same woodchip samples. By characterizing these microorganisms, it may be possible to develop a strategy to enhance denitrification activity of woodchip bioreactors using bioaugmentation and biostimulation strategies. Consequently, the objective of this study was to (i) identify low temperature-adapted denitrifiers by comparative 16S rRNA (gene) analysis, (ii) isolate low temperature-adapted denitrifiers by culture method, and (iii) characterize these denitrifying strains.

Results

Occurrence of denitrification in the microcosms. To identify cold-adapted denitrifiers in the woodchip bioreactors, we established a series of reproducible woodchip bioreactor microcosms to evaluate the following five treatments: (i) W, woodchip without incubation, (ii) WINA, woodchip microcosm incubated with nitrate and acetate; (iii) WIN, woodchip microcosm incubated with nitrate but without acetate; (iv) WIA, woodchip microcosm incubated with acetate but without nitrate; and (v) WI, woodchip microcosm incubated without nitrate and acetate.

Accumulation of N₂O was observed in the microcosms supplemented with nitrate regardless of the addition of acetate (Fig. 1), suggesting that denitrification occurred in these conditions (i.e., treatments WINA and WIN). The N₂O concentrations were not significantly different ($p = 0.7084$ by ANOVA) between WINA and WIN treatments and nitrous oxide was not detected in the microcosms without addition of nitrate, indicating that denitrification did not occur in these conditions (i.e., treatments WIA, and WI). Concentrations of N₂O in the microcosms incubated ≥ 24 h were significantly larger ($p < 0.05$ by ANOVA) than those incubated ≤ 12 h, suggesting that denitrification activity greatly increased after 12 h.

Microbial communities in the microcosms. RNA and DNA were extracted from the microcosms after 0-, 24-, 36-, and 48-h incubations, and used for the microbial community analyses (Table S1). A total of 2,731,477 and 3,741,963 sequence reads were obtained from 39 DNA and 39 cDNA samples, respectively. The number of sequences per sample ranged from 28,609 to 115,611 and from 21,530 to 181,499 for DNA and cDNA samples, respectively. Numbers of sequences were normalized to the smallest number among the DNA and cDNA samples by random subsampling for further downstream analyses. The subsampled sequences provided sufficient resolution of the microbial communities, as indicated by Good's coverage ranging from 0.962 to 0.979 (Table S2) and by analysis of rarefaction curves (Fig. S1).

Table S2 also shows species richness estimated by observed operational taxonomic units (OTUs) and Chao1 index, and species diversity represented by Shannon and Simpson indices, for microbial community in each DNA and cDNA sample. These diversity indices were significantly lower in the microbial communities from the woodchips incubated with nitrate (i.e., treatments WINA and WIN) than those from the woodchips incubated without nitrate (i.e., treatments WIA and WI) ($p < 0.05$ by ANOVA). However, no significant differences were

observed between the microbial communities from the woodchips incubated with acetate (i.e., treatments WINA and WIA) and those from the woodchips incubated without acetate (i.e., treatments WIN and WI) ($p > 0.05$ by ANOVA). This suggested that α diversity in a microbial community is more influenced by the nitrate addition than by the addition of acetate. Moreover, the addition of nitrate influenced the β diversity as well. Microbial communities in the microcosms incubated with nitrate (i.e., treatments WINA and WIN) clustered differently from those in the microcosms incubated without nitrate (i.e., treatments WIA and WI) based on principal coordinate analysis (PCoA) plots with Bray-Curtis dissimilarity for both DNA (Fig. 2A) and cDNA (Fig. 2B) samples. No clustering of microbial communities was observed by acetate addition (Fig. 2A and 2B), suggesting that the addition of external C source such as acetate had minimal impact on α and β diversities of the microbial communities.

Microbial taxa responsive to denitrification. The OTUs responsive to the denitrification-inducing conditions were identified by comparative 16S rRNA (gene) analysis (Fig. 3). OTUs (266 and 232) were identified as having different relative abundance between three sample types (i.e., microcosms incubated with nitrate [treatments WINA and WIN], microcosms incubated without nitrate [treatments WIA and WI], and no incubation control [treatment W]) by ANOVA test (FDR $p < 0.05$), for DNA and cDNA samples, respectively. Among the 266 OTUs identified in the DNA analysis, those classified to the genera *Dechloromonas*, *Flavobacterium*, *Hydrogenphaga*, *Janthinobacterium*, *Mycoplana*, *Polaromonas*, and *Pseudomonas* were significantly more abundant in microcosms incubated with nitrate addition than those incubated without nitrate (Fig. 3A). Among the 232 OTUs identified in the RNA (cDNA) analysis, those classified to the genera *Agrobacterium*, *Cellulomonas*, *Cryobacterium*, *Devosia*, *Mycoplana*, *Polaromonas*, *Propionicimonas*, *Pseudomonas*, and *Sphingobium* were significantly more

abundant in microcosms incubated with nitrate addition than those incubated without nitrate (Fig. 3B). Since these OTUs increased their abundance in response to denitrifying conditions, they are most likely denitrifiers or nitrate reducers. *Pseudomonas* and *Polaromonas* were significantly more abundant in denitrifying conditions than non-denitrifying conditions for both DNA and RNA samples, indicating that they were active and rapidly growing denitrifiers in the woodchip samples at relatively cold conditions (15°C).

Denitrifiers isolated from the woodchip bioreactors. A total of 21 isolates were identified as nitrate-reducing and N₂O-producing bacteria by the acetylene inhibition assay. Most isolates belonged to three genera: *Cellulomonas* (3 strains), *Clostridium* (14 strains), and *Microvirgula* (3 strains). Since bacteria reducing nitrate to ammonium (i.e., dissimilatory nitrite reduction to ammonium; DNRA) can also produce N₂O in the acetylene inhibition test (Tiedje, 1994), we measured concentrations of nitrate and ammonium to discriminate DNRA bacteria from denitrifying bacteria. Bacteria that reduced >10% of nitrate to ammonium were considered as DNRA bacteria. By this analysis, four strains of *Clostridium* spp. and one *Cellulomonas* spp. strains remained as denitrifying bacteria (Table S3).

The genus *Cellulomonas* was commonly detected by both culture-dependent and – independent approaches. Compared with the control microcosms, the abundance of members of the genus *Cellulomonas* significantly increased in the RNA samples collected from the denitrifying microcosms ($p < 0.05$ by ANOVA), but not in those collected from the non-denitrifying microcosms ($p = 0.33$ by ANOVA) (Fig. 4). Taken together, these results suggested that *Cellulomonas* spp. strains are likely one of the most active denitrifying bacteria in the woodchip bioreactor samples.

Whole genome sequencing of *Cellulomonas* sp. strain WB94. The presence of denitrification functional genes could not be detected by PCR with commonly used primers. To identify genes related to denitrification and cellulose degradation, we sequenced the genome of *Cellulomonas* sp. strain WB94 by using the PacBio platform. The genome of strain WB94 (accession number NZ_QEES000000000) was represented by seven contigs, with a total genome size of 3,868,980 bp and mole% G+C content ranging from 0.70 to 0.73% (Table S4). The genome contained 3,387 protein-coding sequences (CDS), 137 pseudogenes, 46 tRNAs, six rRNAs (two rRNA operons), and three noncoding RNAs. The average nucleotide identity (ANI) between the genomes of strain WB94 and *Cellulomonas cellasea* DSM 20118 were 98%, which is greater than the cutoff value for species discrimination (95% to 96%) (Goris et al., 2007; Richter and Rosselló-Móra, 2009). Therefore, strain WB94 most likely belonged to *Cellulomonas cellasea*.

The genome of Strain WB94 harbored the nitrate reductase genes *narIJHG* and *napA* as well as the dissimilatory NO-forming nitrite reductase gene *nirK* (Table S5), suggesting that Strain WB94 can reduce nitrate to nitrite and to nitric oxide. The deduced NirK amino acid sequence was most closely related to the NirK from *Actinosynnema mirum* DSM43827 [CP001630], but was also similar to those from other *Cellulomonas* species (>57% identity) (Fig. 5). Other denitrification-related genes were not found on the genome. The genome also contained the assimilatory NAD(P)H-dependent nitrite reductase genes *nirBD*, suggesting that Strain WB94 can use nitrate and nitrite as a N source. The genome also contained genes related to the biodegradation of complex polysaccharides, including cellulose, xylan, starch and glycogen (Table S5).

Role of *Cellulomonas* spp. in the woodchip bioreactors. To verify the role of *Cellulomonas* spp. in the woodchip bioreactor microcosm, we measured the transcription levels of *Cellulomonas nirK* (Fig. 6). Levels of *nirK* transcription were significantly higher in the denitrifying microcosms than in non-denitrifying microcosms ($p < 0.01$ by ANOVA). Interestingly, however, the *nirK* transcription levels in the no incubation controls were also significantly greater than those in the non-denitrifying microcosms ($p < 0.01$ by ANOVA) but not significantly different from those in the denitrifying microcosms ($p = 0.87$). The biodegradation of cellulose by *Cellulomonas* sp. Strain WB94 was also verified by using the cellulase assay (data not shown).

Discussion

While woodchip bioreactor technology is a promising approach to reduce nutrient loading from agricultural fields to surrounding and downstream water bodies (E. Christianson et al., 2012), limited research has been done to identify low temperature-adapted denitrifiers in these bioreactors. In this study, we used both culture-dependent and -independent approaches to identify nitrate-reducing and denitrifying microorganisms active at low temperature conditions in a woodchip bioreactor.

Similar amounts of N_2O were produced from triplicate woodchip bioreactor microcosms, suggesting that denitrification occurred reproducibly in the microcosms used in this study. The amount of N_2O significantly increased after 12-h incubation at $15^\circ C$, suggesting that the microorganisms actively performed denitrification after 12 h. Addition of acetate did not increase the amount of N_2O produced, indicating that C was not limited. This lack of improvement in nitrate removal rate with acetate addition to woodchips is in contrast to a recent

laboratory column study that showed enhanced performance at 15 and 5°C (Roser et al., 2018). Others have shown that woodchip nitrate removal performance is negatively affected as the woodchips age (Robertson, 2010; David et al., 2016). Thus, in the current study, even though 4-year old woodchips were used, there was still enough C available for denitrification from the woodchips that the addition of readily available C (acetate) did not enhance denitrification rate. This difference could be methodological or attributed to a robust microbial community in this experiment.

A comparative 16S rRNA (gene) sequencing approach was used to identify nitrate-reducing and denitrifying microorganisms. A similar approach was previously successfully used to identify denitrifying bacteria in rice paddy soils (Ishii et al. 2009). While this previous study used conventional clone library analysis with >1,000 clones/library, here we used Illumina MiSeq high-throughput sequencing technology with >20,000 reads/sample. As a result, we sequenced enough DNA to cover the majority of microorganisms in the samples. In addition, Ishii et al. (2009) only used DNA samples, whereas here we sequenced the 16S rRNA (gene) from both DNA and RNA to identify total and metabolically active microorganisms, respectively. Sequencing 16S rRNA was previously shown useful to detect metabolically active microorganisms (Gremion et al., 2003; Yoshida et al., 2012) because more ribosomes are present in metabolically active cells than resting or starved cells (Nomura et al., 1984). Microbial community structures were different between DNA- and RNA-based analyses, similar to previous studies (Gentile et al., 2006; Moeseneder Markus et al., 2006; Lanzén et al., 2011), suggesting that only parts of the microbial populations were active in the environments.

Several genera were identified as potential nitrate-reducing and denitrifying bacteria. *Pseudomonas* spp. and *Polaromonas* spp. were commonly detected both by DNA- and RNA-

based analyses. The genus *Pseudomonas* includes well-studied denitrifying strains such as *Pseudomonas stutzeri* strain ZoBell and *Pseudomonas aeruginosa* strain PAO1 and is reported to be one of the most active denitrifiers in natural environments (Knowles, 1982). In addition, some strains such as *P. aeruginosa* strain PKE117 and *Pseudomonas putida* strain mt-2 strains are reported to have strong extracellular lignin peroxidase activities to degrade woodchips (Yang et al., 2007; Ahmad et al., 2010), suggesting that *Pseudomonas* spp. could perform denitrification and use woodchips as a C source. *Polaromonas* species are also known to be psychrophiles with temperature optima 4-12°C (Irgens et al., 1996). Nitrate reduction of the *Polaromonas* strains have been reported (Mattes et al., 2008; Margesin et al., 2012), and a complete set of denitrification functional genes is present in the draft genome of *Polaromonas glacialis* R3-9 strain (GenBank accessions NZ_KL448323 and NZ_KL448327) (Wang et al., 2014), suggesting that *Polaromonas* spp. could perform denitrification at low temperature conditions.

Some genera were detected by the DNA- or the RNA-based analyses, but not by both methods. For example, the genera *Cellulomonas*, *Cryobacterium*, *Propionicimonas*, *Devosia*, *Agrobacterium*, and *Sphingobium* were detected only by the RNA-based analysis. The difference may be due to the growth rates of bacteria. Metabolically active cells may also replicate and increase their rRNA gene copies in the environment; however, there is a time lag between metabolic activity and genome replication (Rolfe et al., 2012). Therefore, active but slow-growing bacteria may not always be detected by the DNA-based analysis.

Cellulomonas spp. were commonly detected by both culture-independent analysis and culture-dependent isolation methods. Other genera identified as nitrate-reducing and denitrifying bacteria by the culture-independent analysis were not obtained by our isolation method, probably

due to the bias caused by the medium used (i.e., R2A-NA). Growth media can largely influence results of bacterial isolation (Davis et al., 2005).

Although denitrification by *Cellulomonas* strains has not been reported thus far, an incomplete set of denitrification functional genes (e.g., *narG* and *nirK*) is present in several genomes of the *Cellulomonas* sp. strains (GenBank accessions CP001964, CP002665, CP002666, and CP021430). Our *Celluomonas* sp. strain WB94 also possessed denitrification functional genes, including *narG* and *nirK*, and was able to reduce nitrate. The *nirK* of Strain WB94 was similar to those from other *Cellulomonas* species. Transcription levels of the *Cellulomonas nirK* were significantly higher in the denitrifying microcosms than the non-denitrifying microcosms, suggesting that *Cellulomonas* strains were actively involved in denitrification process in woodchip bioreactors. Genes responsible for nitric oxide (NO) reductase were not found on the genome. Since WB94 produced N₂O by the acetylene inhibition assay, this strain should have NO reductase on its genome. Further data mining is necessary to identify the NO reductase of this strain.

Cellulomonas spp. are also well known for their ability to use endoglucanases and exoglucanases to degrade cellulose (Thayer et al., 1984). Our strain, *Cellulomonas* sp. strain WB94, also had the ability to degrade cellulose. In addition, various genes related to the biodegradation of complex polysaccharides were found on the genome of Strain WB94. These results suggest that *Cellulomonas* spp. could play an important role in nitrate reduction as well as degradation of woodchips.

Conclusions

Based on a series of culture-independent and –dependent analyses, we identified *Pseudomonas* spp., *Polaromonas* spp., and *Cellulomonas* spp. as being important bacteria responsible for nitrate reduction and denitrification in woodchip bioreactor microcosms under relatively cold temperature conditions. Since *Cellulomonas* spp. identified in this study can also degrade cellulose and other complex polysaccharides, they may provide a C source and electron donors to themselves and other denitrifiers in woodchip bioreactors. By inoculating these cold-adapted denitrifiers (i.e., bioaugmentation), it might be possible to increase the nitrate removal rate of woodchip bioreactors under cold temperature conditions.

This microcosm-based study was designed to mimic field conditions of N concentration and temperature, but the study's batch method differed from the continuous flow of field bioreactors. To examine if the low temperature-adapted denitrifiers identified in this study are also active in the field conditions, it is necessary to analyze samples collected from the field, which should be done in the future.

Experimental Procedures

Woodchip bioreactor microcosms. Woodchip samples were collected from a field bioreactor near Willmar, MN, on 2 October 2014. Woodchip samples were kept at 4°C until used. Five grams of woodchips were placed in 210-mL vials, and mixed with 5 mL of synthetic tile drain water (see Table S6 for chemical composition) supplemented with or without 3.57 mM nitrate (50 ppm as N) and/or 3.95 mM acetate. Nitrate concentrations of 50 ppm-N have been observed in tile drain water in the field (Gamble et al., 2018). The concentration of acetate used provided a C/N molar ratio of around 2.0, which was previously reported as the minimum value needed to reduce almost all of the nitrate to dinitrogen (N₂) gas (Her and Huang, 1995). The vial

headspace was replaced with N₂ and acetylene (C₂H₂), in a 90:10 ratio, for measuring denitrification via the accumulation of N₂O (Tiedje 1994), or with N₂ alone for microbial analysis. In both cases, microcosms were incubated at 15°C for up to 48 h. A total of five treatments were prepared: (i) W, woodchip without incubation, (ii) WINA, woodchip microcosm incubated with nitrate and acetate; (iii) WIN, woodchip microcosm incubated with nitrate but without acetate; (iv) WIA, woodchip microcosm incubated with acetate but without nitrate; (v) WI, woodchip microcosm incubated with neither nitrate nor acetate.

To determine the occurrence of denitrification, microcosms were incubated in triplicate at 15°C with the vial headspace containing 10% C₂H₂. The concentration of N₂O in the head space was measured at 0, 4, 8, 12, 24, 36, and 48 h after incubation, by using a gas chromatograph (GC) (Model 5890, Hewlett-Packard/Agilent Technologies) equipped with an electron capture detector and PoraPak Q column (Sigma-Aldrich) as previously described (Maharjan and Venterea, 2013).

RNA and DNA extractions. For RNA and DNA extractions, a different set of woodchip microcosms were prepared with the vial headspace filled with 100% N₂. Nine vials were prepared for each treatment (a total of 36 vials). The microcosms were incubated as described above. Three microcosms were sacrificed 24, 36, and 48 h after incubation, and the RNA and DNA were extracted from woodchip samples (2 g) collected from each of the microcosms. In addition, RNA and DNA were extracted from woodchip samples (n=3) without incubation (treatment W).

RNA and DNA were extracted by using a PowerSoil RNA Isolation kit (MOBIO, Carlsbad, CA) and RNA PowerSoil DNA Elution Accessory kit (MOBIO, Carlsbad, CA), respectively, according to the manufacturer's instructions. For the extracted RNA samples,

possible genomic DNA residue was removed using Turbo DNA free kit (Ambion, Austin, TX). No DNA contamination in the resulting RNA samples was confirmed by PCR targeting the 16S rRNA gene as described previously (Ishii et al., 2016). Complementary DNA (cDNA) was synthesized from the RNA samples (200 ng) by using PrimeScript RT Reagent kit (Takara Bio, Mountain View, CA) according to the manufacturer's instructions.

Microbial community analysis. Thirty nine DNA and cDNA samples shown in Table S1 were individually used to amplify the V4 region of the 16S rRNA gene and 16S rRNA using the 515F-806R primer set, respectively, as described previously (Caporaso et al., 2012). Resulting amplicons were purified and used to prepare Illumina sequencing libraries with the TruSeq kit (Illumina, San Diego, CA). Paired-end sequencing reaction was done using a MiSeq platform (Illumina) with V3 chemistry (300-bp read length) at the University of Minnesota Genomics Center (Minneapolis, MN).

The paired-end raw read data were assembled, quality-filtered and trimmed using NINJA-SHI7 (Al-Ghalith GA, 2017), which is a fastq-to-combined-fasta processing pipeline. The assembled sequences were clustered into OTUs at 97% sequence similarity using NINJA-OPS (Al-Ghalith et al., 2016), which is a complete OTU-picking pipeline with advantage of the Burrows-Wheeler alignment using BowTie2. The resulting OTU tables, in sparse BIOM 1.0 format, were used for further statistical analyses done using QIIME 1.9.1 (Caporaso et al., 2010). Taxonomic assignment of the OTUs were done using the Greengenes 97 reference data set (McDonald et al., 2011).

Culture-independent identification of denitrifiers. Microbes responsive to the denitrification-inducing conditions (i.e., denitrifiers) were identified by comparing the microbial communities in denitrification-inducing conditions (i.e., treatments WINA and WIN) and those

in non-denitrification conditions (i.e., treatments WIA and WI). The following steps were used for this analysis: 1) OTUs showing more than 1% relative abundance in at least one of the triplicate samples were chosen as major and represented microbial taxa; 2) OTUs showing a significant difference between the three sample types (i.e., microcosms incubated with nitrate [treatments WINA and WIN], microcosms incubated without nitrate [treatments WIA and WI], and no incubation control [treatment W]) were identified by analysis of variance (ANOVA) test (FDR $p < 0.05$); and 3) OTUs that satisfied both steps 1 and 2 were visualized by heatmap analysis done with the Bray-Curtis distance indices. The OTU heatmaps were created by the heatmap.2 and vegdist subroutines within the gplots and vegan packages, respectively, for R.

Isolation and identification of denitrifiers. Denitrifying bacteria were also directly isolated from the woodchip samples collected from the same field bioreactor near Willmar, MN. In brief, 1 g of the woodchip sample was mixed with phosphate buffered saline (PBS, pH 7.4). The woodchip suspension was then spread-plated onto R2A agar plates, supplemented with 5 mM nitrate and 10 mM acetate (R2A-NA). The plates were incubated under anaerobic conditions, by using AnaeroPak system (Mitsubishi Gas Chemical), at 15°C for 1 to 2 weeks. Colonies were picked and restreaked onto new R2A-NA agar plates to obtain well-isolated single colonies.

The ability of the strains to denitrify was examined by using the acetylene inhibition assay (Tiedje, 1994). In brief, fresh cell cultures (300 μ l) were inoculated into R2A-NA broth (10 ml) in 27 ml test tubes. After replacing the air phase with Ar:C₂H₂ (90:10) gas, the test tubes were incubated at 30°C. After 2-week incubation, gas samples were taken via a gastight syringe and analyzed for N₂O production by GC as described above. In addition, liquid samples were collected and analyzed for nitrate, nitrite and ammonium concentrations using the SEAL AA3

HR AutoAnalyzer. Strains that reduced $\geq 40\%$ nitrate, converted $< 10\%$ of nitrate to ammonium, and produced significant amount of N_2O (> 100 ppm) were considered as denitrifiers. The GC system used in this study was too sensitive, and the upper quantification limit was often exceeded. Therefore, we could not calculate the percentage of nitrate reduced to N_2O .

Genomic DNA were isolated by heating cells in $100 \mu\text{l}$ 0.05 M NaOH at 95°C for 15 min (Ashida et al., 2010). After centrifugation, the supernatant was diluted 10 fold in MilliQ water, and used for PCR to amplify the 16S rRNA gene. The reaction mixture ($50 \mu\text{l}$) contained $1\times$ Ex Taq buffer (Takara Bio, Otsu, Japan), $0.2 \mu\text{M}$ of each primer (m-27F and m-1492R; (Tyson et al., 2004)), 0.2 mM of each dNTP, 1 U of Ex Taq DNA polymerase (Takara Bio), and $2 \mu\text{l}$ of DNA template. PCR was carried out using a Veriti™ Thermal Cyclers (Life Technologies) and the following conditions: initial annealing at 95°C for 5 min, followed by 30 cycles of 95°C for 30 s, 55°C for 30 s and 72°C for 90 s, and one cycle of 72°C for 7 min. Amplification was confirmed by using agarose gel electrophoresis. The PCR products were purified using AccuPrep PCR Purification Kit (Bioneer) and then quantitated using PicoGreen dsDNA quantitation assay (Thermo Scientific). The purified PCR products were sequenced by the Sanger method using a 3730xl DNA Analyzer (Applied Biosystems) at the University of Minnesota Genomics Center. The forward (m-27F) and reverse (m-1492R) reads were assembled using the phred, phrap, consed software (Ewing et al.). Strain identity was determined by using a Naïve Bayesian classifier (Wang et al., 2007).

Whole genome sequencing. *Cellulomonas* sp. strain WB94 was selected for genome sequencing since this bacterium increased its relative abundance under denitrifying conditions based on the comparative 16S rRNA sequencing analysis. Genomic DNA was extracted from pure cell cultures using PowerSoil DNA Isolation Kit (MOBIO) according to the manufacturer's

instructions. Sequencing libraries were prepared using the PacBio SMRT kit (Pacific Biosciences), and the genome was analyzed by using the PacBio RS II platform (Pacific Biosciences). Extracted DNA was used to generate a SMRTbell library (20 kbp insert) which was sequenced at the Mayo Clinic's Molecular Biology Core (Rochester, MN). After quality filtering, reads were assembled de novo using the hierarchical genome assembly process (HGAP3) in the SMRT Link portal (v 2.3.0). Genome annotation was done using the NCBI Prokaryotic Genome Annotation Pipeline (Tatusova et al., 2016). Average Nucleotide Identity (ANI) values were calculated using JSpecies (Richter and Rosselló-Móra, 2009).

Transcription analysis of the *Cellulomonas nirK*. Primers WB94_nirK_F (5'-AGACGCTGTGGACCTACAAC-3') and WB94_nirK_R (5'-CGACGAACTGGTACGTCAAC-3') were designed based on the genome sequence of *Cellulomonas* sp. WB94 and used to amplify *nirK* transcripts of *Cellulomonas*. The reaction mixture for qPCR (10 μ L) contained 1 \times SYBR Premix ExTaq ROX plus (Takara Bio), 0.2 μ M each primer, and 2 μ L of cDNA samples. The qPCR was performed using StepOnePlus Real-Time PCR System v. 2.3 (Applied Biosystem) with the following conditions: 95°C for 30 sec., followed by 45 cycles of 95°C for 5 sec, 60°C, and 83°C for 30 sec. Melting curve analysis and agarose gel electrophoresis were done to confirm correct amplification of the PCR products. In addition to the *Cellulomonas nirK*, the quantity of 16S rRNA was measured by qPCR with Eub338 (5'-ACTCCTACGGGAGGCAGCAG-3') and Eub518 (5'-ATTACCGCGGCTGCTGG-3') primers (Muyzer et al., 1993). Levels of *nirK* transcripts were normalized using the quantity of 16S rRNA.

Statistical analyses. The PAST software was used to perform one-way ANOVA test to analyze statistical significance in the quantitative data obtained in microcosm treatments (Hammer, 2001).

Nucleotide sequence accession numbers. The 16S rRNA amplicon sequences were deposited to the Short Read Archive under accession number SRP149200. The 16S rRNA gene sequences of the isolated strains and the whole genome sequence of strain WB94 have been deposited in the DDBJ/EMBL/GenBank databases under accession numbers MH196452–MH196472 and NZ_QEES00000000, respectively.

Acknowledgments

This work was supported by Minnesota Department of Agriculture (Project No. 108837) and the Minnesota's Discovery, Research and Innovation Economy (MnDRIVE) initiative of the University of Minnesota. EA was supported, in part, by the USDA North Central Region Sustainable Agriculture Research and Education (NCR-SARE) Graduate Student Grant Program.

Conflicts of Interest

The authors declare no conflict of interests.

References

- Ahmad, M., Taylor, C.R., Pink, D., Burton, K., Eastwood, D., Bending, G.D., and Bugg, T.D.H. (2010) Development of novel assays for lignin degradation: comparative analysis of bacterial and fungal lignin degraders. *Mol Biosyst* **6**: 815-821.
- Al-Ghalith, G.A., Montassier, E., Ward, H.N., and Knights, D. (2016) NINJA-OPS: Fast Accurate Marker Gene Alignment Using Concatenated Ribosomes. *PLOS Comput Biol* **12**: e1004658.
- Al-Ghalith GA, A.K., Hillmann B, Shields-Cutler R, Knights D. (2017). SHI7: A streamlined short-read iterative trimming pipeline.
- Ashida, N., Ishii, S., Hayano, S., Tago, K., Tsuji, T., Yoshimura, Y. et al. (2010) Isolation of functional single cells from environments using a micromanipulator: application to study denitrifying bacteria. *Appl Microbiol Biotechnol* **85**: 1211-1217.
- Bhattarai, S.P., Huber, S., and Midmore David, J. (2005) Aerated subsurface irrigation water gives growth and yield benefits to zucchini, vegetable soybean and cotton in heavy clay soils. *Ann Appl Biol* **144**: 285-298.
- Caporaso, J.G., Lauber, C.L., Walters, W.A., Berg-Lyons, D., Huntley, J., Fierer, N. et al. (2012) Ultra-high-throughput microbial community analysis on the Illumina HiSeq and MiSeq platforms. *ISME J* **6**: 1621.
- Caporaso, J.G., Kuczynski, J., Stombaugh, J., Bittinger, K., Bushman, F.D., Costello, E.K. et al. (2010) QIIME allows analysis of high-throughput community sequencing data. *Nat Methods* **7**: 335.

- Christianson, L., Bhandari, A., Helmers, M., Kult, K., Sutphin, T., and Wolf, R. (2012) Performance evaluation of four field-scale agricultural drainage denitrification bioreactors in Iowa. *Trans ASABE* **55**: 2163.
- David, M.B., Gentry, L.E., Cooke, R.A., and Herbstritt, S.M. (2016) Temperature and substrate control woodchip bioreactor performance in reducing tile nitrate loads in east-central Illinois. *J Environ Qual* **45**:822–829.
- Davis, K.E.R., Joseph, S.J., and Janssen, P.H. (2005) Effects of growth medium, inoculum size, and incubation time on culturability and isolation of soil bacteria. *Appl Environ Microbiol* **71**: 826-834.
- Christianson, L.E., Bhandari, A., and Helmers, M.J. (2012) A practice-oriented review of woodchip bioreactors for subsurface agricultural drainage. *Appl Eng Agric* **28**: 861.
- Gentile G, Giuliano L, D'Auria G, Smedile F, Azzaro M, De Domenico M, Yakimov MM. (2006) Study of bacterial communities in Antarctic coastal waters by a combination of 16S rRNA and 16S rDNA sequencing. *Environ Microbiol* **8**: 2150-2161.
- Gamble, J.D., Feyereisen, G.W., Papiernik, S.K., Wentz, C.D., and Baker, J.M. (2018) Summer fertigation of dairy slurry reduces soil nitrate concentrations and subsurface drainage nitrate losses compared to fall injection. *Front Sustain Food Syst* **2**: 15
- Gentry, L.E., David, M.B., Smith, K.M., and Kovacic, D.A. (1998) Nitrogen cycling and tile drainage nitrate loss in a corn/soybean watershed. *Agric Ecosyst Environ* **68**: 85-97.
- Ghane, E., Fausey, N.R., and Brown, L.C. (2015) Modeling nitrate removal in a denitrification bed. *Water Res* **71**: 294-305.

- Goris, J., Konstantinidis, K.T., Klappenbach, J.A., Coenye, T., Vandamme, P., and Tiedje, J.M. (2007) DNA–DNA hybridization values and their relationship to whole-genome sequence similarities. *Int J Syst Evol Microbiol* **57**: 81-91.
- Gremion, F., Chatzinotas, A., and Harms, H. (2003) Comparative 16S rDNA and 16S rRNA sequence analysis indicates that Actinobacteria might be a dominant part of the metabolically active bacteria in heavy metal-contaminated bulk and rhizosphere soil. *Environ Microbiol* **5**: 896-907.
- Hammer, Ø., Harper, D.A.T., Ryan, P.D. (2001) PAST: Paleontological statistics software package for education and data analysis. *Palaeontol Electronica* **4**: 9.
- Hathaway, S.K., Porter, M.D., Rodríguez, L.F., Kent, A.D., and Zilles, J.L. (2015) Impact of the contemporary environment on denitrifying bacterial communities. *Ecol Eng* **82**: 469-473.
- Healy, M.G., Barrett, M., Lanigan, G.J., João Serrenho, A., Ibrahim, T.G., Thornton, S.F. et al. (2015) Optimizing nitrate removal and evaluating pollution swapping trade-offs from laboratory denitrification bioreactors. *Ecol Eng* **74**: 290-301.
- Her, J.-J., and Huang, J.-S. (1995) Influences of carbon source and C/N ratio on nitrate/nitrite denitrification and carbon breakthrough. *Bioresour Technol* **54**: 45-51.
- Irgens, R.L., Gosink, J.J., and Staley, J.T. (1996) *Polaromonas vacuolata* gen. nov., sp. nov., a psychrophilic, marine, gas vacuolate bacterium from Antarctica. *Int J Syst Evol Microbiol* **46**: 822-826.
- Ishii, S., Ashida, N., Otsuka, S., and Senoo, K. (2011) Isolation of oligotrophic denitrifiers carrying previously uncharacterized functional gene sequences. *Applied and Environmental Microbiology* **77**: 338-342.

- Ishii, S., Joikai, K., Otsuka, S., Senoo, K., and Okabe, S. (2016) Denitrification and nitrate-dependent Fe(II) oxidation in various *Pseudogulbenkiania* strains. *Microbes Environ* **31**: 293-298.
- Ishii, S., Yamamoto, M., Kikuchi, M., Oshima, K., Hattori, M., Otsuka, S., and Senoo, K. (2009) Microbial populations responsive to denitrification-inducing conditions in rice paddy soil, as revealed by comparative 16S rRNA gene analysis. *Appl Environ Microbiol* **75**: 7070-7078.
- Jones, C.M., Stres, B., Rosenquist, M., and Hallin, S. (2008) Phylogenetic analysis of nitrite, nitric oxide, and nitrous oxide respiratory enzymes reveal a complex evolutionary history for denitrification. *Mol Biol Evol* **25**: 1955-1966.
- Knowles, R. (1982) Denitrification. *Microbiol Rev* **46**: 43-70.
- Lanzén, A., Jørgensen, S.L., Bengtsson, M.M., Jonassen, I., Øvreås, L., and Urich, T. (2011) Exploring the composition and diversity of microbial communities at the Jan Mayen hydrothermal vent field using RNA and DNA. *FEMS Microbiol Ecol* **77**: 577-589.
- Lepine, C., Christianson, L., Sharrer, K., and Summerfelt, S. (2016) Optimizing hydraulic retention times in denitrifying woodchip bioreactors treating recirculating aquaculture system wastewater. *J Environ Qual* **45**: 813-821.
- Maharjan, B., and Venterea, R.T. (2013) Nitrite intensity explains N management effects on N₂O emissions in maize. *Soil Biol Biochem* **66**: 229-238.
- Margesin, R., Spröer, C., Zhang, D.-C., and Busse, H.-J. (2012) *Polaromonas glacialis* sp. nov. and *Polaromonas cryoconiti* sp. nov., isolated from alpine glacier cryoconite. *Int J Syst Evol Microbiol* **62**: 2662-2668.

- Mattes, T.E., Alexander, A.K., Richardson, P.M., Munk, A.C., Han, C.S., Stothard, P., and Coleman, N.V. (2008) The genome of *Polaromonas* sp. strain JS666: insights into the evolution of a hydrocarbon- and xenobiotic-degrading bacterium, and features of relevance to biotechnology. *Appl Environ Microbiol* **74**: 6405-6416.
- McDonald, D., Price, M.N., Goodrich, J., Nawrocki, E.P., DeSantis, T.Z., Probst, A. et al. (2011) An improved Greengenes taxonomy with explicit ranks for ecological and evolutionary analyses of bacteria and archaea. *ISME J* **6**: 610.
- Moeseneder, M.M., Arrieta, J.M., and Herndl, G.J. (2006) A comparison of DNA- and RNA-based clone libraries from the same marine bacterioplankton community. *FEMS Microbiol Ecol* **51**: 341-352.
- MPCA (2014) *The Minnesota Nutrient Reduction Strategy*. St. Paul, MN: Minnesota Pollution Control Agency.
- Muyzer, G., de Waal, E.C., and Uitterlinden, A.G. (1993) Profiling of complex microbial populations by denaturing gradient gel electrophoresis analysis of polymerase chain reaction-amplified genes coding for 16S rRNA. *Appl Environ Microbiol* **59**: 695-700.
- Nomura, M., Gourse, R., and Baughman, G. (1984) Regulation of the synthesis of ribosomes and ribosomal components. *Annu Rev Biochem* **53**: 75-117.
- Philippot, L. (2002) Denitrifying genes in bacterial and archaeal genomes. *BBA-Gene Struct Expr* **1577**: 355-376.
- Porter, M.D., Andrus, J.M., Bartolero, N.A., Rodriguez, L.F., Zhang, Y., Zilles, J.L., and Kent, A.D. (2015) Seasonal patterns in microbial community composition in denitrifying bioreactors treating subsurface agricultural drainage. *Microb Ecol* **70**: 710-723.

- Richter, M., and Rosselló-Móra, R. (2009) Shifting the genomic gold standard for the prokaryotic species definition. *Proc Natl Acad Sci USA* **106**: 19126-19131.
- Robertson, W.D. (2010) Nitrate removal rates in woodchip media of varying age. *Ecol Eng* **36**: 1581-1587.
- Rolfe, M.D., Rice, C.J., Lucchini, S., Pin, C., Thompson, A., Cameron, A.D.S. et al. (2012) Lag phase is a distinct growth phase that prepares bacteria for exponential growth and involves transient metal accumulation. *J Bacteriol* **194**: 686-701.
- Roser, M.B., Feyereisen, G.W., Spokas, K.A., Mulla, D.J., Strock, J.S., and Gutknecht, J. (2018) Carbon dosing increases nitrate removal rates in denitrifying bioreactors at low-temperature high-flow conditions. *J Environ Qual* **47**: 856-864.
- Schipper, L.A., Robertson, W.D., Gold, A.J., Jaynes, D.B., and Cameron, S.C. (2010) Denitrifying bioreactors—an approach for reducing nitrate loads to receiving waters. *Ecol Eng* **36**: 1532-1543.
- Sharrer, K.L., Christianson, L.E., Lepine, C., and Summerfelt, S.T. (2016) Modeling and mitigation of denitrification ‘woodchip’ bioreactor P releases during treatment of aquaculture wastewater. *Ecol Eng* **93**: 135-143.
- Yang, J.S., Ni, J.R., Yuan, H.L., and Wang, E. (2007) Biodegradation of three different wood chips by *Pseudomonas* sp. PKE117. *Int Biodeterior Biodegradation* **60**: 90-95.
- Tatusova, T., DiCuccio, M., Badretdin, A., Chetvernin, V., Nawrocki, E.P., Zaslavsky, L. et al. (2016) NCBI prokaryotic genome annotation pipeline. *Nucleic Acids Res* **44**: 6614-6624.
- Thayer, D.W., Lowther, S.V., and Phillips, J.G. (1984) Cellulolytic activities of strains of the genus *Cellulomonas*. *Int J Syst Evol Microbiol* **34**: 432-438.

- Tiedje, J. (1994) Denitrifiers. In *Methods of Soil Analysis Part 2: Microbiological and Biochemical Properties*. Weaver R.R., Angel, S., Bottomley, P., Bezdiecek, D., Smith, S., Tabatabai, A., Wollum, A. et al. (eds) Madison, WI: Soil Science Society of America, pp. 245-267.
- Tyson, G.W., Chapman, J., Hugenholtz, P., Allen, E.E., Ram, R.J., Richardson, P.M. et al. (2004) Community structure and metabolism through reconstruction of microbial genomes from the environment. *Nature* **428**: 37-43.
- USEPA (2008) Gulf Hypoxia Action Plan 2008. In: Force, M.R.G.o.M.W.N.T. (ed).
- Wang, Q., Garrity, G.M., Tiedje, J.M., and Cole, J.R. (2007) Naïve Bayesian classifier for rapid assignment of rRNA sequences into the new bacterial taxonomy. *Appl Environ Microbiol* **73**: 5261-5267.
- Wang, Z., Chang, X., Yang, X., Pan, L., and Dai, J. (2014) Draft genome sequence of *Polaromonas glacialis* strain R3-9, a psychrotolerant bacterium isolated from Arctic glacial foreland. *Genome Announc* **2**: e00695-00614.
- Warneke, S., Schipper, L.A., Matiasek, M.G., Scow, K.M., Cameron, S., Bruesewitz, D.A., and McDonald, I.R. (2011) Nitrate removal, communities of denitrifiers and adverse effects in different carbon substrates for use in denitrification beds. *Water Res* **45**: 5463-5475.
- Yoshida, M., Ishii, S., Fujii, D., Otsuka, S., and Senoo, K. (2012) Identification of active denitrifiers in rice paddy soil by DNA- and RNA-based analyses. *Microbes Environ* **27**: 456-461.
- Zumft, W.G. (1997) Cell biology and molecular basis of denitrification. *Microbiol Mol Biol Rev* **61**: 533-616.

Figure legends

Figure 1. N₂O production from the microcosms supplemented with nitrate (i.e., treatments WINA and WIN) during 48-h incubation. N₂O production was not observed from the microcosms without nitrate addition (i.e., treatments WIA and WI). Legends: ▲, microcosms incubated with nitrate and acetate (i.e., treatment WINA) and □, microcosms incubated with nitrate only (i.e., treatment WIN).

Figure 2. Principal coordinate analysis (PCoA) plots showing β diversity between microbial communities for (A) DNA and (B) cDNA samples. The β diversity was calculated using Bray-Curtis dissimilarity. Legends: Red, microcosms without incubation (i.e., treatment W); blue, microcosms incubated with acetate (i.e., treatments WINA and WIN); and orange, microcosms incubated without acetate (i.e., treatments WIN and WI). Microbial communities in the microcosms incubated with nitrate (i.e., treatments WINA and WIN) were clustered together.

Figure 3. Heatmaps showing relative abundance of sequence reads in operational taxonomic units (OTUs) for (A) DNA and (B) cDNA samples. Only OTUs that showed different abundance between incubation conditions are shown. Assigned genus names are shown for the OTUs that showed significant differences between the three sample types (i.e., microcosms incubated with nitrate [treatments WINA and WIN], microcosms incubated without nitrate [treatments WIA and WI], and no incubation control [treatment W]) by analysis of variance (ANOVA) test. For detailed sample information, see Table S1.

Figure 4. Relative abundance (%) of *Cellulomonas* rRNA in the sequencing libraries. Mean \pm SD ($n = 3$) is shown. Legend: W, woodchip microcosms without incubation; WINA, woodchip microcosms incubated with nitrate and acetate additions; WIN, woodchip

microcosms incubated with nitrate addition; WIA, woodchip microcosms incubated with acetate addition; WI, woodchip microcosms incubated without any additives.

Figure 5. Phylogenetic tree generated based on the deduced NirK sequences using the maximum likelihood method. GenBank accession numbers are shown in square brackets. Bootstrap values (%) were generated from 1000 replicates, and the values >70% are shown. Branch lengths correspond to sequence differences as indicated by the scale bar.

Figure 6. Transcription level of *Cellulomonas nirK* in the woodchip microcosms. Transcription levels were normalized by the amount of the 16S rRNA. Mean \pm SD ($n = 3$) is shown.

Legend: W, woodchip microcosms without incubation; WINA, woodchip microcosms incubated with nitrate and acetate additions; WIN, woodchip microcosms incubated with nitrate addition; WIA, woodchip microcosms incubated with acetate addition; WI, woodchip microcosms incubated without any additives.

Supporting Information

Cold-Adapted Denitrifying Bacteria in Woodchip Bioreactors

Jeonghwan Jang¹, Emily Anderson², Rodney T. Venterea^{2,3}, Michael J. Sadowsky^{1,2}, Carl Rosen², Gary W. Feyereisen³, Satoshi Ishii^{1,2}

¹BioTechnology Institute, University of Minnesota, St. Paul, MN

²Department of Soil, Water, and Climate, University of Minnesota, St. Paul, MN

³USDA-ARS, Soil and Water Management Research Unit, St. Paul, MN

* Corresponding author: Dr. Satoshi Ishii, BioTechnology Institute, University of Minnesota, 1479 Gortner Ave., 140 Gortner Labs, St. Paul, MN. Email: ishi0040@umn.edu

This file contains 1 figure and 6 tables.

Figure S1. Rarefaction curve generated based on the 16S rRNA (gene) sequences obtained in this study. Total sequence reads were normalized to 28,609 and 21,530 reads per library for DNA and cDNA samples, respectively.

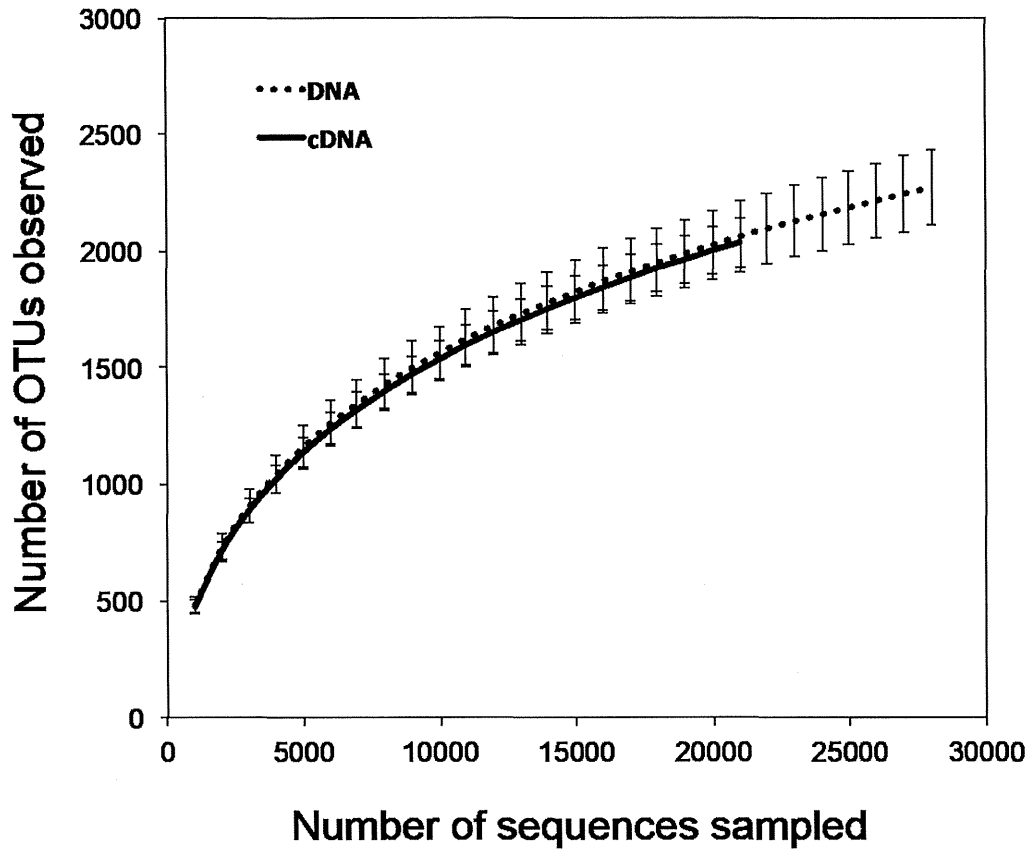


Table S1. Samples prepared for the MiSeq 16S rRNA (gene) sequencing and *nirK* qPCR analyses.

Sample ID	Treatment ID	Supplement		Incubation time (h)	Sample type
		Nitrate	Acetate		
DNA01	W	–	–	0	DNA
DNA02	W	–	–	0	DNA
DNA03	W	–	–	0	DNA
DNA04	WINA	+	+	24	DNA
DNA05	WINA	+	+	24	DNA
DNA06	WINA	+	+	24	DNA
DNA07	WIN	+	–	24	DNA
DNA08	WIN	+	–	24	DNA
DNA09	WIN	+	–	24	DNA
DNA10	WINA	+	+	36	DNA
DNA11	WINA	+	+	36	DNA
DNA12	WINA	+	+	36	DNA
DNA13	WIN	+	–	36	DNA
DNA14	WIN	+	–	36	DNA
DNA15	WIN	+	–	36	DNA
DNA16	WINA	+	+	48	DNA
DNA17	WINA	+	+	48	DNA
DNA18	WINA	+	+	48	DNA
DNA19	WIN	+	–	48	DNA
DNA20	WIN	+	–	48	DNA
DNA21	WIN	+	–	48	DNA
DNA22	WIA	–	+	24	DNA
DNA23	WIA	–	+	24	DNA
DNA24	WIA	–	+	24	DNA
DNA25	WI	–	–	24	DNA

DNA26	WI	-	-	24	DNA
DNA27	WI	-	-	24	DNA
DNA28	WIA	-	+	36	DNA
DNA29	WIA	-	+	36	DNA
DNA30	WIA	-	+	36	DNA
DNA31	WI	-	-	36	DNA
DNA32	WI	-	-	36	DNA
DNA33	WI	-	-	36	DNA
DNA34	WIA	-	+	48	DNA
DNA35	WIA	-	+	48	DNA
DNA36	WIA	-	+	48	DNA
DNA37	WI	-	-	48	DNA
DNA38	WI	-	-	48	DNA
DNA39	WI	-	-	48	DNA
cDNA01	W	-	-	0	RNA (cDNA)
cDNA02	W	-	-	0	RNA (cDNA)
cDNA03	W	-	-	0	RNA (cDNA)
cDNA04	WINA	+	+	24	RNA (cDNA)
cDNA05	WINA	+	+	24	RNA (cDNA)
cDNA06	WINA	+	+	24	RNA (cDNA)
cDNA07	WIN	+	-	24	RNA (cDNA)
cDNA08	WIN	+	-	24	RNA (cDNA)
cDNA09	WIN	+	-	24	RNA (cDNA)
cDNA10	WINA	+	+	36	RNA (cDNA)
cDNA11	WINA	+	+	36	RNA (cDNA)
cDNA12	WINA	+	+	36	RNA (cDNA)
cDNA13	WIN	+	-	36	RNA (cDNA)
cDNA14	WIN	+	-	36	RNA (cDNA)
cDNA15	WIN	+	-	36	RNA (cDNA)

cDNA16	WINA	+	+	48	RNA (cDNA)
cDNA17	WINA	+	+	48	RNA (cDNA)
cDNA18	WINA	+	+	48	RNA (cDNA)
cDNA19	WIN	+	-	48	RNA (cDNA)
cDNA20	WIN	+	-	48	RNA (cDNA)
cDNA21	WIN	+	-	48	RNA (cDNA)
cDNA22	WIA	-	+	24	RNA (cDNA)
cDNA23	WIA	-	+	24	RNA (cDNA)
cDNA24	WIA	-	+	24	RNA (cDNA)
cDNA25	WI	-	-	24	RNA (cDNA)
cDNA26	WI	-	-	24	RNA (cDNA)
cDNA27	WI	-	-	24	RNA (cDNA)
cDNA28	WIA	-	+	36	RNA (cDNA)
cDNA29	WIA	-	+	36	RNA (cDNA)
cDNA30	WIA	-	+	36	RNA (cDNA)
cDNA31	WI	-	-	36	RNA (cDNA)
cDNA32	WI	-	-	36	RNA (cDNA)
cDNA33	WI	-	-	36	RNA (cDNA)
cDNA34	WIA	-	+	48	RNA (cDNA)
cDNA35	WIA	-	+	48	RNA (cDNA)
cDNA36	WIA	-	+	48	RNA (cDNA)
cDNA37	WI	-	-	48	RNA (cDNA)
cDNA38	WI	-	-	48	RNA (cDNA)
cDNA39	WI	-	-	48	RNA (cDNA)

Table S2. Richness and α diversity indices of the microbial communities in the woodchip microcosms. Total sequence reads were normalized to 28,609 and 21,530 reads per library for DNA and cDNA samples, respectively.

Sample ID	Good's coverage	Richness		Diversity	
		Observed OTUs	Chao1	Shannon	Simpson
DNA01	0.973	2222	3171.4	9.093	0.995
DNA02	0.973	2320	3174.3	9.263	0.996
DNA03	0.973	2289	3203.8	9.257	0.996
DNA04	0.974	2162	3133.3	9.071	0.995
DNA05	0.973	2285	3126.7	9.100	0.995
DNA06	0.974	2215	3066.8	9.111	0.995
DNA07	0.973	2212	3186.4	9.232	0.996
DNA08	0.973	2265	3190.2	9.162	0.995
DNA09	0.975	2100	2954.7	9.038	0.995
DNA10	0.974	2220	3078.0	9.212	0.996
DNA11	0.977	2020	2719.1	8.865	0.992
DNA12	0.975	2167	3012.5	9.181	0.996
DNA13	0.973	2266	3169.2	9.284	0.996
DNA14	0.976	1984	2876.5	8.404	0.986
DNA15	0.973	2264	3115.8	9.160	0.995
DNA16	0.972	2264	3294.6	9.168	0.995
DNA17	0.974	2190	3055.3	8.843	0.991
DNA18	0.971	2303	3463.6	9.222	0.995
DNA19	0.979	1839	2531.2	7.988	0.974
DNA20	0.976	2030	2791.6	8.878	0.994
DNA21	0.974	2188	3066.2	9.162	0.995
DNA22	0.973	2432	3326.9	9.472	0.996
DNA23	0.974	2332	3170.4	9.384	0.996
DNA24	0.970	2594	3691.2	9.643	0.997

DNA25	0.973	2389	3323.0	9.487	0.997
DNA26	0.970	2588	3559.2	9.624	0.997
DNA27	0.972	2403	3401.2	9.495	0.997
DNA28	0.971	2488	3467.5	9.567	0.997
DNA29	0.969	2564	3716.6	9.539	0.997
DNA30	0.972	2422	3402.6	9.446	0.996
DNA31	0.974	2370	3223.7	9.488	0.997
DNA32	0.975	2262	3011.6	9.383	0.997
DNA33	0.974	2326	3170.2	9.432	0.997
DNA34	0.974	2396	3241.4	9.508	0.997
DNA35	0.975	2317	3113.7	9.457	0.997
DNA36	0.974	2357	3166.1	9.475	0.997
DNA37	0.972	2500	3336.3	9.554	0.997
DNA38	0.972	2430	3386.5	9.487	0.997
DNA39	0.975	2394	3232.1	9.583	0.997
cDNA01	0.965	2088	3101.0	9.198	0.996
cDNA02	0.965	2082	3080.0	9.152	0.995
cDNA03	0.964	2124	3088.4	9.204	0.996
cDNA04	0.971	1821	2532.3	8.576	0.990
cDNA05	0.967	1997	2817.2	8.923	0.994
cDNA06	0.967	2000	2827.2	9.051	0.995
cDNA07	0.969	1954	2698.5	9.036	0.995
cDNA08	0.966	2019	2894.3	9.045	0.995
cDNA09	0.969	1912	2663.6	9.024	0.995
cDNA10	0.967	2018	2848.3	9.124	0.996
cDNA11	0.966	1938	2922.6	8.771	0.992
cDNA12	0.967	2056	2862.6	9.199	0.996
cDNA13	0.966	1965	2954.4	8.927	0.993
cDNA14	0.970	1752	2614.0	8.534	0.990

cDNA15	0.965	1996	2920.4	9.035	0.995
cDNA16	0.967	1968	2829.5	9.036	0.995
cDNA17	0.967	1966	2896.3	8.961	0.994
cDNA18	0.966	2012	2937.3	9.094	0.995
cDNA19	0.967	1960	2815.2	9.016	0.995
cDNA20	0.969	1929	2751.6	9.090	0.995
cDNA21	0.966	2009	2931.0	9.117	0.995
cDNA22	0.966	2169	3019.9	9.239	0.994
cDNA23	0.966	2146	2980.5	9.276	0.995
cDNA24	0.962	2258	3265.6	9.407	0.996
cDNA25	0.967	2119	2832.1	9.269	0.995
cDNA26	0.964	2208	3147.2	9.373	0.996
cDNA27	0.965	2072	3134.6	9.218	0.995
cDNA28	0.966	2135	3003.2	9.347	0.996
cDNA29	0.963	2243	3145.0	9.333	0.995
cDNA30	0.966	2093	2915.7	9.051	0.992
cDNA31	0.964	2107	3136.8	9.161	0.994
cDNA32	0.968	1993	2825.1	9.123	0.994
cDNA33	0.967	2031	2942.4	9.154	0.994
cDNA34	0.964	2185	3238.6	9.401	0.996
cDNA35	0.966	2122	2962.4	9.294	0.995
cDNA36	0.967	2108	2953.5	9.278	0.995
cDNA37	0.963	2210	3177.3	9.420	0.996
cDNA38	0.965	2227	3080.0	9.417	0.996
cDNA39	0.966	2170	3074.3	9.335	0.995

Table S3. Nitrate reducing and denitrifying strains obtained in this study. Strains shown in bold reduced $\geq 40\%$ nitrate, converted $< 10\%$ of nitrate to ammonium, and produced significant amount of N_2O (> 100 ppm), and therefore, were considered as denitrifiers.

Isolate ID	Proportion of N converted to ammonium (%)	Nitrate reduced (%)	N ₂ O produced (ppm)	Identification (genus)
WB17	40.9	98.3	1401.1	<i>Microvirgula</i>
WB18	44.9	98.3	1479.3	<i>Microvirgula</i>
WB19	4.1	BDL	63.1	<i>Clostridium</i>
WB21	5.8	BDL	224.0	<i>Clostridium</i>
WB22	42.1	98.4	1496.5	<i>Microvirgula</i>
WB23	7.0	BDL	9.5	<i>Clostridium</i>
WB24.2	7.3	BDL	7.1	<i>Clostridium</i>
WB26	BDL	33.5	2.5	<i>Clostridium</i>
WB29	BDL	32.0	1.3	<i>Clostridium</i>
WB39	7.1	39.4	68.8	<i>Clostridium</i>
WB40	2.0	3.8	5.1	<i>Clostridium</i>
WB49	6.8	39.6	103.2	<i>Clostridium</i>
WB53	0.8	58.2	843.6	<i>Clostridium</i>
WB66	5.0	45.1	112.1	<i>Clostridium</i>
WB76	BDL	44.4	147.0	<i>Clostridium</i>
WB80	5.9	49.8	603.2	<i>Clostridium</i>
WB81	4.1	47.5	0.3	<i>Clostridium</i>
WB91	7.0	38.7	169.7	<i>Desulfobacterium</i>
WB94	6.5	49.2	116.0	<i>Cellulomonas</i>
WB102	2.5	60.3	BDL	<i>Cellulomonas</i>
WB104	73.1	29.1	994.9	<i>Cellulomonas</i>

Table S4. Summary of the sequenced genome of *Cellulomonas* sp. strain WB94.

Contig No.	Accession number	Size (bp)	GC content (%)
0	NZ_QEES01000002.1	2,780,765	71.9
1	NZ_QEES01000005.1	329,035	70.2
2	NZ_QEES01000001.1	235,040	70.3
3	NZ_QEES01000007.1	151,423	71.1
4	NZ_QEES01000004.1	162,011	72.2
5	NZ_QEES01000003.1	157,415	72.7
6	NZ_QEES01000006.1	53,291	71.9

Table S5. Genes associated with denitrification or polysaccharide catabolism identified on the genome of *Cellulomonas* sp. strain WB94.

	Function	Gene	Locus_tag	Product	
Denitrification	Nitrate Reduction	<i>narI</i>	DDP54_03075	respiratory nitrate reductase subunit gamma	
		<i>narJ</i>	DDP54_03080	nitrate reductase molybdenum cofactor assembly chaperone	
		<i>narH</i>	DDP54_03085	nitrate reductase subunit beta	
		<i>narG</i>	DDP54_03090	nitrate reductase subunit alpha	
	Nitrite reduction	<i>nirD</i>	DDP54_03030	nitrite reductase (NAD(P)H) small subunit	
		<i>nirB</i>	DDP54_03035	nitrite reductase (NAD(P)H)	
			DDP54_03150	Molybdopterin-binding nitrite reductase	
		<i>nirK</i>	DDP54_17680	NO-forming nitrite reductase	
	Polysaccharide catabolism	Cellulose degradation		DDP54_00625	endoglucanase
			<i>malQ</i>	DDP54_01650	4-alpha-glucanotransferase
			DDP54_0629	1,3-beta-glucanase	
<i>malQ</i>			DDP54_17500	4-alpha-glucanotransferase	
			DDP54_09215	cellobiose phosphorylase	
Xylan degradation			DDP54_00375	1,4-beta-xylanase	
Starch/glycogen degradation			DDP54_12980	alpha-amylase	
			DDP54_13300	alpha-amylase	
		DDP54_12980	alpha-amylase		

DDP54_13300 alpha-amylase
DDP54_15400 glucoamylase
DDP54_1540 glucoamylase

Table S6. Composition of the synthetic agricultural wastewater

Chemical	Concentration (mg/L)
CaCl ₂	220.5
MgCl ₂ .6H ₂ O	421.5
KH ₂ PO ₄	1.3
Na ₂ SO ₄	10.4
H ₃ BO ₃	0.1
FeSO ₄ .7H ₂ O	0.625
CuSO ₄ .5H ₂ O	0.0775
MnSO ₄ .H ₂ O	0.025
ZnSO ₄ .7H ₂ O	0.1